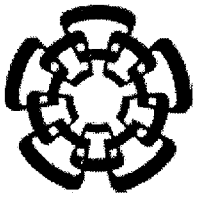

CENTRO DE INVESTIGACIÓN Y DE ESTUDIOS
AVANZADOS DEL INSTITUTO POLITÉCNICO NACIONAL

**Unidad Zacatenco**

**Departamento de Computación**

# Modelo continuo para el problema de localización de ambulancias

T E S I S

Que presenta

**Sergio Antonio del Ángel Morales Pacheco**

Para obtener el grado de

**Maestro en Ciencias en Computación**

Director de la Tesis

**Dr. Oliver Steffen Schütze**

**México, D.F.** **Diciembre, 2015**

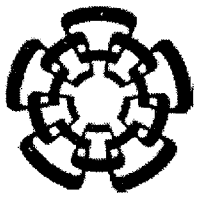

Centro de Investigación y de Estudios
Avanzados del Instituto Politécnico Nacional

**Zacatenco Campus**

**Computer Science Department**

# Solving the Ambulance Location Problem using a Continuous Location Model

Submitted by

**Sergio Antonio del Ángel Morales Pacheco**

As a fulfillment of the requirement for the degree of

**Master in**

**Computer Science**

Advisor

**Dr. Oliver Steffen Schütze**

**México, D.F.** **December 2015**

# Contents

# Acknowledgment

I dedicate, as a symbol of my gratefulness, this thesis work to the members of my family: Elena, Feliú and Moisés. The importance and help they represent to me, can not be encrypted into words, so I will keep it simple: Thank you, I love you.

This thesis work summarizes the work and the collaboration over one year with the Tijuana Red Cross Unit and the Technological Institute of Tijuana (ITT). I would like to thank to, the head of the Tijuana Red Cross Unit, Dr. Carlos Vega for his guidance in the development of this work and for providing us the information needed to model the Ambulance Location Problem; and I thank as well to Dr. Leonardo Trujillo Reyes from the ITT, who has been with us from the beginning of the project: offering new ideas; commenting, discussing and interpreting all the results of this work, and who also received me at the ITT to provided me a better understanding of the problem we were dealing with.

I especially thank to my thesis advisor, Dr. Oliver Schutze, who offered me the opportunity to participate in this project, for his big help and the time dedicated to every step and obstacle that this thesis work have brought to us.

Finally, I thank to the Consejo Nacional de Ciencia y Tecnología (CONACYT) for its financial support throughout my Master on Computer Science program.

# List of Figures

# List of Tables

# Chapter 1

# Introduction

Determining the location of the ambulances along a city is one of the most important problems to solve in order to guarantee the proper delivery of Emergency Medical Services (EMS). The set of ambulances must be located along the city, such that the area considered by the problem is covered within a time response tolerance threshold.

The present work is the result of a collaboration with the Tijuana Red Cross Unit[1] to find an efficient and applicable solution for the problem of determining the location of the ambulances available along Tijuana city. In Section 1.1, the main aspects of the collaboration with the Red Cross are detailed along with the reasons that sustain this work. An introduction to the ambulance location problem is included in Section 1.2. In Section 1.3, the aims of this work are drawn. Finally, Section 1.4 lists the contributions of this thesis work.

## 1.1 Motivation

The fleet of the Red Cross Unit of Tijuana currently consists of 14 ambulances, 11 of which are in service every day. These 11 ambulances cover approximately 98 % of the EMS demand in Tijuana. In 2013, the Red Cross provided EMS care to more than 37,000 persons with their fleet of ambulances. The population of Tijuana contains about 1.6 million inhabitants. Thus, there is in average one ambulance available for each 141,000 inhabitants, while the international recommendation is to have one ambulance unit for at most 20,000 inhabitants. Furthermore, in 2013 the average response time for an ambulance in Tijuana to arrive to an emergency call was roughly 14 minutes, with a standard deviation of 4 minutes. In 75% of the cases the ambulance arrived within 18 minutes and in 90 % of the cases the ambulance arrived within 23 minutes. The cost for the maintenance and operation of the fleet is about 25 million Mexican Pesos per year (approx. 1.7 million US Dollars) while the service is free of charge for the users.

Given the size of the city, the limited resources available for the Red Cross, and the social impact of the problem, it is evident that the EMS systems must strive

[1] http://www.cruzrojatijuana.org.mx/

towards high efficiency and close to optimal deployment.

In particular, this work deals with the problem of determining the best locations for ambulance bases across Tijuana city based on historical information of EMS calls. With the solution to the ambulance location problem it is expected to reduce the average arrival time of the Red Cross EMS units, the reduction will be achieved by modeling and solving the problem for this particular case, this is: taking into consideration the number and the type of EMS calls received in the different districts of Tijuana city to locate the ambulances where they are more needed.

The reduction of the average time is at the same time an improvement of the Emergency Medical Services quality, which can be interpreted as a reduction in the number of deaths caused by the delay of the arrival of ambulances.

## 1.2 Problem

The problem of locating ambulances may be treated as a problem of locating facilities and allocating customers (taking into consideration the time response restrictions). This problem involves the main topics of distribution system design, that is, in cases when the quality of the service provided by the facility depends on its location and the location of other facilities. There exists a large variety of approaches in the literature regarding the solution of this, and other related problems, that include linear, single-facility, deterministic, static, dynamic, continuous and discrete models, among others [12], [20], [36].

Proposed solutions must attempt to model the most relevant features of the particular urban area for which EMS are being planned for, as well as the characteristics of the service provider for that city. This problem is known as the ambulance location problem, which has been studied in several previous research works [4, 26]. One approach is to model it as a graph covering problem, with several proposals in relevant literature. In these models, the problem is defined on a graph $G$, where the vertices denote either demand points (locations or areas within a city that might require EMS services) or feasible bases (potential sites to place ambulances within the city); where $V$ is the set of all demand points and $W$ is the set of all feasible bases. The edges in $G$ are weighted by a factor $t_{ij}$ that denotes the expected travel time (or potentially, any other measure of cost) between vertex $i$ and vertex $j$. A demand point $i \in V$ is *covered* by site $j \in W$ if and only if $t_{ij} \leq r$ where $r$ represents a minimum coverage requirement or standard. For instance, the location set covering model (LSCM) [37] aims to minimize the number of ambulances needed to cover all demand points. Another popular model is the double standard model (DSM) proposed by Gendreau et al. [16], that uses two coverage standards $r_1$ and $r_2$, with $r_1 < r_2$. In this model, all demand points must be covered by an ambulance located within $r_2$ time units (or cost units), and a proportion $\alpha$ of the demand points must be within $r_1$ time units of an ambulance. For example, in the *United States Emergency Medical Services Act* of

1973 $r_1$ is set to 10 minutes[2] and $\alpha$ to 0.95 while there is no specification for $r_2$.

In [19], Jaramillo et al. applied genetic algorithms (GA) techniques to solve a wide set of theoretical location problems. The representative location models chosen were the fixed charge location problem (uncapacitated and capacitated version) and the maximum covering problem from non-competitive location theory and the centroid and medianoid models from competitive location theory. This work concluded that GAs do not outperform specialized heuristics in the facility location problems, however, the solutions that the GAs produce are no worse than and in fact sometimes superior to the ones produced by these other methods. In literature, there are a broad amount of examples of applications for the GA to facility location problem. For instance, in [28] Marić applied successfully a GA to solve the uncapacitated facility location problem. Other examples can be found in [13, 22, 23].

## 1.3 Aim

The aim of this thesis is to model the ambulance location problem and to find the solution to this problem for the particular case discussed (Tijuana Red Cross Unit). The real impact of the project along with the interest in finding an accurate continuous multi-objective model, for such situations where the time is a key factor, are the main goals for this work.

## 1.4 Contribution

The following are the contributions achieved:

- A continuous location model for the ambulance location problem.
- A multiobjective continuous model for the ambulance location problem.
- A software package for free scientific use.
- One conference paper published [31] in the proceedings of the IEEE Congress on Evolutionary Computation, 2015.
- The development and completion of a Master thesis.

## 1.5 Thesis Organization

The following chapters of the present document are organized as follows:

[2]The National EMS Information System reports an average arrival time under ten minutes in the years of 2010 and 2011, data retrieved from www.nedarc.org/emsDataSystems/nemsisReports/2010_11EMSTimes.html

- In Chapter 2, we introduce the concept of continuous optimization and continuous location optimization problem along with the models and solution methods in the state-of-the-art that address these problems.
- In Chapter 3 the continuous location model that we propose to solve the ambulance location and the details of its implementation are described.
- In Chapter 4 are presented the multi-objective extension of the continuous location model and the multi-criteria model.
- Chapter 5 includes the description of the experiments performed and their respective results for all the models previously mentioned.
- Finally, in chapter 7, we give our conclusions after discussing the results obtained and their implications, along with the future work that we consider pertinent and important, in order to improve or correct the flaws observed in our computations.

# Chapter 2

# Background and Related Work

This work proposes a continuous optimization model (the definition for these models is given in Section 2.1) for the ambulance location problem. Furthermore, this model is extended to a multi-objective model (Section 2.2); both optimization problems are solved using genetic algorithms (GAs); in particular, the multi-objective problem is solved by the NSGA-II method (Section 2.3).

The optimization problem we use is an adaption of the Multi-source Weber Problem (Section 2.4.1), which is an extension of the Weber facility location problem (Section 2.4). In addition, in order to address the time restrictions inherent in the ambulance location problem, a set of constraints considered in the Limited Distance Minisum Problem is adapted to the proposed model (Section 2.4.2).

In Section 2.5, the most relevant models that regard either the ambulance location problem or the ambulance location/relocation problem are described.

## 2.1 Continuous Optimization

In continuous optimization, the variables in the model are nominally allowed to take on a continuous range of values, usually real numbers. This feature distinguishes continuous optimization from discrete or combinatorial optimization, in which the variables may be binary (restricted to the values 0 and 1), integer (for which only integer values are allowed), or more abstract objects drawn from sets with finitely many elements.

An important distinction in continuous optimization is between problems in which there are no constraints on the variables and problems in which there are constraints on the variables. Unconstrained optimization problems arise directly in many practical applications; they also arise in the reformulation of constrained optimization problems in which the constraints are replaced by a penalty term in the objective function. Constrained optimization problems arise from applications in which there are explicit constraints on the variables. There are many subfields of constrained optimization for which specific algorithms are available.

In this work, a constrained optimization problem is proposed, this family of prob-

lems considers the problem of optimizing an objective function subject to constraints on the variables. In general terms, a single objective optimization problem reads as

$$\min_{x \in \mathbb{R}^n} f(x)$$

subject to

$$h(x) \leq 0$$
$$g(x) = 0$$

$$f : \mathbb{R}^n \mapsto \mathbb{R}$$

$$g : \mathbb{R}^n \mapsto \mathbb{R}^m, \qquad g(x) = (g_1(x), g_2(x), ..., g_m(x))^T$$
$$g_i : \mathbb{R}^n \mapsto \mathbb{R}, \qquad i = 1, ..., m$$

$$h : \mathbb{R}^n \mapsto \mathbb{R}^p, \qquad h(x) = (h_1(x), h_2(x), ..., h_p(x))^T$$
$$h_i : \mathbb{R}^n \mapsto \mathbb{R}, \qquad i = 1, ..., p$$

The feasible set $S$ is the set of points $x$ that satisfy the equality and the inequality constraints.

$$S = \{x \in \mathbb{R}^n | g(x) \leq 0, h(x) = 0\}$$

There are several strategies in the literature to approach to the solution of these problems, some of these strategies implement mathematical programming techniques like convex programming, integer programming and non-linear programming [14],[35]; however, the are strategies which do not implement mathematical programming techniques to find optimal solutions, examples of such strategies are the bio-inpired metaheuristics (particle swarm optimization [41], ant colony optimization [8] and genetic algorithms [40]).

While others strategies are improved by using more than one method to solve the problem: examples of these strategies are the hybrid optimization algorithms [5],[33] and the memetic algorithms [25],[34].

## 2.2 Multi-Objective Optimization

The need to face real applications renders the hypothesis of a single-objective function to be optimized subject to a set of constraints no longer suitable, and the introduction of a multi-objective optimization framework allows one to manage more information. If we regard the ambulance location problem from different points of view, i.e., in terms of social needs for a quick response, or in terms of economic issues or geographic coverage, it is clear that a model that considers simultaneously two or more such objectives could produce solutions with a higher level of equity.

A multi-objective optimization problem can be described in mathematical terms as follows:

$$\min_{x \in \mathbb{R}^n} (f_1(x), f_2(x), f_3(x), ..., f_k(x))$$

subject to

$$h(x) \leq 0$$
$$g(x) = 0,$$

where $k > 1$.

The concept of *optimality* does not apply directly in the multi-objective setting. Here, the notion of Pareto optimality has to be introduced. Essentially, a feasible vector $x^* \in S$ is said to be Pareto optimal for a multi-objective problem if all other feasible vectors have a higher value for at least one of the objective functions $f_i$, with $i = 1, ..., k$, or have the same value for all the objective functions. Formally speaking, we have the following definitions:

**Definition** A point $x^* \in S$ is said to be a weak Pareto optimum or a weak efficient solution for the multi-objective problem if and only if there is no feasible $x$ such that $f_i(x) < f_i(x^*) \quad \forall i \in 1, ..., k$.

**Definition** A point $x^* \in S$ is said to be a strict Pareto optimum or a strict efficient solution for the multi-objective problem if and only if there is no feasible $f_i(x) \leq f_i(x^*)$ $\forall i \in 1, ..., k$, with at least one strict inequality.

The set of all the Pareto points is called the Pareto set $Q$.

$$Q = \{x^* \in S \quad | \nexists x \in S : f_i(x) < f_i(x^*) \quad \forall i = 1, ..., k\}$$

The image of the efficient set $Q$, i.e., the image of all the efficient solutions, is called Pareto front. Examples in the literature of these problems can be found in [7], [32], [39].

## 2.3 Genetic Algorithms

Since the 1960s there has been increasing interest in imitating living beings to develop powerful algorithms for difficult optimization problems, *evolutionary computation* is the term in common use to refer such techniques. The best known algorithms in this class include genetic algorithms, developed by Holland [18]; evolutionary programming, developed by Fogel et al. [15]; and genetic programming, developed by Koza [21].

A genetic algorithm is a method for solving both constrained and unconstrained optimization problems based on a natural selection process that mimics biological evolution. The algorithm repeatedly modifies a population of individual solutions. At each step, the genetic algorithm randomly selects individuals from the current population and uses them as parents to produce the children for the next generation. Over successive generations, the population "evolves" toward an optimal solution.

One can apply genetic algorithms to solve problems that are not well suited for standard optimization algorithms, including problems in which the objective function is discontinuous, nondifferentiable, stochastic, or highly nonlinear.

In general, a genetic algorithm has five basic components, as sumarized by Michalewicz [30]:

1. A genetic representation of solutions of the problem.

2. A way to create an initial population of solutions.

3. An evaluation function rating solutions in terms of their fitness.

4. Genetic operators that alter the genetic composition of children during reproduction.

5. The values for the parameters that use the genetic algorithm.

The conventional genetic algorithm, considered in detail in [27], maintains a population of individuals, say $P(t)$, for generation $t$. Each individual is evaluated with the objective function, the function for which an optimal solution is required, to give some measure of its fitness. Some individuals undergo stochastic transformations by means of genetic operations to form new individuals. There are two types of transformation: *mutation*, which creates new individuals by making changes in a single in a single individual, *crossover*; which creates new individuals by combining parts from two individuals. A new population is formed by selecting the fittest individuals from the parent population and the offspring population, this is, the individuals best evaluated according to the objective function. By allowing the best individual(s) from the current generation to carry over to the next unaltered, the algorithm, eventually converges to a solution, which is not guaranteed to be the same as the global solution.

## 2.4 The Weber facility location problem

The problem where the objective is to locate a single facility in the plane $\mathbb{R}^2$, so that the sum of distances from the facility to a set of demand points is minimized is often referred to in the literature as the Weber (or Fermat-Weber) problem [2]. It traces back to Fermat in the $17^{th}$ century who posed a purely geometrical version of the problem with only three points.

Drezner, Mehrez and Wesolowsky investigated in [9] the Weber problem for the case in which the distance functions are constant after given threshold values, which they call the facility location problem with limited distances. This problem has applications in situations where the service provided by the facility is useless after a given threshold (time or distance units). For example, imagine the problem of locating a fire station, where every demand point has a distance limit after which the service offered is neglected.

The authors consider a situation where a certain damage occurs in a property located in $p_i$, for $i = 1, .., n$. The service station is located at the point $y \in \mathbb{R}^2$, and the time needed to arrive at this point increases up to $\lambda_i$ (time tolerance threshold), so the service is insensitive after this given $\lambda_i$ time threshold. By denoting $d(p_i, y)$ the distance between point $p_i$ and the service station located at $y$, and $\Omega$ the proportion of damage at zero distance then the proportion of damage in $p_i$ is given by

$$\Omega + (1 - \Omega)d(p_i, y)/\lambda_i$$

in the case $d(p_i, y) < \lambda_i$, and 1 otherwise. The corresponding facility location problem is then expressed as:

$$\min_{y \in \mathbb{R}^2} \sum_{i=1}^{n} \left( \Omega + (1 - \Omega) \frac{\min\{d(p_i, y), \lambda_i\}}{\lambda_i} \right). \tag{2.1}$$

By removing the constant terms from this problem and introducing binary variables $v_i$ that select between $d(p_i, y)$ and $\lambda_i$ to the summation of the objective function we end up with the following minimization problem:

$$\min_{y \in \mathbb{R}^2, v \in \{0,1\}^n} \sum_{i=1}^{n} \frac{1}{\lambda_i} (\lambda_i (1 - v_i) + d((p_i, y), v_i). \tag{2.2}$$

### Continuous location models

Continuous location models (models in the plane) are caracterized through two essential attributes: (a) the solution space is continuous, that is, it is feasible to locate facilities on every point in the plane, (b) distance is measured by a suitable metric.

Continuous location models require to calculate coordinates $(x, y) \in \mathbb{R}^m \times \mathbb{R}^m$ for $m$ facilities. The objective is to minimize the sum of distances between the facilities and $m$ given demand points.

The subject of the Weber problem is to determine the coordinates of a single facility, this is when $m = 1$ and $(x, y) \in \mathbb{R} \times \mathbb{R}$, such that the sum of the weighted distances $w_k d_k(x, y)$ to given demand points $k \in K$ located in $(a_k, b_k)$ is minimized, where $K$ denotes the set of demand points.

The corresponding optimization problem is expressed as:

$$\min_{(x,y)} \sum_{k \in K} w_k d_k(x, y). \tag{2.3}$$

### 2.4.1 The Multi-source Weber Problem

To locate more than one facility, an extended version of the Weber Problem is required, which is known as the *Multi-source Weber Problem* [20], this problem is NP-hard [29], heuristic approaches for the solution of this problem can be found in [3],[10] and [38]. To be more precise, the aim is to locate $m$ facilities, $1 < m < |K|$, and to allocate demand to the chosen facilities. This problem can be modeled as the following non-linear mixed conditional integer problem:

$$\min_{\substack{(x,y) \in \mathbb{R}^m \times \mathbb{R}^m \\ u \in \{0,1\}^{m \times |K|}}} \sum_{k \in K} \sum_{j=1}^{m} w_k d(p_k, (x_j, y_j)) u_{kj} \tag{2.4}$$

subject to:

$$\begin{aligned} &\sum_{j=1}^{m} u_{kj} = 1 && \forall k \in K, \\ &u_{kj} \in \{0, 1\} && \forall k \in K, j = 1, ..., m \\ &x, y \in \mathbb{R}^m. \end{aligned}$$

where set of constraints $\sum_{j=1}^{m} u_{kj} = 1$ guarantees that demand is satisfied only once, this is, point $k$ can only be assigned to one facility $j$.

### 2.4.2 Limited Distance Minisum Problem with Side Constraints

Consider that there are $n$ demand points with threshold distances $\lambda_i > 0$ and weights $w_i \geq 0$, $i = 1, ..., n$. The LDMPSC as proposed in [12] is expressed as follows:

$$\min_{\substack{(x,y) \in \mathbb{R} \times \mathbb{R} \\ v \in \{0,1\}}} \sum_{i=1}^{n} w_i (\lambda_i (1 - v_i) + ||p_i - (x, y)||_q v_i) \tag{2.5}$$

subject to:

$$||p_i - (x, y)||_q v_i \leq \lambda_i$$

$$L \leq \sum_{i=n}^{n} v_i \leq U,$$

where $||p_i - (x, y)||_q$ denotes the $l_q$-distance definded as

$$||x||_q = (|x_1|^q + |x_2|^q + |x_3|^q + ... + |x_n|^q)^{\frac{1}{q}}$$

between a point $p_i$ and the facility located at $(x, y)$ in the plane $\mathbb{R}^2$.

The variable $v_i$ can be equal to 1 only if the distance between $p_i$ and the facility located at $(x, y)$ is inferior (or equal) to the distance limit $\lambda_i$, which is expressed in the former set of constraints. The latter set of constraints defines bounds $L$ and $U$ on the number of variables $v_i$, which can be equal to 1.
By removing its constant terms, problem (2.5) can be rewritten as:

$$\min_{\substack{(x,y)\in\mathbb{R}\times\mathbb{R} \\ v\in\{0,1\}}} \sum_{i=1}^{n} w_i(||p_i - (x, y)|| - \lambda_i)v_i. \tag{2.6}$$

subject to:

$$||p_i - (x, y)||v_i \leq \lambda_i,$$

$$L \leq \sum_{i=n}^{n} v_i \leq U.$$

The LDMPSC has applications in situations where the service provided by the facility is sensitive after a given amount of time, for instance consider the problem of minimizing the call center staffing [1] or the problem of locating a fire station [11].

## 2.5 State-of-the-Art

### 2.5.1 Static Ambulance Location

The static ambulance location (SAL)[1] problem can be defined on a graph $G$, where the vertices denote either demand points (locations or areas within a city that might require Emergency Medical Services (EMS)) or feasible bases (potential sites to place ambulances within the city); where $V$ denotes the set of demand points and $W$ the set of feasible bases.

The edges in $G$ are weighted by a travel time $t_{ij}$ that denotes the expected travel time between vertex $i$ and vertex $j$. Then, we can define that a demand point $i \in V$ is covered by the site $j \in W$ if and only if $t_{ij} \leq r$, where $r$ is the minimum or standard

[1]this model is called static because its solution does not consider the problem of dispatching the ambulances after they have been located.

coverage requirement. Also, let $W_i = \{j \in W : t_{ij} \leq r\}$ be the set of location sites covering the demand point $i$.

The SAL problem has been modeled by the location set covering model (LSCM), whose objective is to minimize the number of ambulances needed to cover all demand points, using a binary variable $x_j$, which is equal to 1 if and only if an ambulance is located at the vertex $j$; then the LSCM is defined as the following constrained optimization problem:

$$\min_{j \in W} \sum x_j \tag{2.7}$$

subject to:

$$\sum_{j \in W_i} x_j \geq 1 (i \in V). \tag{2.8}$$

$$x_j \in \{0, 1\} (j \in W) \tag{2.9}$$

The disadvantages of this model are:

- An over simplification of the real problem, since it considers the minimization of the number of ambulances ignoring the information available about the weight associated to each demand point, this is, the cost for traveling from a feasible base towards a demand point.
- The model assumes the existance of $|W|$ ambulances available, but this number may decrease when an emergency occurs and an emergency unit is dispatched to it.

### Double Standard Model (DSM)

The DSM was proposed by Gendreau et al. [17], using two coverage standards $r_1$ and $r_2$, with $r_1 < r_2$. In this model, all demand points must be covered by an ambulance located within $r_2$ time units, and a proportion $\alpha$ of the demand points must be within $r_1$ time units of an ambulance. The objective of DSM is to maximize the demand covered twice within the time standard $r_1$ (maximize the number of demand sites covered by two ambulances within $r_1$ time units) considering that there are $\rho$ ambulances available, and $\rho_j$ ambulances at most per site $j$.

Let $W_i^1 = \{j \in W : t_{ij} \leq r_1\}$ and $W_i^2 = \{j \in W : t_{ij} \leq r_2\}$ be the sets of service points covering demand point $i$ within $r_1$ and $r_2$ time standards, respectively, $y_j$ the total number of ambulances located at site $j \in W$, $q_i$ is a quantification of EMS's demand at the point $i \in V$, and the binary variable $x_i^j$ which is equal to 1 if and only if the demand at vertex $i \in V$ is covered $k$ times ($k = 1$ or 2) within $r_1$ time units. The DSM optimization problem is defined as:

$$\max_{i \in V} \sum q_i x_i^2 \tag{2.10}$$

subject to:

$$\sum_{j \in W_i^2} y_j \geq 1 \qquad i \in V, \tag{2.11}$$

$$\sum_{i \in V} q_i x_i^1 \geq \alpha \sum_{i \in V} q_i, \tag{2.12}$$

$$\sum_{j \in W_i^1} y_j \geq x_i^1 + x_i^2 \qquad i \in V, \tag{2.13}$$

$$x_i^2 \leq x_i^1 \qquad i \in V \wedge x_i^k \in \{0,1\}, \tag{2.14}$$

$$\sum_{j \in W} y_j = \rho \qquad y_j \in \mathbb{Z}^+, \tag{2.15}$$

$$y_j \leq \rho_j \qquad j \in W, \tag{2.16}$$

In constraint (2.11), the number of ambulances that covers every demand point $i$ within $r_2$ time units must be equal or greater than 1, in constraint (2.12) the proportion of demand points $d_i$ covered within $r_1$ time units is required to be greater or equal than $\alpha$. Constraint (2.13) states that the sum of ambulances that covers a demand point $i$ within $r_1$ should be greater than 1 if the point $i$ is covered once ($x_i^1 = 1$) and greater than 2 if the point $i$ is covered twice ($x_i^2 = 1$). Constraint (2.14) states that a point may not be covered twice if it is not covered at least once. Constraint (2.15) establishes the maximum number of ambulance available. Finally, constraint (2.16) establishes the maximum number of ambulances allowed to be located at each feasible service point.

The DSM model has proven to be very useful and applicable to real world scenarios. However, researchers have also worked on extending the model to include a variety of more realistic constraints and objectives, which are reviewed next.

### 2.5.2 Dynamic Double Standard Model (DDSM)

When an ambulance is dispatched, from a service point, to attend an emergency that occurs at some demand point in the city, one or more of the remaining demand points

may result uncovered. If this is the case, the location of the ambulances requires to be updated. When the model considers this kind of situations, then the problem to be solved is known as the ambulance relocation problem.

The DDSM, presented in [24], considers the ambulance relocation problem (ARP), which involves determining the best deployment of $\rho$ ambulances over a series of discrete time instances, subject to restrictions regarding the movement or re-positioning of ambulances between consecutive instances. DDSM aggregates a number of practical considerations which addresses the dynamic nature of the problem: (a) Vehicles moved in successive redeployment cannot always be the same. (b) Repeated round-trips between two locations should be avoided. (c) The number of long trips among initial and final location sites should be small.

In this model, the ARP is solved at every discrete moment $t$ on which an ambulance is deployed to attend a medical emergency.

The dynamic aspect of the redeployment of ambulances is captured by time dependent variables $M_{jl}^t$, whose value is equal to a quantification of the cost of repositioning an ambulance $l$ from its current site to site $j \in W$ at time $t$. The idea is that every variable $M_{jl}^t$ captures the historical movements and activity of ambulance $l$, this is, if ambulance $l$ has been frequently repositioned then its $M_{jl}^t$ associate variable's value should be large.

The movements of each ambulance are also subject to the constraints of the problem, such that unfeasible movements are disallowed. There are also binary variables $y_{jl}$ which are equal to 1, if and only if, ambulance $l$ is moved to site $j$. The DDSM maximization problem is defined as:

$$\max_{i \in V} \sum q_i x_i^2 - \sum_{j \in W} \sum_{l=1}^{\rho} M_{jl}^t y_{jl} \tag{2.17}$$

subject to:

$$\sum_{j \in W_i^2} \sum_{l=1}^{\rho} y_j \geq 1 \qquad i \in V, \tag{2.18}$$

$$\sum_{i \in V} q_i x_i^1 \geq \alpha \sum_{i \in V} q_i, \tag{2.19}$$

$$\sum_{j \in W_i^1} \sum_{l=1}^{\rho} y_{jl} \geq x_i^1 + x_i^2 \qquad i \in V, \tag{2.20}$$

$$x_i^2 \leq x_i^1 \qquad i \in V \wedge x_i^k \in \{0, 1\}, \tag{2.21}$$

$$\sum_{j \in W} y_{jl} = 1 \qquad l = 1, ...\rho \wedge y_{jl} \in \{0, 1\}, \tag{2.22}$$

$$\sum_{l=1}^{\rho} y_{jl} \leq \rho_j \qquad j \in W. \tag{2.23}$$

The constraints of the DDSM model are similar to the ones of the static DSM model. The main difference is in the objective function, where the sum of the $M_{jl}^t$ penalization for redeployment variables is included.

# Chapter 3

# A Continuous Location Model for the Tijuana Red Cross Ambulance Fleet

The task of this work is to define a model for the optimal placement of the Tijuana Red Cross ambulance fleet. For this, we propose in the following a model for this problem and go then into detail about the implementation of the optimization. The model will be static, i.e., we measure the response time by the (estimated) travel time from the base station of an ambulance to a demand point.

## 3.1 Continuous Location Model

The Multi-source Weber Problem serves as a starting point for our model, since it considers both multiple facilities (ambulances) and multiple demand points (persons requesting EMS). Note, however, that problem (2.4) does not involve any time constraints, such constraints are of great importance for the problem at hand since if the time to reach a certain demand point is greater than a given threshold, then the service is probably of no use. Even worse, the decision to move the ambulance to this demand point comes with a potential waste of resources since the ambulance might not be able to attend another demand that may be requested during that time.

In the following, we will consider the minimization of all response times from the ambulances to the demand points, such minimization may be interpreted as a maximization of the number of demands covered.

Taking this into consideration, we have decided to integrate elements from the LDMPSC problem [12] and the multi-source Weber problem [20] to model the Tijuana Red Cross ambulance problem as follows:

Assume we are given $m$ ambulances building the fleet $A = \{a_1, \ldots, a_m\}$ and $n$ demand points $\rho_1, \ldots, \rho_n$ located in a certain region. Denote by $t_k(\rho_k, (x_j, y_j))$ the (estimated) time that it takes for the ambulance $a_j$ to arrive from its base station at

the demand point $\rho_k$ located at $(x_{\rho_k}, y_{\rho_k})$, where $k$ goes from 1 to $n$. $\tau_k$ is defined as the tolerance time threshold value for the demand point $\rho_k$ and $\omega_k$ is its associated weight value. The definition of the weight values $\omega_k \in \mathbb{R}$ is discussed in Section 3.2.2. The corresponding fleet location problem can then be expressed as follows

$$\min_{(x,y)\in\mathbb{R}^m\times\mathbb{R}^m} f_{location}(x,y) = \sum_{j=1}^{m} f_{weightedSum}(x_j, y_j) \tag{3.1}$$

subject to:

$$\sum_{j=1}^{m} U\Big(\tau_k - t_k\big(\rho_k, (x_j, y_j)\big)\Big) \geq 1 \qquad \forall k \in K,$$

where $f_{weightedSum}(x_j, y_j)$ is defined as:

$$f_{weightedSum}(x_j, y_j) = \begin{cases} \sum\limits_{k\in K} \omega_k t_k\big(\rho_k, (x_j, y_j)\big) U\Big(\tau_k - t_k\big(\rho_k, (x_j, y_j)\big)\Big) \\ if \ \sum_{k=1}^{n} U\Big(\tau_k - t_k\big(\rho_k, (x_j, y_j)\big)\Big) > 0 \\ 10000 \qquad otherwise. \end{cases} \tag{3.2}$$

The function $U : \mathbb{R} \mapsto \{0, 1\}$, is given by:

$$U(x) = \begin{cases} 1 \quad if \ x \geq 0 \\ 0 \quad otherwise. \end{cases} \tag{3.3}$$

The set of constraints assures that at least 1 ambulance covers each demand point $\rho_k$, this is, when $t_k(\rho_k, (x_j, y_j)) \leq \tau_k$, the function $U$ retrieves a value equals to 1, enough to satisfy the $k$-th inequality, if this does not occur, then this constraint will be active.
The function $f(x_j, y_j)$ is equal to the sum of distances from the ambulance $a_j$ located at $(x_j, y_j)$ if this ambulance covers at least 1 demand point, else it is set to $f(x_j, y_j) = 10,000$ which is a penalization value. Thus, this function *pushes* the location of all the ambulances inside the feasible region defined by the set of demand points and its respective tolerance time thresholds values $\tau_k$.

Note that problem (3.1) is an optimization problem consisting of $2m$ continuous variables.

## 3.2 Implementations

For the implementation of problem (3.1) for the Tijuana Red Cross ambulance fleet we have used the following realizations.

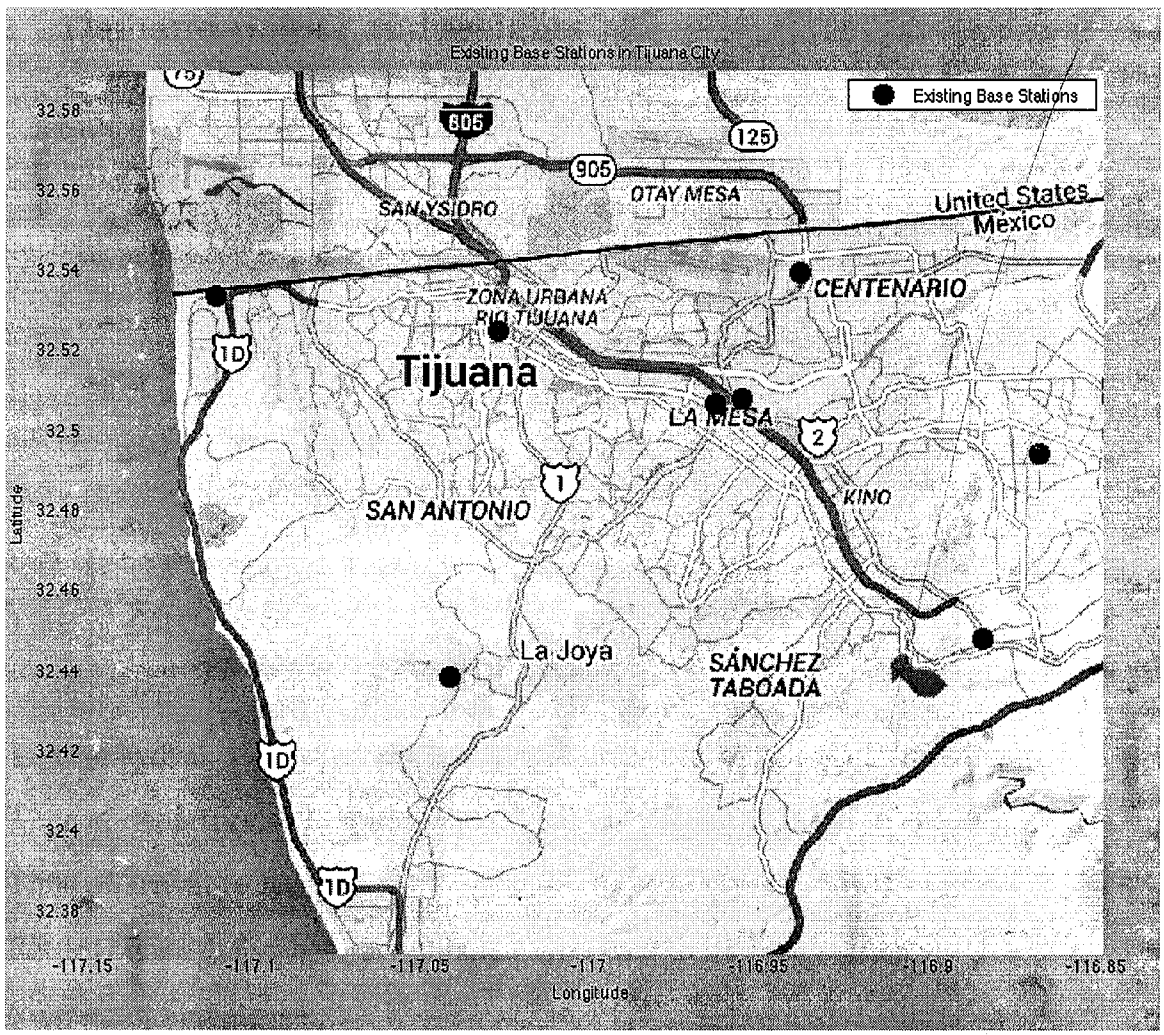


Figure 3.1: The domain $Q$ for the location of the ambulances. The circles show the eight actual base stations of the Red Cross Tijuana fleet.

### 3.2.1 Domain

The possible location for every base point of an ambulance is in the city of Tijuana, Mexico. To be more precise, we restricted the search to $x \in [-117.15, -116.8]$ (longitude) and $y \in [32.4, 32.6]$ (latitude), i.e., we have set the domain as

$$Q = [-117.15, -116.8] \times [32.4, 32.6] \subset \mathbb{R}^2 \tag{3.4}$$

which is the box in the plane that tightly covers Tijuana.

The Tijuana Red Cross Unit has currently eight base stations (though three of them are equipped with two ambulances) distributed all over the city, Figure 3.1 shows the domain $Q$ together with the eight base stations of the Tijuana Red Cross Unit.

### 3.2.2 Demand points and weights

One crucial aspect is the proper choice of the demand points and the weights since they determine the *optimal* location of the fleet. Thus, a random selection of these values would yield misleading results. Instead, we have selected the demand points based on the actual demands that took place and which were recorded from the Tijuana Red Cross Unit in the period from 01/01/2014 to 08/31/2014. The data base contains a total of more than 23,000 of EMS requests, the table in which the requests are store contains the following fields:

- Base station assignment: the name and the number of the base where the emergency call was received.
- Date (day, month, year).
- Day of the week.
- Time of call .
- Time of departure: time when the ambulance is dispatched.
- Time of arrival: time when the ambulance arrives at the place of the emergency.
- Time of departure to hospital: time when the patient is taken to the hospital.
- Time of arrival to hospital.
- Return time: time when the ambulance returns to its base station.
- Number of ambulance.
- State.
- Administrative district.
- Street: name of the street where the emergency occurs.
- Adjoining street_1: adjacent to the street where the emergency occurred.
- Adjoining street_2: adjacent to the street where the emergency occurred.
- Neighborhood.
- Patient address.
- Priority: In time sensitive increasing order: green (minor bone fracture, sexual assault), yellow (fever), red (chest pain, breathing problems), black (heart attack, choking).
- Longitude and latitude

Each demand point that we chose for the optimization model stands for a particular district of Tijuana (to be more precise, its center point), and every weight value was calculated directly proportional to:

- Density Criteria: the total number of EMS requests from this district within the given time period, i. e., the weight value for the $k$-th district is calculated by

$$\omega_k = \frac{N_T - N_k}{N_T(n-1)},$$

where $N_k$ is the number of EMS registers inside the area of the $k-$th district, $N_T$ is the total number of EMS registers in the database and $n$ is the total number of districts.

- Priority Criteria: the mean priority of the requests from the district (emergencies which requires immediate attendance such as heart attacks are associated to the highest priority value 4 (black color), downwards to the emergencies with a wider time tolerance threshold, therefore, associated to the lowest value 1 (green color)):

$$\omega_k = \frac{dp_{total} - \overline{dpr_k}}{dp_{total}(n-1)},$$

where $\overline{dpr}_k$ is the average priority EMS value of the $k$-th district and

$$dp_{total} = \sum_{i=1}^{n} \overline{dpr_i}$$

To allocate the contribution of every entry in the data base with its respective demand point weight value we followed two approaches:

- Longitude and latitude coordinates available: by looking for the closest demand point to the point in the map where the request was registered, to determine the closest point the estimated travel time was used instead of the geometric distance.

  Note: Even though every ambulance is provided with a GPS device to assert the position of the emergency at the time the ambulance arrives, on very few cases the ambulance operators recall to store this information, since their highest priority is to attend the patient emergency. In less than the 10% of the requests this information was available, this is why the information from other fields was used to determine the position of the emergency.

- Emergency address available: when latitude and longitude coordinates were not available but the emergency address was (street, neighborhood, adjoining street 1, adjoining street 2), then we used the geocoding service from GOOGLE MAPS[1] to determine the coordinates of the request, and finally look for the nearest demand point.

  The precision of the service relies on the amount of the address information available, this is, in the cases where only the street and neighborhood information but no the adjoining streets names are included, the approximation for the point where the emergency occurred is worse. All the requests in which no address information or geographical coordinates were available were dismissed.

In Figures 3.2 and 3.3 appear the demand points which represents the districts of Tijuana. The symbols representing the districts are associated to its weight value.

Finally, as time threshold we have set 10 minutes for each demand which is an acceptable value for most demands.

### 3.2.3 Expected travel time

To evaluate the objective, it remains to determine the expected travel time $t_k$ between two locations. For this, we have used the estimations provided by OpenStreetMap[2] which are sufficiently accurate for the purpose of our study (note that the exact travel time depends on numerous factors which can hardly be known a priori).

In particular we have used the Table Service from the Open Source Routing Machine Project (OSRM-Project) Server API[3], that receives the coordinates of the points in the domain $Q$ and returns an array including the estimated travel time between such points.

We handle the Problem (3.1) as a discrete problem due to the restrictions of OpenStreetMap[4]. We have first constructed a discretization of the area under consideration. That is, we have determined a grid of coordinates within the boundaries of Tijuana and have stored the expected travel time from one coordinate to each other one in a lookup table. Every time that a time distance $t_k$ is required during the algorithm execution, this table is consulted.

In our computations we have used different grids to discretize $Q$ and solve the problem, obtaining different results, the largest discretization table is a $31 \times 31$ grid, where $Q$ represents an area of 472.5 km$^2$, and every point in the grid stands for 0.49 km$^2$.

[1] `https://developers.google.com/maps/documentation/geocoding/intro`

[2] `https://www.openstreetmap.org`

[3] `https://github.com/Project-OSRM/osrm-backend/wiki/Server-api`

[4] the maximum number of distances between points allowed to retrieve per query is one hundred, and the time it takes to retrieve such information depends of the quality of the internet connection and the traffic into the OpenStreeMap server

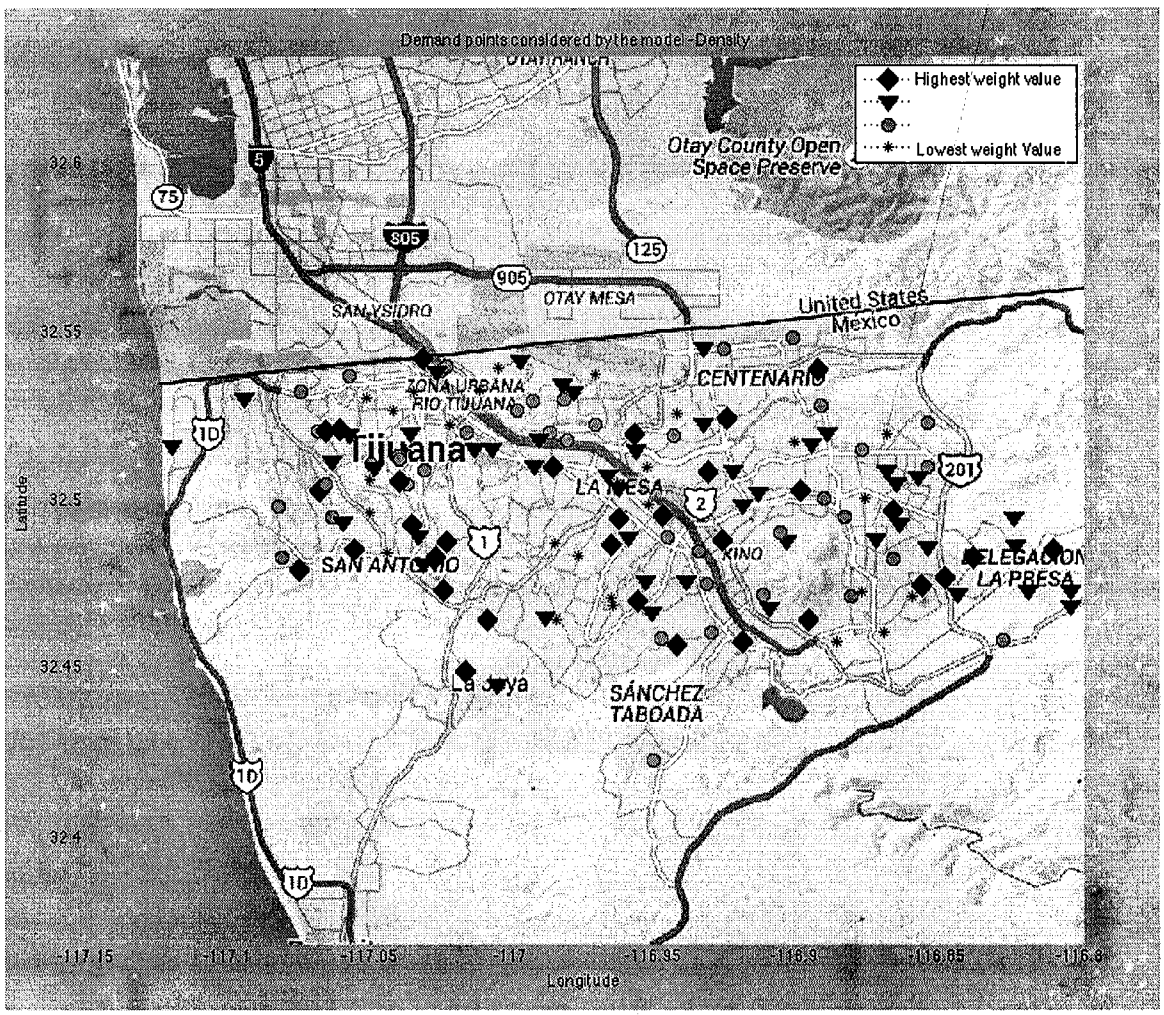


Figure 3.2: Demand points classified by the average number of EMS requests

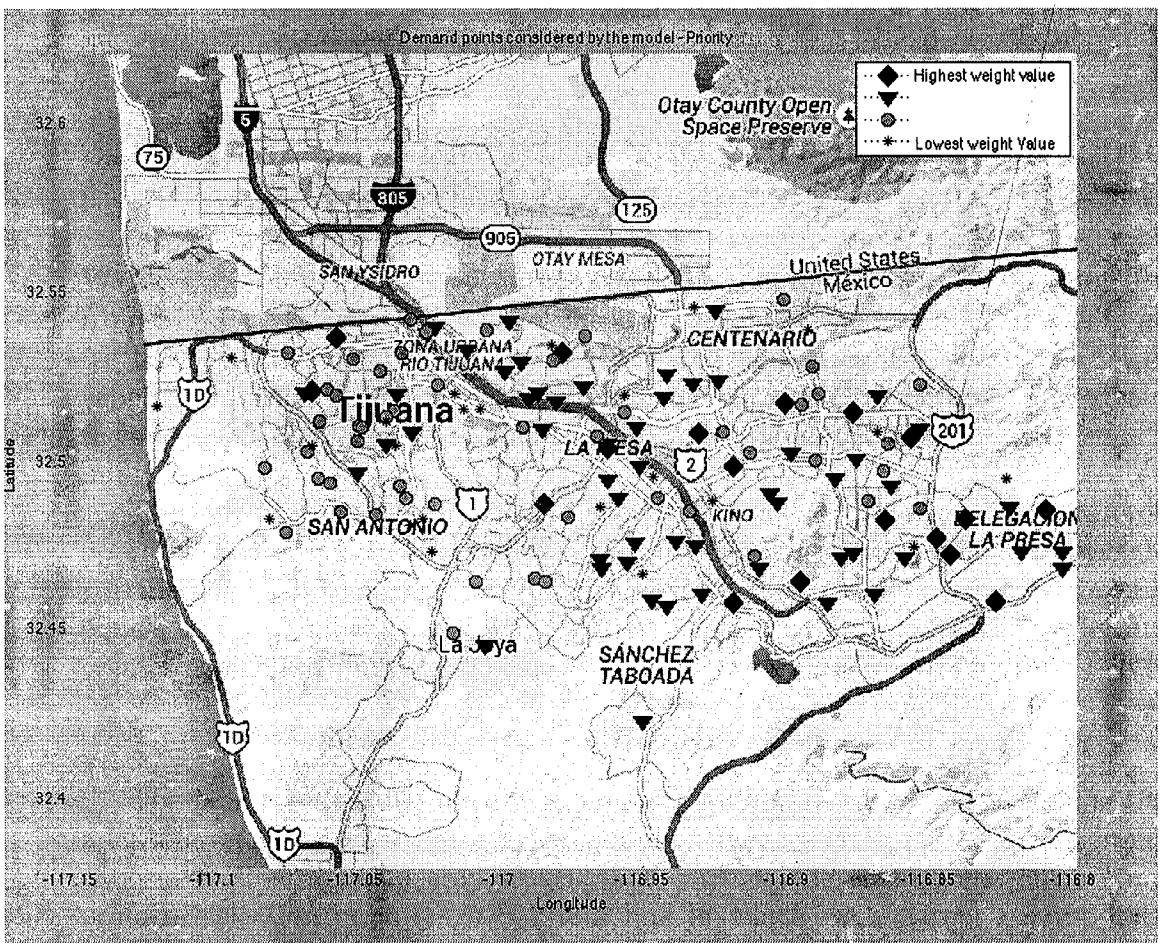


Figure 3.3: Demand points classified by the mean priority of EMS requests

The estimated travel time look up table was build, as mentioned before, looking for the time distance between all the points in the grid, for example, in the case of the $31 \times 31$ grid discretization the size of the look up table is

$$\frac{31 \times 31 \times 31 \times 31}{2},$$

which is the same as saying the the size $n \times n$ of the discretization of $Q$ grows quadratically, the time it takes to retrieve the time estimations from OpenStreetMap grows quadratically as well, we calculated that the time it took to fill the largest discretization table was of almost 96 hours.

## 3.3 Chosen Algorithm and Setting for the Continuous Location Problem

We have chosen to use the genetic algorithm `GA` from the Global Optimization Toolbox from MATLAB[5]. Since this is an initial study about the feasibility of the approach, we have omitted comparisons to other search heuristics, but leave this important aspect for future research. Comparisons to 'classical' mathematical programming techniques do not seem to be adequate since the ambulance location problem is highly multi-modal.

The settings used to run `GA` are shown in Table 4.1, the intermediate crossover operator creates children by taking a weighted average of the parents, the weights are specified by a single parameter, *Ratio*, which can be a scalar or a row vector of length equals to the number of variables. A default vector of all 1's is used. The function creates the child from $parent1$ and $parent2$ using the following formula

$$child = parent1 + rand * Ratio * (parent2 - parent1).$$

The adaptive feasible mutation operator randomly generates directions that are adaptive with respect to the last successful or unsuccessful generation. The mutation chooses a direction and step length that satisfies the constraints. The stochastic uniform selection operator lays out a line in which each parent corresponds to a section of the line of length proportional to its scaled value. The algorithm moves along the line in steps of equal size. At each step, the algorithm allocates a parent from the section it lands on. The first step is a uniform random number less than the step size.

The function tolerance stopping criteria causes the algorithm to terminate if the average relative change in the best fitness function value over a certain number of generations (50) is less than or equal to the function tolerance value ($1e-6$).

[5] `http://mathworks.com`

Table 3.1: Design parameters used by the algorithm GA of MATLAB.

| Design parameter | value/kind |
|---|---|
| Population size | 20 |
| Crossover operator | intermediate |
| Crossover rate | 0.8 |
| Elite count | 2 |
| Mutation operator | adapt feasible |
| Selection operator | stochastic uniform |
| Stopping criteria | function tolerance: |
| | average relative change over |
| | 50 generations $\leq 1e-6$ |

# Chapter 4

# A Multi-Objective Location Model for the Tijuana Red Cross Ambulance Fleet

By solving the optimization problem defined in Equation (3.1) (in page 18) the most relevant aspects of the ambulance location problem are addressed: the time restrictions which state the pertinence of the service within the time thresholds and the coverage of whole set of demand points. Of course, there are many more aspects to consider for this problem; their importance is, nevertheless, not as big as it is for the mentioned aspects. The aim of the multi-objective ambulance location problem is to address other design aspects and to provide a well pondered solution without forgetting to comply with the most important restrictions of the original problem (time and coverage).

An immediate example of these relegated aspects is the geographical coverage: with the solution of the single objective problem in Section 5.1 (in page 34) it is easy to see that there are areas in Tijuana city which are not covered by any ambulance, areas in which the historical amount of EMS services required is not enough to consider them relevant points for the model. Aware of this fact, the question for the designers and decision makers could be: Is there a way to deploy the ambulances in the city covering all the demand points at the set time all, or the most, of the geographical area is covered? Thinking in terms of *fairness*, this is the question we pursue to answer with the extension of the model, the geographical coverage model is presented in Section 4.3.

As mentioned in the former chapter, two set of weight values have been designed and used to solve the single objective problem (the demand criteria set and the priority criteria set presented in Section 3.2.2), by proposing a multi-objective model the possibility of finding an optimized solution for both sets at the same time arises, along with the possibility of designing and including future sets of weight values which stand for criteria that the final user finds eventually relevant, we have named such model the multi-criteria model (Section 4.2).

## 4.1 The Multi-Objective Location Model

The multi-objective model proposed consists on two objectives: the continuous location model and the continuous coverage model; the corresponding optimization problem is expressed as follows

$$\min_{(x,y)\in\mathbb{R}^m\times\mathbb{R}^m} [f_{location}(x,y), f_{coverage}(x,y)] \tag{4.1}$$

subject to:

$$\sum_{j=1}^{m} U\Big(\tau_k - t_k\big(\rho_k,(x_j,y_j)\big)\Big) \geq 1 \qquad \forall k \in K,$$

$$C_{Demand} - \sum_{k=1}^{n} U\Big(\tau_k - t_k\big(\rho_k,(x_j,y_j)\big)\Big) \geq 0 \qquad \forall j \in A,$$

where the $f_{location}$ objective has been previously defined in Equation (3.1), and the $f_{coverage}$ objective is defined in Section 4.3 in Equation (4.6).

The former set of constraints guarantees that every demand point $k$ is covered at least by one ambulance, as in Equation (3.1).

The latter set of constraints is defined to discard solutions in which the maximum number $C_{Demand}$ of demand points that an ambulance $a_j$ is allowed to cover is exceeded, the sum

$$\sum_{k=1}^{n} U\Big(\tau_k - t_k\big(\rho_k,(x_j,y_j)\big)\Big),$$

retrieves the total number of demand points $k$ that the ambulance $a_j$ is covering, this number is limited by the constant $C_{Demand}$.

A small value for $C_{Demand}$ forces the genetic algorithm to find solutions in which the ambulances are better distributed all over the area, a big value for $C_{Demand}$ will favor solutions in which the ambulances might be concentrated at specific areas of the city, leaving others completely uncovered.

## 4.2 The $f_{location}$ Objective And The Multi-criteria Model

The $f_{location}$ function is defined as:

$$f_{location}(x,y) = \sum_{j=1}^{m} f_{weightedSum}(x_j,y_j) \tag{4.2}$$

where $f_{weightedSum}(x_j, y_j)$ is defined as:

$$f_{weightedSum}(x_j, y_j) = \begin{cases} \sum_{k \in K} \omega_k t_k\big(\rho_k, (x_j, y_j)\big) U\Big(\tau_k - t_k\big(\rho_k, (x_j, y_j)\big)\Big) \\ if \ \sum_{k=1}^{n} U\Big(\tau_k - t_k\big(\rho_k, (x_j, y_j)\big)\Big) > 0 \\ 10000 \qquad otherwise. \end{cases} \tag{4.3}$$

The information that describes the particular conditions of the location problem: the amount of EMS demand, the areas where the demand is higher, the type of emergencies occurring at different locations, etcetera, is contained and represented in the set of weights values $\omega_k$

As previously mentioned in Section 3.2, we have designed two sets of weight values according to different criteria: the density and the priority criteria, this implies that the solution to the Problem 3.1 will depend on the criteria selected for the setting of the problem.

The multi-criteria model aims to find the compromised solution of both criteria, i.e., the multi-criteria model is a multi-objective model in which every objective is mathematically defined the same way, but its corresponding set of weight values will represent different criteria, and therefore, its optimized solution will be different.

This design feature leads to the possibility for the inclusion of more objectives, in which the new objectives will be defined the same way $f_{location}$ objective is defined, but containing a different set of weights standing for different and conflictive aspects of the problem, the multi-criteria model is expressed as:

$$f_{extendedMO} = [f^{\omega_1}_{location}(x, y), f^{\omega_2}_{location}(x, y), f^{\omega_3}_{location}(x, y), ..., f^{\omega_z}_{location}(x, y)] \tag{4.4}$$

Hereby, where every objective $f^{\omega_i}_{location}$ stands for a different design criteria, and there are $z$ different sets of weight values. This problem is subject to the same restrictions that the Problem 4.1 is subject to, the multi-objective optimization problem is defined as:

$$\min_{(x,y) \in \mathbb{R}^m \times \mathbb{R}^m} f_{extendedMO} = [f^{\omega_1}_{location}(x, y), f^{\omega_2}_{location}(x, y), ..., f^{\omega_z}_{location}(x, y)] \tag{4.5}$$

subject to:

$$\sum_{j=1}^{m} U\Big(\tau_k - t_k\big(\rho_k, (x_j, y_j)\big)\Big) \geq 1 \qquad \forall k \in K,$$

$$C_{Demand} - \sum_{k=1}^{n} U\Big(\tau_k - t_k\big(\rho_k, (x_j, y_j)\big)\Big) \geq 0 \qquad \forall j \in A.$$

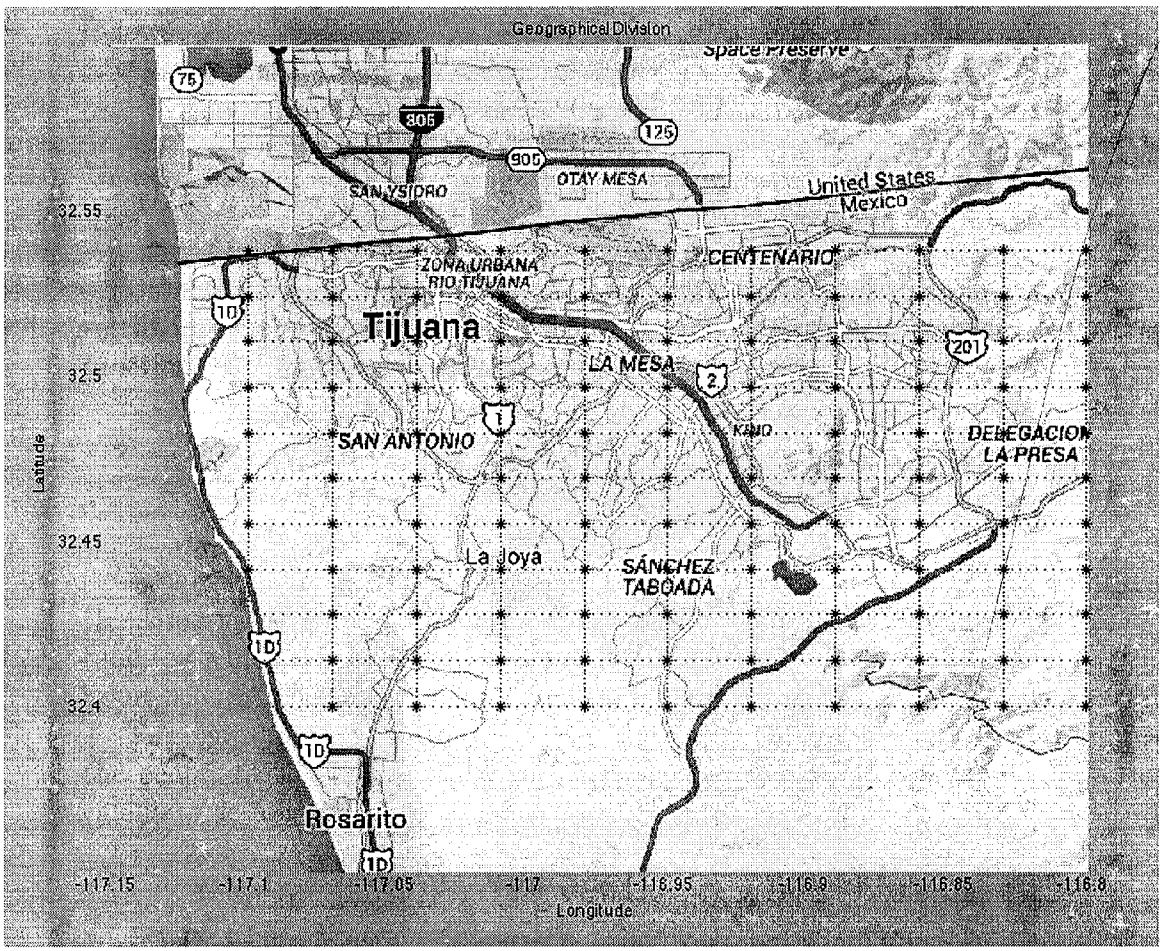


Figure 4.1: Geographical Division of Tijuana

## 4.3 Continuous Coverage Model

While trying to attend all the demand points considered in the Continuous Location Model with a given set of ambulances, some of the geographical areas in the city were not being covered by any ambulance, this occurs due to the fact that the emergency medical services demand is concentrated at very specific areas of the city; in order to find a *fairer* solution which addresses the demand from the first model at the same time that it covers the most of the geographical area, the Continuous Coverage Model is proposed.

To model the coverage of the geographical area, a discretization of the region is used, a grid $G$ of $11 \times 11$ points $\rho_g$ in which every point stands for an area of 3.9 km$^2$, by this, the grid $G$ contains all the possible regions in which a EMS service may be required, this division is shown in Figure 4.1.

The coverage maximization problem of the geographical area is then modeled as

follows:

$$\max_{(x,y)\in\mathbb{R}^m\times\mathbb{R}^m} f_{coverage}(x,y) = \frac{\sum_{g=1}^{h} \overline{f^g_{iscovered}(x,y)}}{h}, \tag{4.6}$$

where $h$ is the number of points $\rho_g$ in the grid $G$,

$$f_{coverage} : \mathbb{R}^m \times \mathbb{R}^m \mapsto [0,1],$$

retrieving the value 1 when the whole geometrical area is considered covered, the function $f^g_{iscovered}(x,y)$ is defined as follows:

$$f^g_{iscovered}(x,y) = \sum_{j=1}^{m} \left(1 + \alpha_G t_g\big(\rho_g,(x_j,y_j)\big)\right)^{-1} U\Big(\tau_g - t_g\big(\rho_g,(x_j,y_j)\big)\Big).$$

$\tau_g$ is the time tolerance threshold assigned to each point in $G$ ($\tau_g = 10$ minutes, the same value is used for the Continuous Location objective parameters), $t_g$ is the function which retrieves the time that it takes to go from the ambulance $(x_j, y_j)$ to the point $\rho_g \in G$, the same time estimation is used for the Continuous Location Model.

Function $f^g_{iscovered}$ verifies whether the point $(x_j, y_j)$ lies within $\tau_g$ minutes from the center of the region $\rho_g$, if so, then the percentage of coverage of this region is calculate as follows:

$$\left(1 + \alpha_G t_g\big(\rho_g,(x_j,y_j)\big)\right)^{-1},$$

where $\alpha_G$ is a constant adjusted to guarantee that when the point $(x_j, y_j)$ is exactly $\tau_g$ minutes from the center of the region $\rho_g$ then the coverage value is equal to 0.5, and when the location of $(x_j, y_j) = \rho_g$ the coverage value is equal to 1 (the maximum value).

If the point $(x_j, y_j)$ does not lay within the tolerance time region $\tau_g$ then $U\Big(\tau_g - t_g\big(\rho_g,(x_j,y_j)\big)\Big) = 0$, therefore, the coverage value will be equal to 0.

The mean of all the contributions to the coverage of every region $g$ is calculated and retrieved as $\overline{f^g_{iscovered}(x,y)}$. Finally $f_{coverage}(x,y)$ is equal to the sum of coverage of every region $g \in G$, divided by the total amount of regions $h$.

### 4.3.1 Chosen Algorithm for the multi-objective location model: NSGA-II

The non-dominated sorting based multi-objective evolutionary algorithm (called the Non-dominated Sorting GA-II or NSGA-II) developed by Deb et al in [6], which alleviates criticized features from other multi-objective evolutionary algorithms which use non-dominated sorting and sharing such as: $O(mN^3)$ computational complexity (where $m$ is the number of objectives and $N$ is the population size); non-elitism approach; and the need for specifying a sharing parameter.

Table 4.1: Design parameters used by the algorithm NSGA-II

| Design parameter | value/kind |
|---|---|
| Population size | 75 |
| Crossover operator | intermediate |
| Crossover rate | 2/numVar |
| Mutation operator | Gaussian |
| Mutation rate | 2/numVar |
| Selection operator | binary tournament |
| Stopping criteria | max generation |

In NSGA-II, the population is initialized as usual. Once the population is initialized the population is sorted based on non-domination into each front. The first front being completely non-dominant set in the current population and the second front being dominated by the individuals in the first front only and the front goes so on. Each individual in the each front are assigned rank (fitness) values or based on front in which they belong to. Individuals in first front are given a fitness value of 1 and individuals in second are assigned fitness value as 2 and so on.

In addition to fitness value a new parameter called crowding distance is calculated for each individual. The crowding distance is a measure of how close an individual is to its neighbors. Large average crowding distance will result in better diversity in the population. Parents are selected from the population by using binary tournament selection based on the rank and crowding distance. An individual is selected in the rank is lesser than the other or if crowding distance is greater than the other 1.

The selected population generates offsprings from crossover and mutation operators. The population with the current population and current offsprings is sorted again based on non-domination and only the best N individuals are selected, where N is the population size. The selection is based on rank and on the crowding distance of the last front.

# Chapter 5

# Experiments and Results

In this chapter we present the experiments we performed first, in Section 5.1, for the Continuous Location Model presented in Chapter 2, comparing our results against the current deployment of the ambulance stations in Tijuana City, in order to show that our approach represents an improvement on the way the ambulances are located.

In Section 5.2, we discuss the experiments performed for the Multi-objective Continuous Location Model, presenting the solution to the problem in different scenarios, which is: by changing the number of points in the discretization of the domain $Q$ and by solving the problem for different values of the constant $C_{demand}$ included in Equation (4.1). A discussion of the units of the Continuous Location Model is also included in Section 5.2.2, this is, what does it imply to reduce the function evaluation from one solution to another along the Pareto front, and how does it affects the quality of the EMS services provided by the Tijuana Red Cross Unit.

Finally, in Section 5.3 the results obtained for the Multi-criteria model are presented, different results were obtained by varying the value of the constant $C_{Demand}$ and by adding a relaxation factor into the coverage constraints.

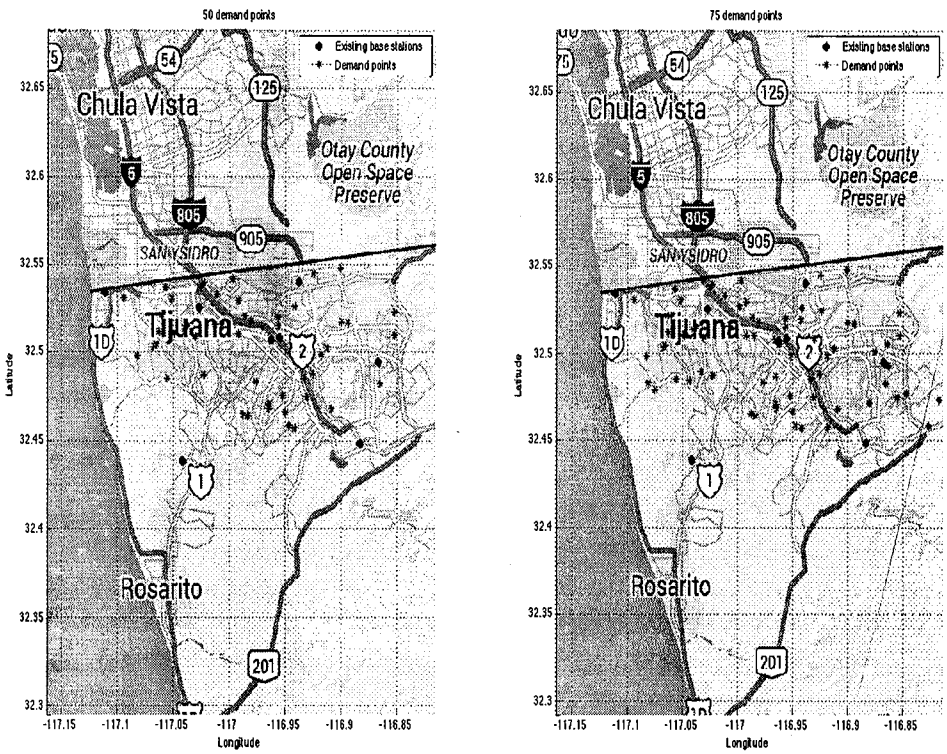


Figure 5.1: Domain $Q$ containing $n = 50, 75$ demand points and the location of the existing base stations.

## 5.1 Continuous Location Model

In our study, we have used $m = 8$ (where $m$ is the number of ambulances available) since the Red Cross Tijuana has currently eight base stations (though three of them are equipped with two ambulances), in order to obtain a fair comparison against the solution of the Problem 3.1 obtained with our computations. Further, we have considered five different situations, in which the number of demand points $n$ increases on every case, i.e., $n = 50$, 75, 100, 125 and 150 demand points. Thus, the instances of Problem 3.1 are of dimensions $2 \times m = 16$, in all cases.

### 5.1.1 Experiments

Figures 5.1, 5.2 and 5.3 shows the five scenarios for which we have compare our computations and results against the current location of the ambulance bases.

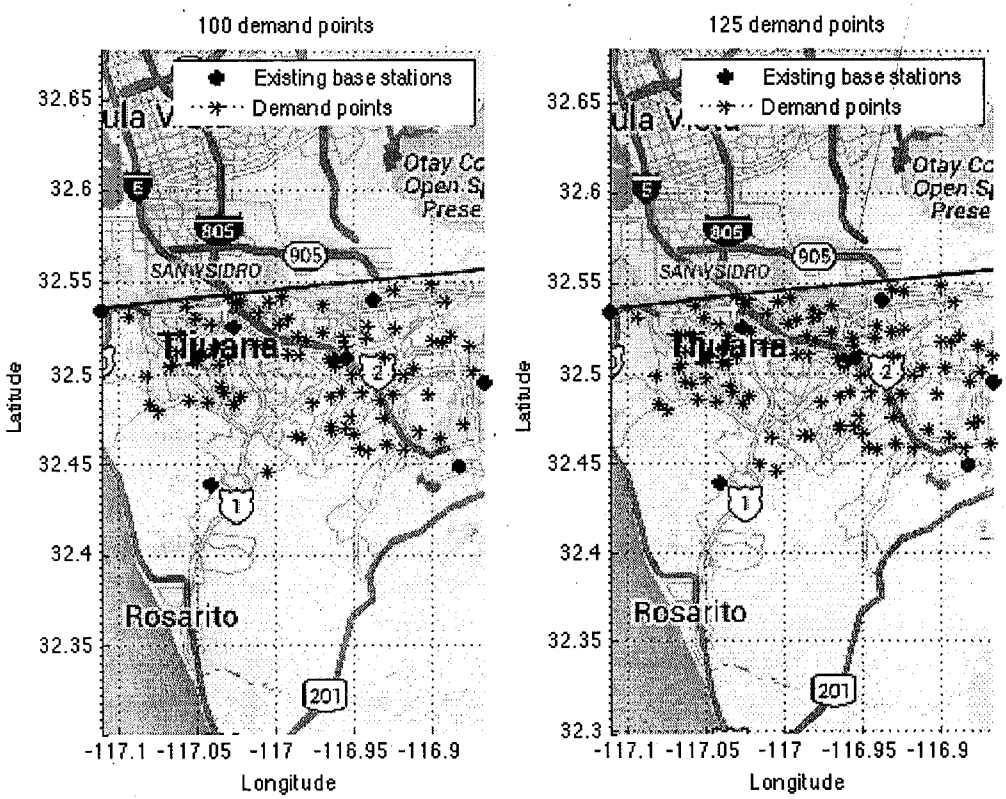


Figure 5.2: Domain $Q$ containing $n = 100, 125$ demand points and the location of the existing base stations.

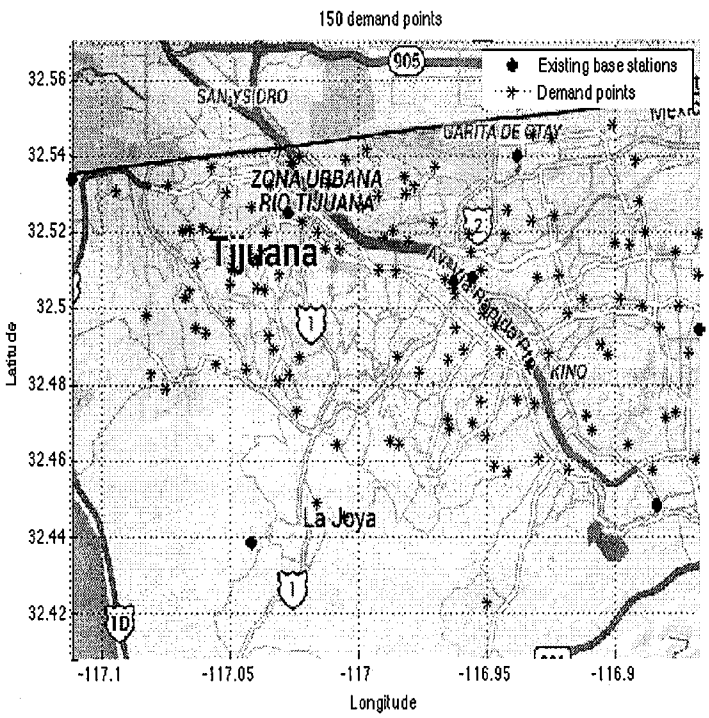


Figure 5.3: Domain $Q$ containing $n = 150$ demand points and the location of the existing base stations.

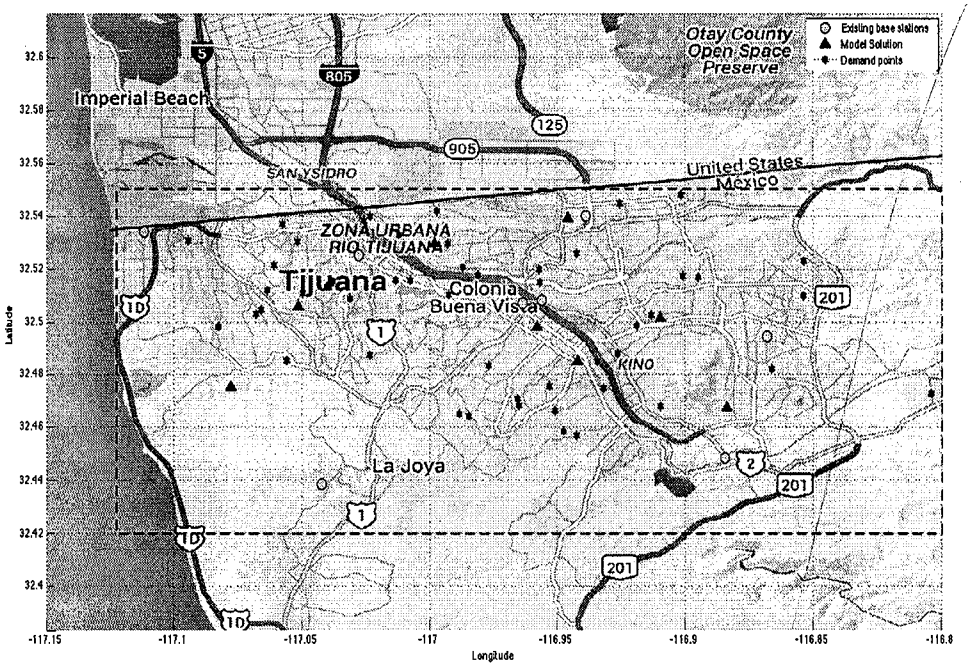


Figure 5.4: Solution for 50 demand points.

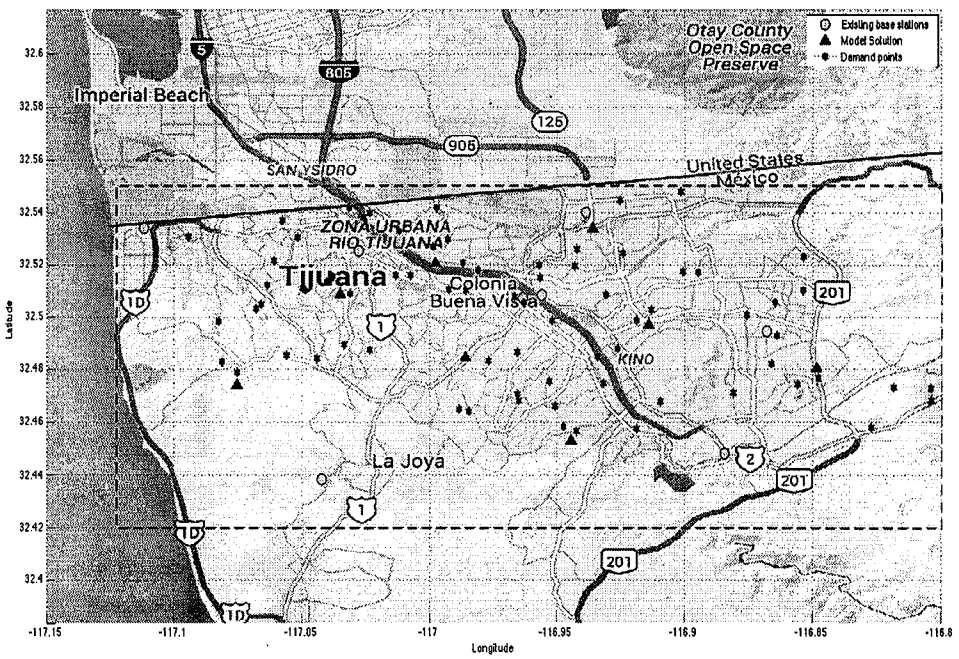


Figure 5.5: Solution for 75 demand points.

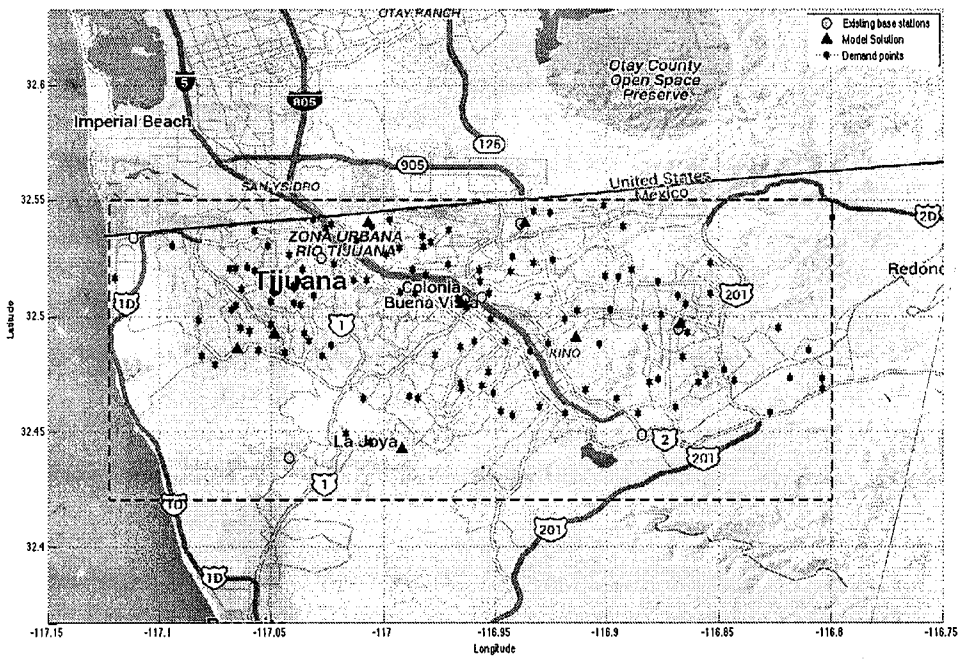


Figure 5.6: Solution for 100 demand points.

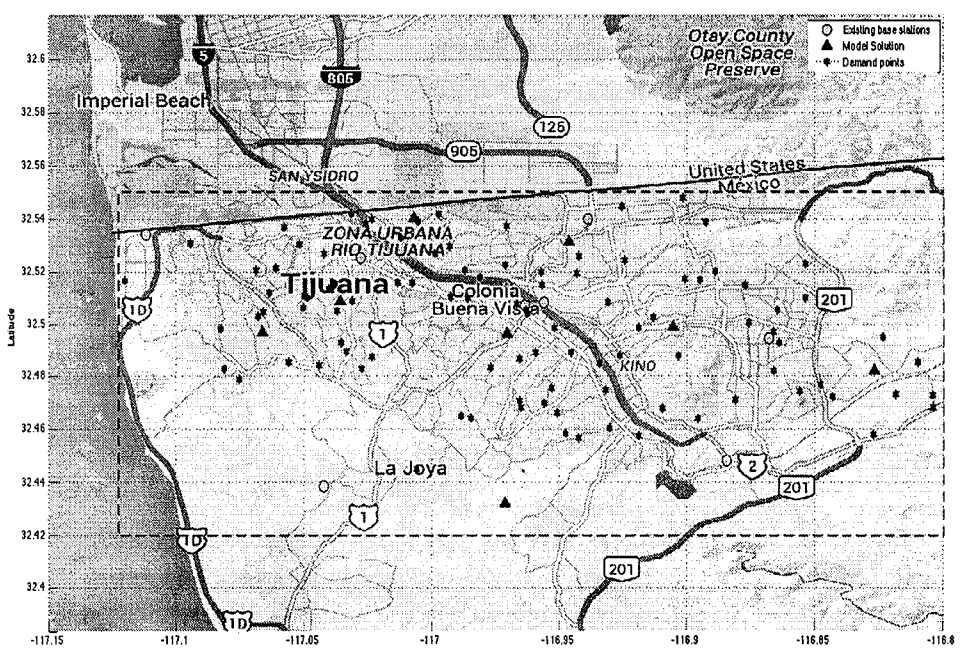


Figure 5.7: Solution for 125 demand points.

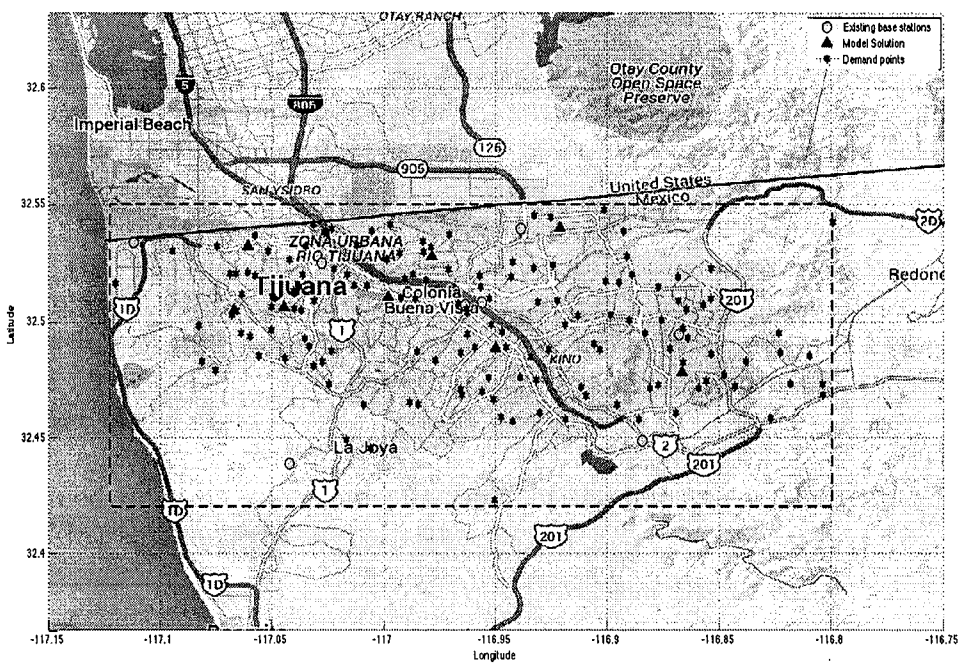


Figure 5.8: Solution for 150 demand points.

### 5.1.2 Interpretation of the Results

Table 5.1 shows the obtained function values and the fractions of the demand covered from the model solution and the existing base stations. All results are averaged over 20 independent runs. Since a comparison of the function value of the objective in Problem (3.1) is hardly fair due to the penalization term, we consider for sake of a better comparison in addition *f_val_alternative*. This function differs from the objective in Problem (3.1) on the fact that the penalization term is dismissed. Instead, all weighted distances among the base stations and the demand points are summed up, *f_val_alternative* is expressed as follows:

$$f\_val\_alternative = \sum_{j=1}^{m}\sum_{k=1}^{n} \omega_k t_k(\rho_k, (x_j, y_j)). \tag{5.1}$$

In both cases, the objective values are better for the new base stations. The difference becomes more apparent when considering the fraction of the demand which can be covered by the fleet: the new fleet is able to cover around 90% of the demands while only around 50% of the demands can be attended by the actual fleet.

When the number of demand points increases then the fraction covered decreases at the same time that the functions evaluation grows, this is because, obviously, the number of contributions to the weighted sum grows and it becomes more difficult for the genetic algorithm to find a solution in which the whole demand set is covered. Nevertheless, for all the cases, the solution obtained is better evaluated than the current deployment of the fleet.

Table 5.1: Obtained function values and fractions of the demand covered from the model solution (MS) and the existing base stations (EB).

| No. demand points | 50 | 75 | 100 | 125 | 150 |
|---|---|---|---|---|---|
| f_val MS | 61 | 214 | 216 | 292 | 261 |
| f_val EB ($\times 10^4$) | 2 | 2 | 2 | 2 | 2 |
| f_val alternative MS | 3400 | 4500 | 5400 | 6000 | 6900 |
| f_val alternative EB | 4000 | 4700 | 5500 | 6400 | 7500 |
| Fraction demand covered MS | 0.92 | 0.90 | 0.90 | 0.85 | 0.85 |
| Fraction demand covered EB | 0.52 | 0.46 | 0.47 | 0.4400 | 0.45 |

Table 5.2 shows the performance of genetic algorithm on the five test instances and Figure 5.9 shows the respective convergence behavior. In all cases the algorithm stopped when the average change in the penalty fitness value was less than the given threshold value ($1e-6$) but the constraints were not all satisfied, this is, some of the demand points in the problem remained uncovered. As it appears in Figure 5.9 the fraction of demand points covered grows on every generation up to, on average, the 90%, after which, the genetic algorithm stopped.

Table 5.2: Performance of the genetic algorithm

| No. demand points | 50 | 75 | 100 | 125 | 150 |
|---|---|---|---|---|---|
| Avg. Time (min) | 5.76 | 8.64 | 11.51 | 14.49 | 16.90 |
| SD Time (min) | 0.0960 | 0.1249 | 0.0182 | 0.1810 | 0.2667 |
| No. generations | 51 | 51 | 51 | 51 | 51 |
| No. function eval | 5201 | 5201 | 5201 | 5201 | 5201 |
| Avg. Solution $t_k$ | 5.3745 | 6.4391 | 5.9346 | 5.9683 | 5.3152 |
| SD Solution $t_k$ | 2.2183 | 0.8695 | 1.5494 | 1.7669 | 1.7736 |

In addition to that, the average time distance from the ambulance fleet to its respectively assigned demand points is of 5.7996 minutes, which is 42% less time than the 10 minutes allowed.
Figures 5.4, 5.5, 5.6, 5.7 and 5.8 show the representative locations of the computed base stations for different numbers of demand points (in fact, no significant deviations in the locations of the ambulances could be observed). Here, the triangles represent the computed base stations, the circles the currently existing base stations, and the stars the demand points.

From Figure 5.4, we can observe that the new locations of the fleet follow the locations of the demand points, but these locations do not necessarily coincide with the location of a specific demand point, since each demand point is subject to cover more than one demand point at time.

Therefore, their resulting location is the weighted geometric center of the demand attended in time units, which is not necessarily the same as the weighted geometric center in length units, this difference comes from the fact that the length units do not consider the urban infrastructure of the city (urban traffic, one-way streets, speed limits, et cetera), instead, the distances in time units are estimated by considering these infrastructure features.

The trend to follow the locations of the demand points becomes less clear when the number of demand points grows in the following Figures, because these points start to pop up almost everywhere, however, on none of the figures appears an ambulance at the left inferior corner, neither at the right inferior one, from the feasible area, where there are no demand points located. And for the current existing base stations we note that some of them do not cover even one demand point and are practically isolated.

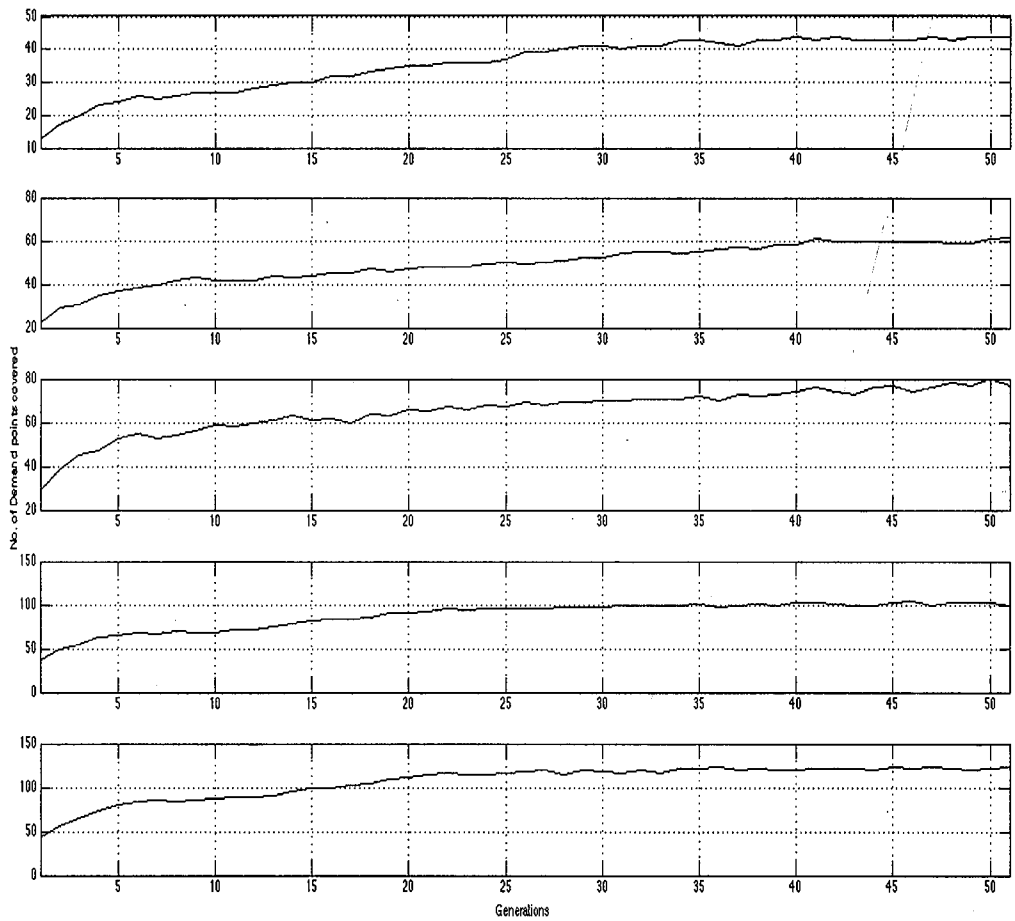


Figure 5.9: Convergence behavior of GA on the three test instances for $n = 50$, 75, 100, 125 and 150 demand points (from top to bottom).

## 5.2 Multi-Objective Location Model

Once we have solved the ambulance location problem, the next question was wether we could enrich the model to attend more features of this problem than the most important (time and demand constraints), such as the geographical coverage.

This section includes the results obtained after addressing the geographical coverage objective. In total this section has 24 experiments, where every experiment is the solution to the multi-objective location model (presented in Section 4.1) given a different setting for the problem.

In particular, we were interested on the changes observed on the solution for different discretization grids of the feasible area, the changes observed when relaxing the coverage constraints and the possible solutions for different values for the constant $C_{Demand}$ which sets an upper limit to the number of demand points each ambulance is allowed to cover.

### 5.2.1 Experiments

As mentioned in Section 3.2.3, we have constructed different discretization grids of the feasible region in order to solve the problem, the discretization grids are described as follows:

- $G = 11 \times 11$: in which every point stands for an area of 3.9 km$^2$ from the feasible region $Q$.
- $G = 21 \times 21$: in which every point stands for an area of 1.07 km$^2$ from the feasible region $Q$.
- $G = 31 \times 31$: in which every point stands for an area of 0.49 km$^2$ from the feasible region $Q$.

For every discretization grid we have also built a look up Table, in which all the travel times from every point to any other in the grid are stored.

The multi-objective optimization Problem (4.1) has been solved at different moments using these grids, in addition to that, we have included another setting to the problem: a relaxation factor into the coverage constraints. When the number of points that the ambulance fleet must cover is reduced, then the possibility to find better solutions for the continuous coverage model increases, as observed after the analysis of the results obtained from this model.

We have also divided the experiments of this section into two sets: the first set are the experiments which were obtained by setting $C_{Demand}$[1]$= 0.15 \times 150 = 22$, and the second set were obtained by setting $C_{Demand} = 0.30 \times 150 = 45$, the maximum number of demand points available is 150, the first set allows every ambulance to cover up to the 15% of the demand, while the second set no more than the 30%.

[1] $C_{Demand}$ is the constant which limits the number of demand points every ambulance is allowed to cover.

We first include the experiments from the first set ($C_{Demand} = 22$,) which give us a total of twelve differed test instances:

1. $G = 11 \times 11$, Relaxation factor $= 0.1$.
2. $G = 11 \times 11$, Relaxation factor $= 0.3$.
3. $G = 11 \times 11$, Relaxation factor $= 0.5$.
4. $G = 11 \times 11$, Relaxation factor $= 0.7$.
5. $G = 21 \times 21$, Relaxation factor $= 0.1$.
6. $G = 21 \times 21$, Relaxation factor $= 0.3$.
7. $G = 21 \times 21$, Relaxation factor $= 0.5$.
8. $G = 21 \times 21$, Relaxation factor $= 0.7$.
9. $G = 31 \times 31$, Relaxation factor $= 0.1$.
10. $G = 31 \times 31$, Relaxation factor $= 0.3$.
11. $G = 31 \times 31$, Relaxation factor $= 0.5$.
12. $G = 31 \times 31$, Relaxation factor $= 0.7$.

A relaxation factor $= 0.1$ means that the solution of the problem must only cover 90% of the set of demand points, this is, 135 instead of 150 demand points. The same logic applies for the subsequent relaxation factors.

Figure 5.10 shows, from top to bottom, the Pareto fronts obtained for the first and the second test instances ($G = 11 \times 11$, Relaxation factor $= 0.1$ and $G = 11 \times 11$, Relaxation factor $= 0.3$.), Figure 5.11 shows, also from top to bottom, the Pareto fronts obtained for the third and the fourth test instances ($G = 11 \times 11$, Relaxation factor $= 0.5$ and $G = 11 \times 11$, Relaxation factor $= 0.7$.).

The Pareto fronts obtained for the test instances from the fifth to the eighth appear at the Figure 5.12 and the Figure 5.13 (from top to bottom). And the Pareto fronts obtained for the test instances from the ninth to the twelfth appear at the Figure 5.14 and the Figure 5.15 (again, from top to bottom).

In every Pareto front, the best solution for objective 1 (Continuous Location Objective over the x-axis) is marked with a green diamond, the best solution for the objective 2 (Continuous Coverage Objective over the y-axis) is marked with a blue star, and the knee point is marked with a purple inverted triangle.

In addition to the Pareto fronts, for six test instances we have included in Appendix A.1 the following graphs (in page 83):

A graph with the locations of the ambulance fleet according to the best solution of the Continuous Location Objective.
A graph with the locations of the ambulance fleet according to the best solution of the Continuous Coverage Objective.
A graph with the locations of the ambulance fleet according to the knee point.
A graph with the locations of all the previous solutions.

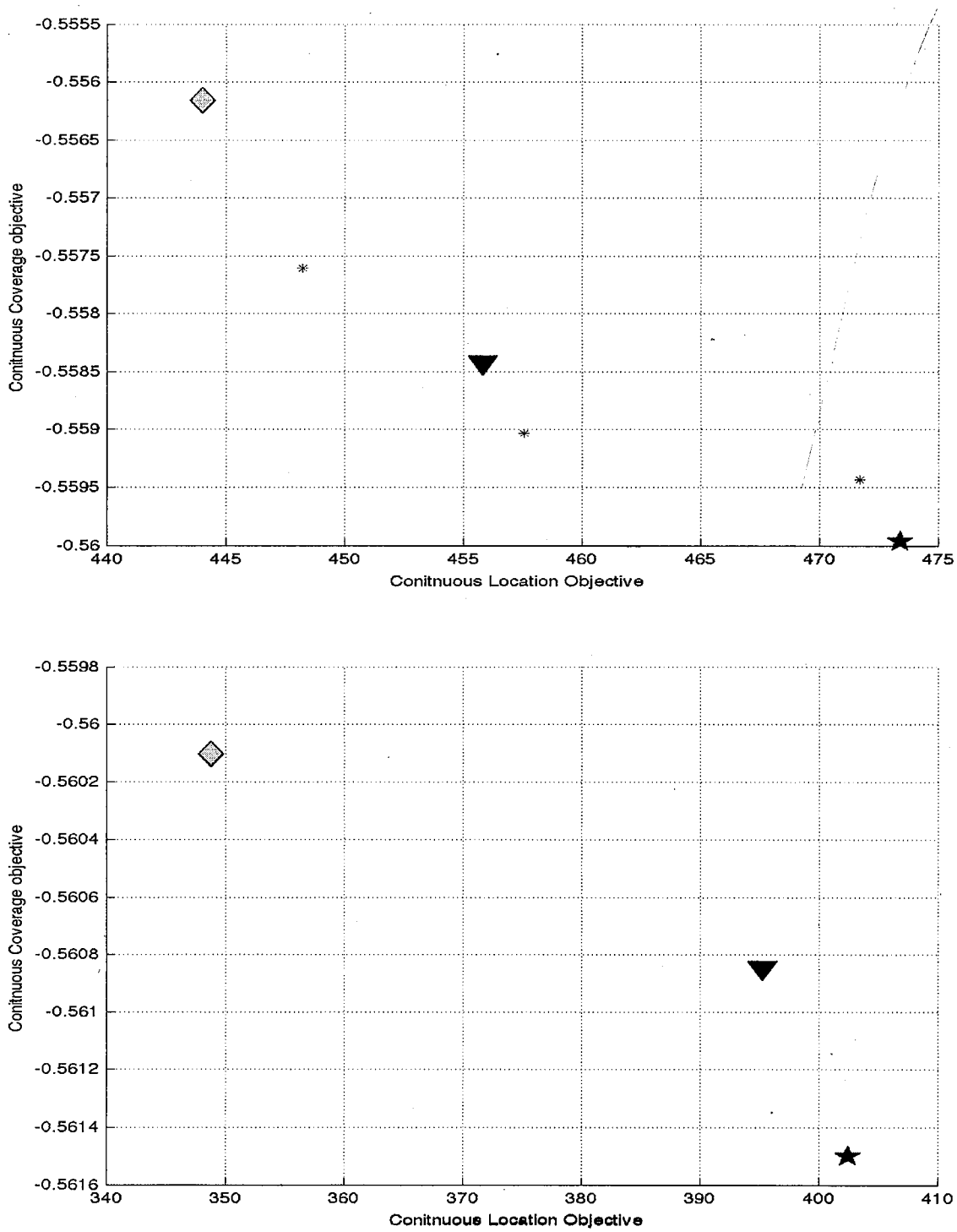


Figure 5.10: Pareto front with grid $G = 11 \times 11$, for relaxation values = 15 and 45 (from top to bottom), Continuous Location Objective (x-axis) vs Continuous Coverage Objective (y-axis).

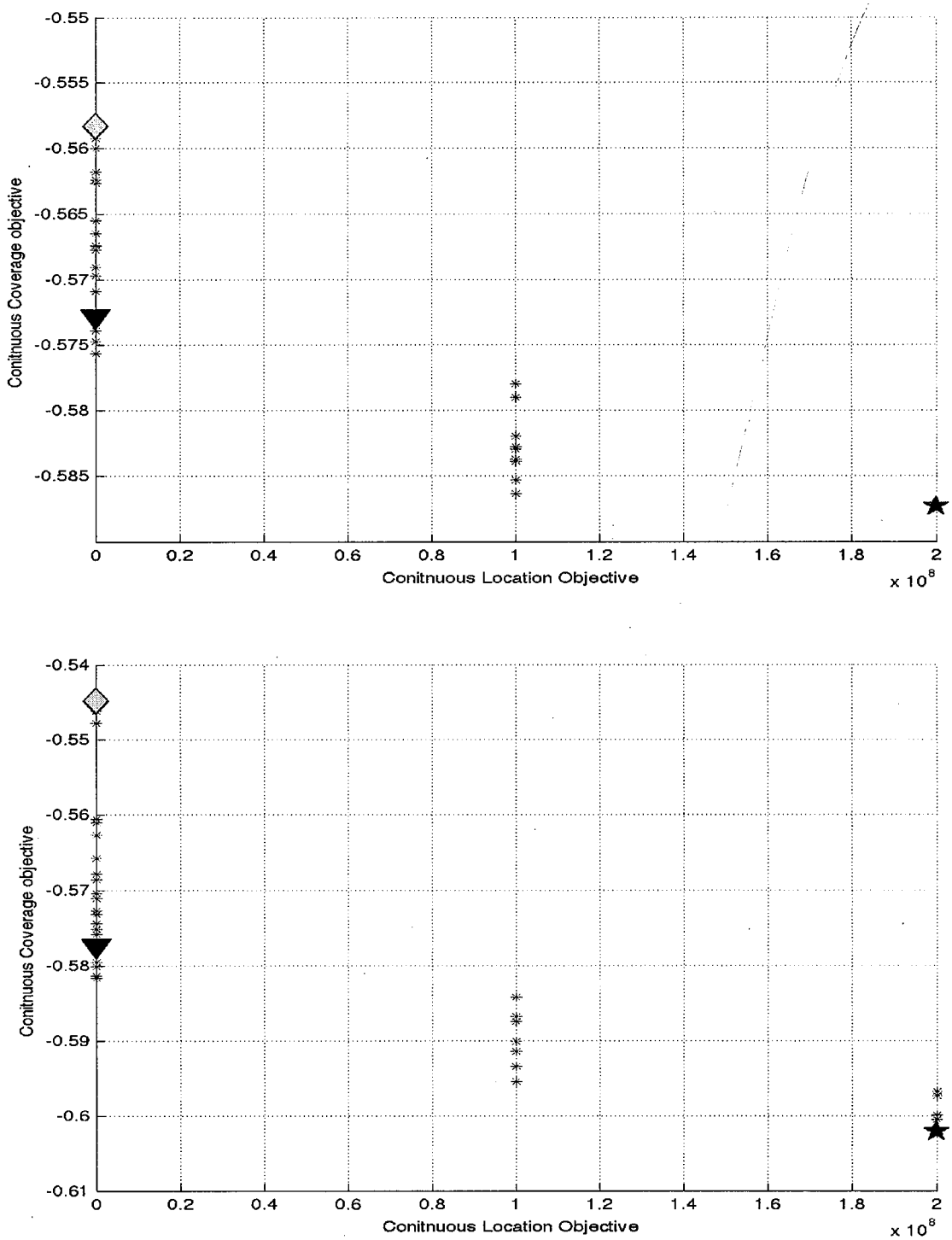


Figure 5.11: Pareto front with grid $G = 11 \times 11$, for relaxation values = 75 and 105 (from top to bottom), Continuous Location Objective (x-axis) vs Continuous Coverage Objective (y-axis).

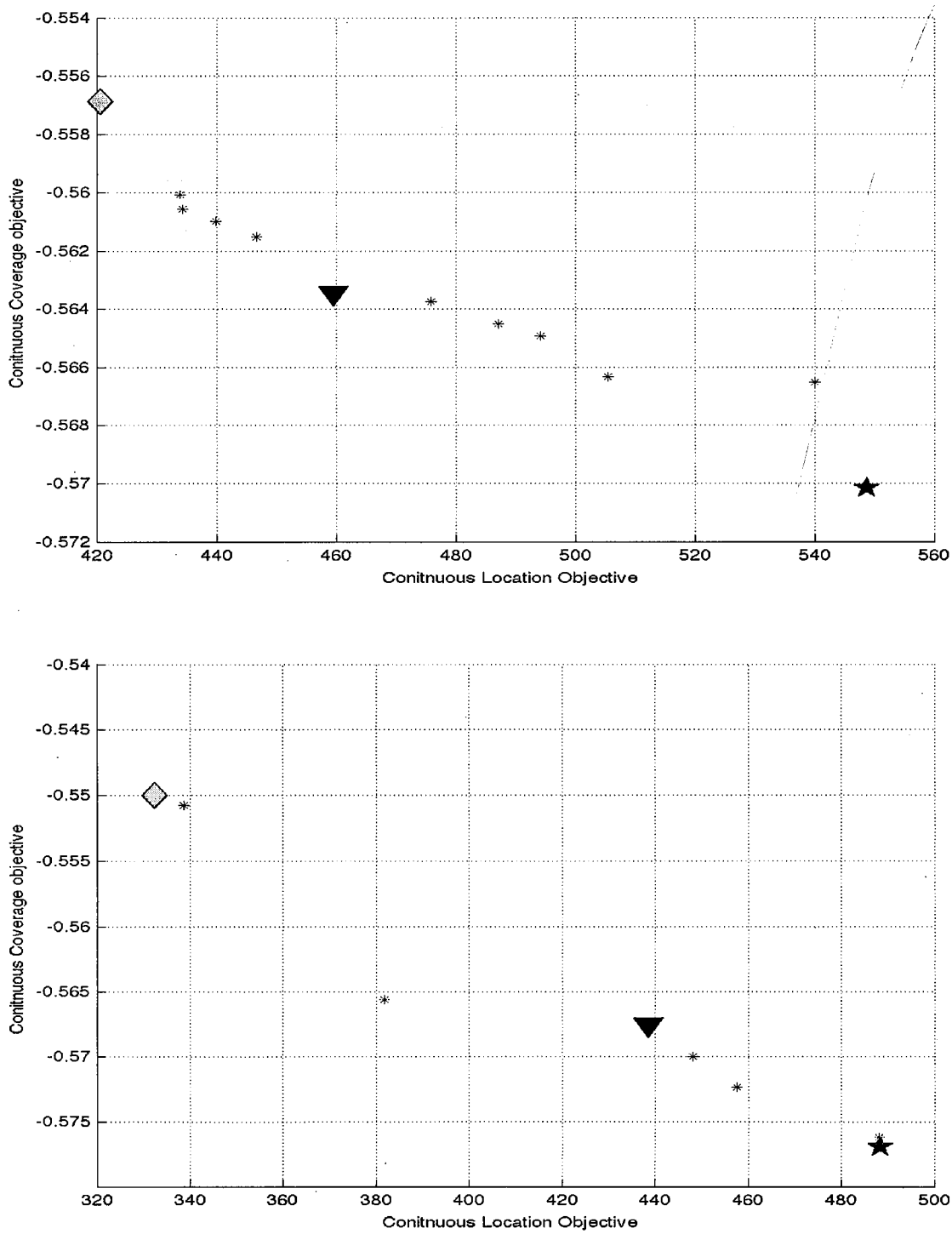


Figure 5.12: Pareto front with grid $G = 21 \times 21$, for relaxation values = 0.1 and 0.3 (from top to bottom), Continuous Location Objective (x-axis) vs Continuous Coverage Objective (y-axis).

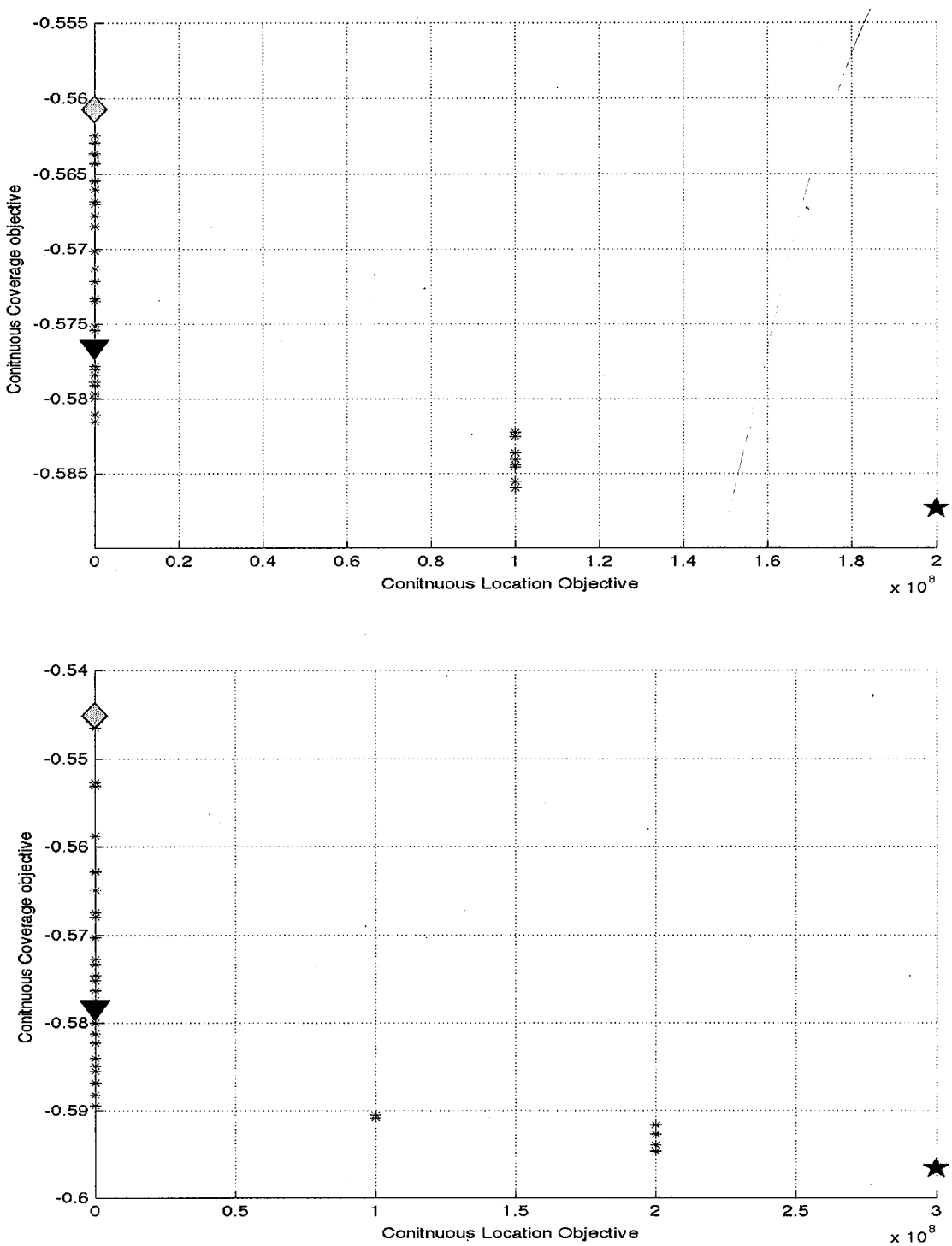


Figure 5.13: Pareto front with grid $G = 21 \times 21$, for relaxation values = 0.5 and 0.7 (from top to bottom), Continuous Location Objective (x-axis) vs Continuous Coverage Objective (y-axis).

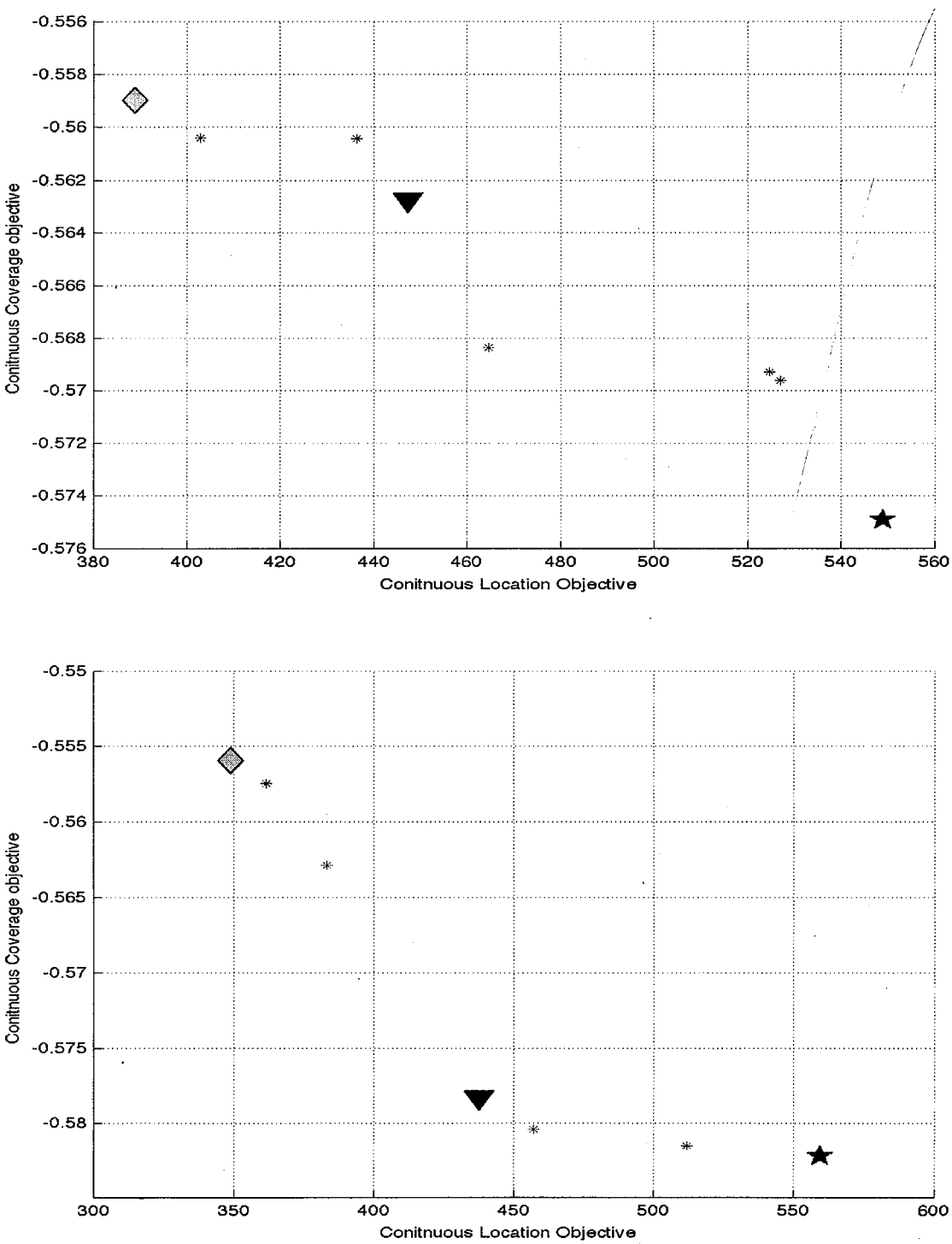


Figure 5.14: Pareto front with grid $G = 31 \times 31$, for relaxation values = 0.1 and 0.3 (from top to bottom), Continuous Location Objective (x-axis) vs Continuous Coverage Objective (y-axis).

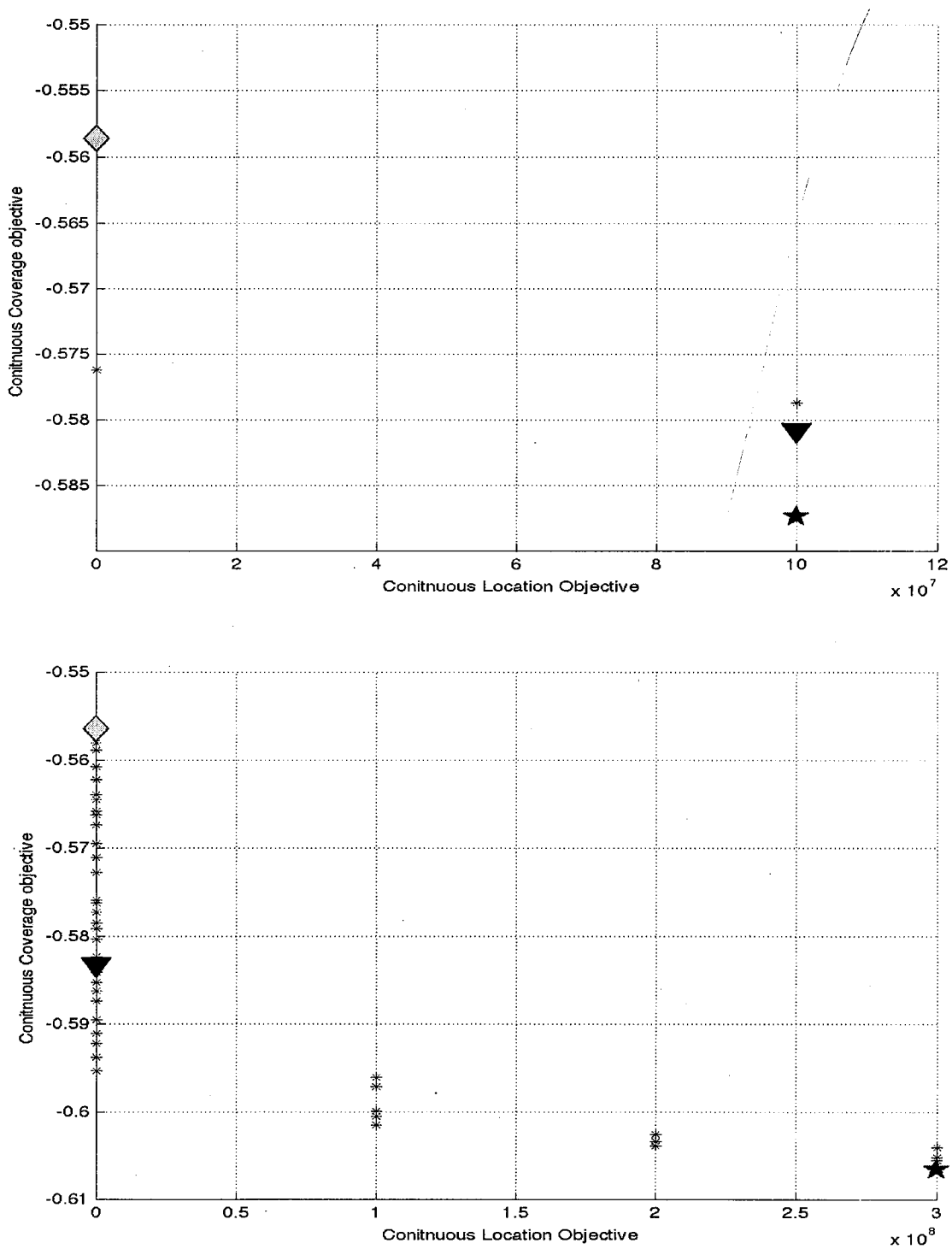


Figure 5.15: Pareto front with grid $G = 31 \times 31$, for relaxation values = 0.5 and 0.7 (from top to bottom), Continuous Location Objective (x-axis) vs Continuous Coverage Objective (y-axis).

The second set of test instances are the ones that were obtained with a value for $C_{Demand} = 45$, the following images are the Pareto fronts generated for this set of test instances (their corresponding locations graphs are shown in Appendix A.2 in page 96).

1. $G = 11 \times 11$, Relaxation factor $= 0.1$.
2. $G = 11 \times 11$, Relaxation factor $= 0.3$.
3. $G = 11 \times 11$, Relaxation factor $= 0.5$.
4. $G = 11 \times 11$, Relaxation factor $= 0.7$.
5. $G = 21 \times 21$, Relaxation factor $= 0.1$.
6. $G = 21 \times 21$, Relaxation factor $= 0.3$.
7. $G = 21 \times 21$, Relaxation factor $= 0.5$.
8. $G = 21 \times 21$, Relaxation factor $= 0.7$.
9. $G = 31 \times 31$, Relaxation factor $= 0.1$.
10. $G = 31 \times 31$, Relaxation factor $= 0.3$.
11. $G = 31 \times 31$, Relaxation factor $= 0.5$.
12. $G = 31 \times 31$, Relaxation factor $= 0.7$.

Figure 5.16 shows, from top to bottom, the Pareto fronts obtained for the first and the second test instances ($G = 11 \times 11$, Relaxation factor $= 0.1$ and $G = 11 \times 11$, Relaxation factor $= 0.3$.), Figure 5.17 shows, also from top to bottom, the Pareto fronts obtained for the third and the fourth test instances ($G = 11 \times 11$, Relaxation factor $= 0.5$ and $G = 11 \times 11$, Relaxation factor $= 0.7$.).

The Pareto fronts obtained for the test instances from the fifth to the eighth appear from the Figure 5.18 to the Figure 5.19. And the Pareto fronts obtained for the test instances from the ninth to the twelfth appear from the Figure 5.20 to the Figure 5.21.

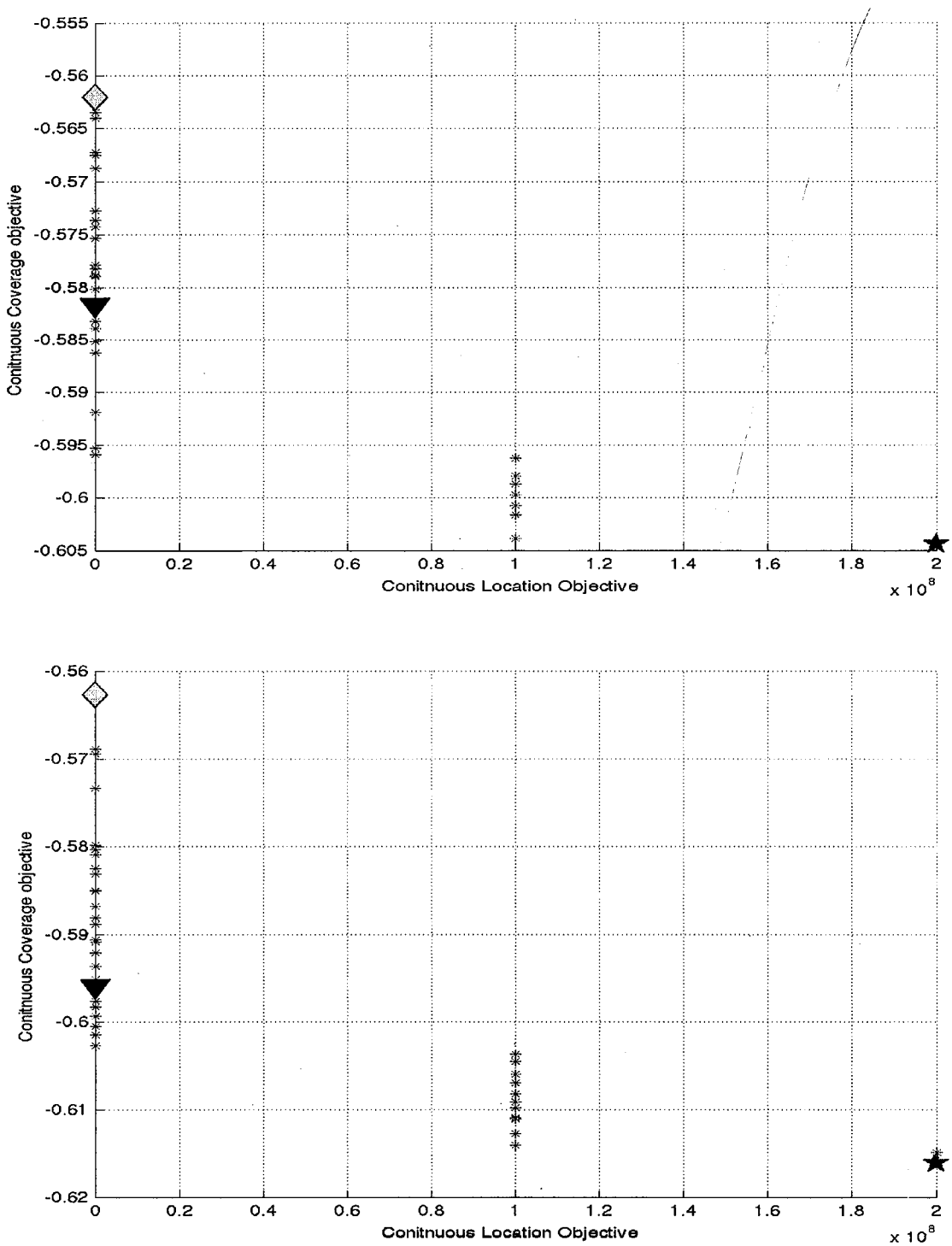


Figure 5.16: Pareto front with grid $G = 11 \times 11$, $C_{Demand=45}$, for relaxation values = 0.1 and 0.3 (from top to bottom), Continuous Location Objective (x-axis) vs Continuous Coverage Objective (y-axis).

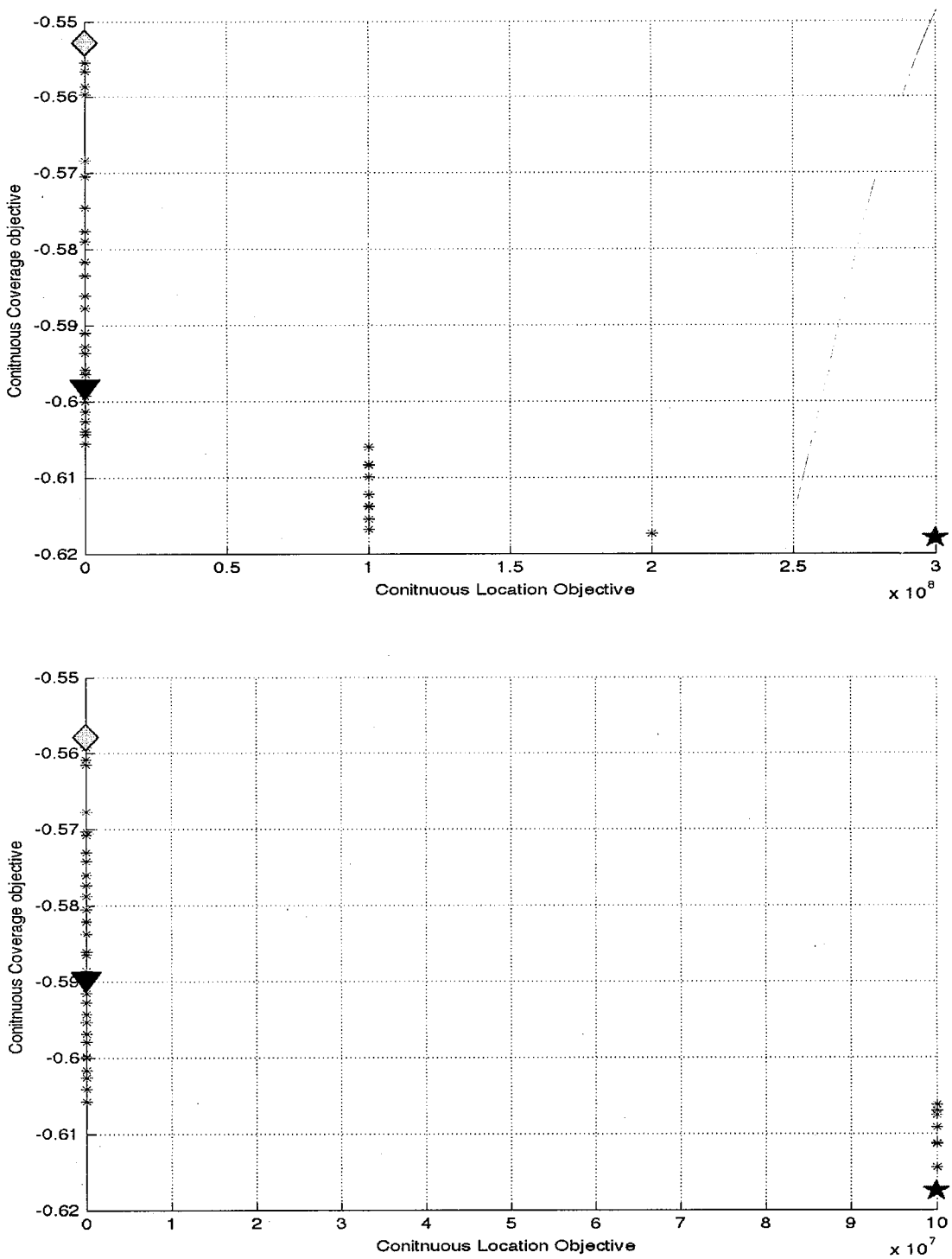


Figure 5.17: Pareto front with grid $G = 11 \times 11$, $C_{Demand=45}$, for relaxation values = 75 and 105 (from top to bottom), Continuous Location Objective (x-axis) vs Continuous Coverage Objective (y-axis).

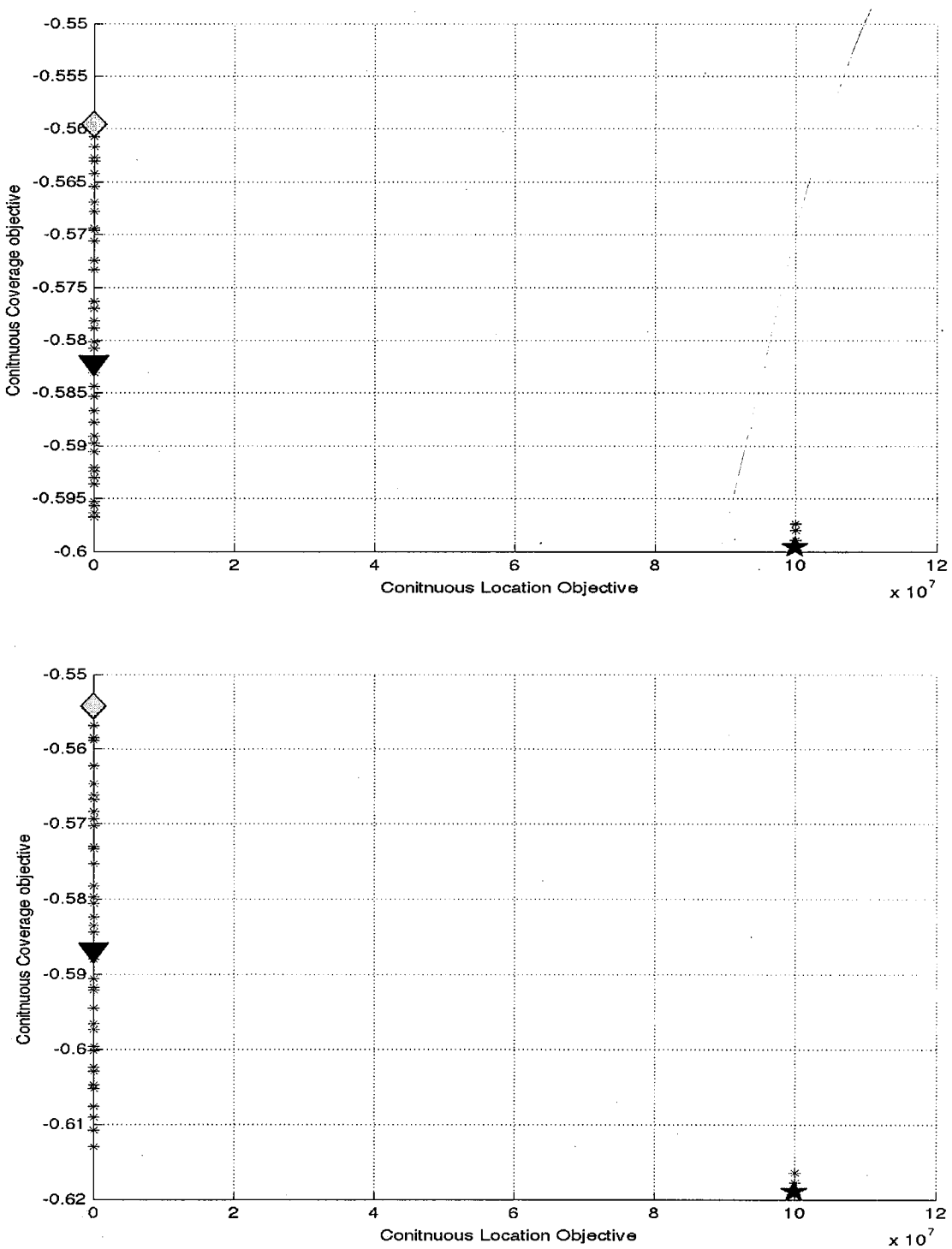


Figure 5.18: Pareto front with grid $G = 21 \times 21$, $C_{Demand=45}$, for relaxation values = 0.1 and 0.3 (from top to bottom), Continuous Location Objective (x-axis) vs Continuous Coverage Objective (y-axis).

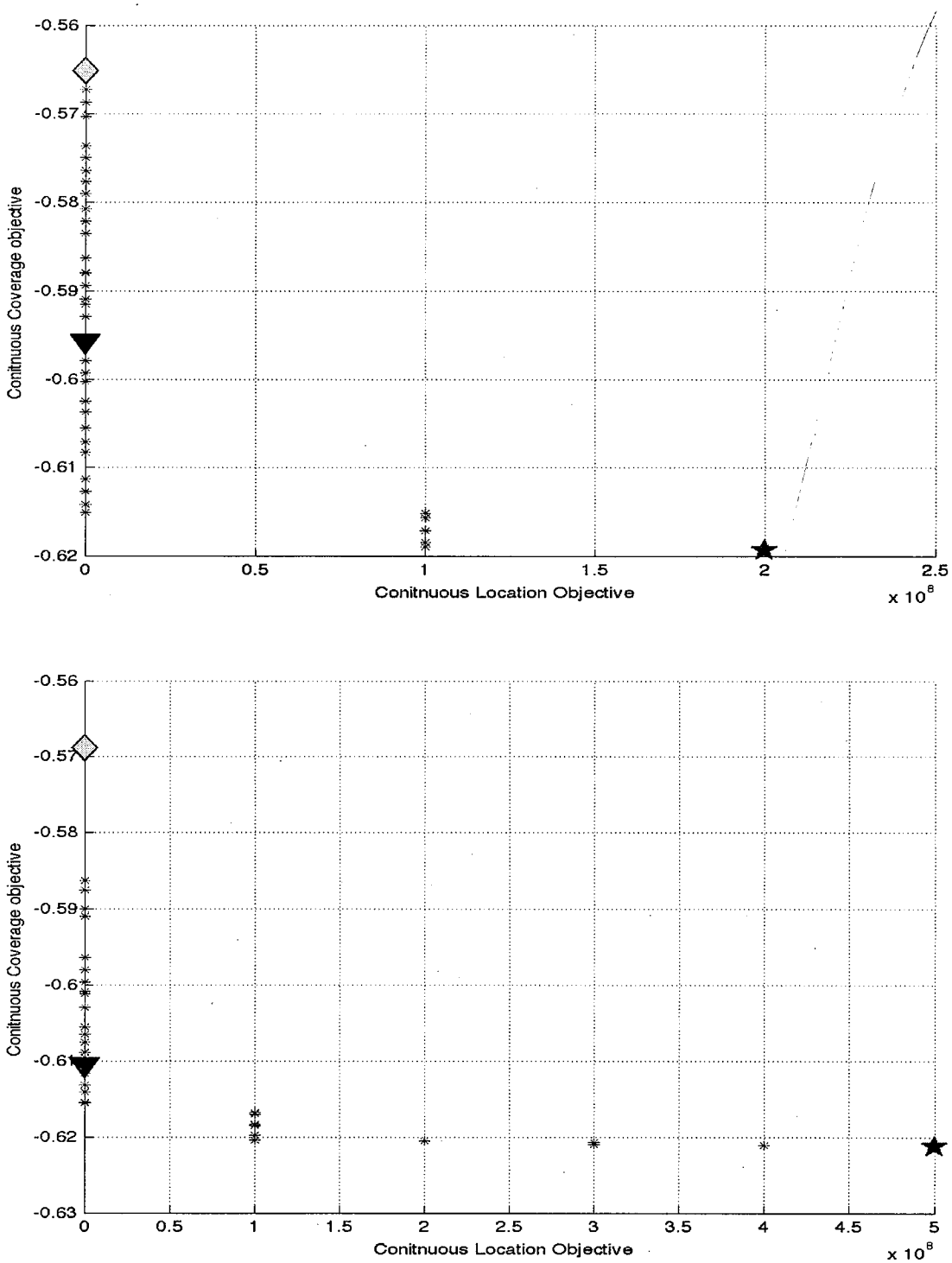


Figure 5.19: Pareto front with grid $G = 21 \times 21$, $C_{Demand=45}$, for relaxation values = 0.5 and 0.7 (from top to bottom), Continuous Location Objective (x-axis) vs Continuous Coverage Objective (y-axis).

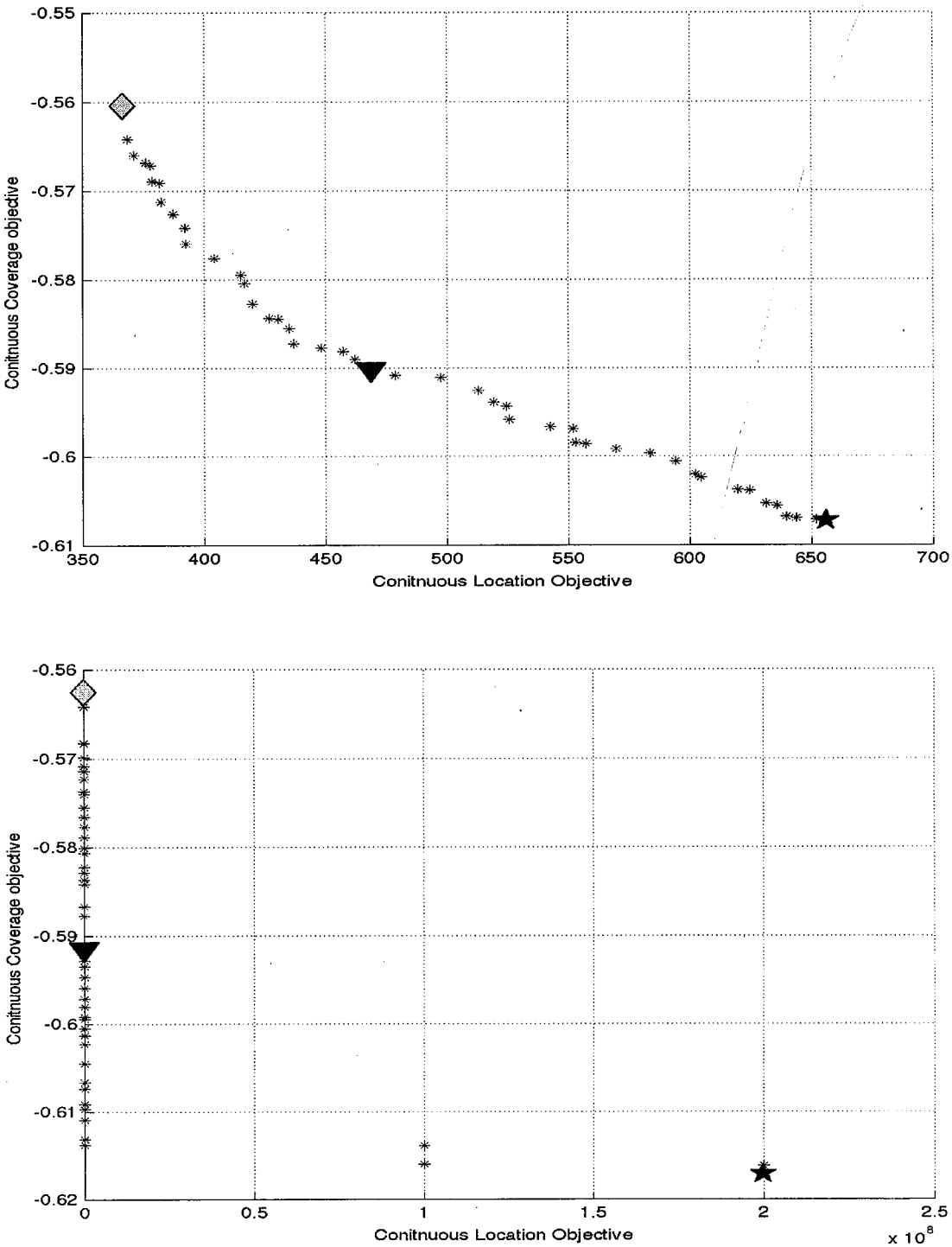


Figure 5.20: Pareto front with grid $G = 31 \times 31$, $C_{Demand=45}$, for relaxation values = 0.1 and 0.3 (from top to bottom), Continuous Location Objective (x-axis) vs Continuous Coverage Objective (y-axis).

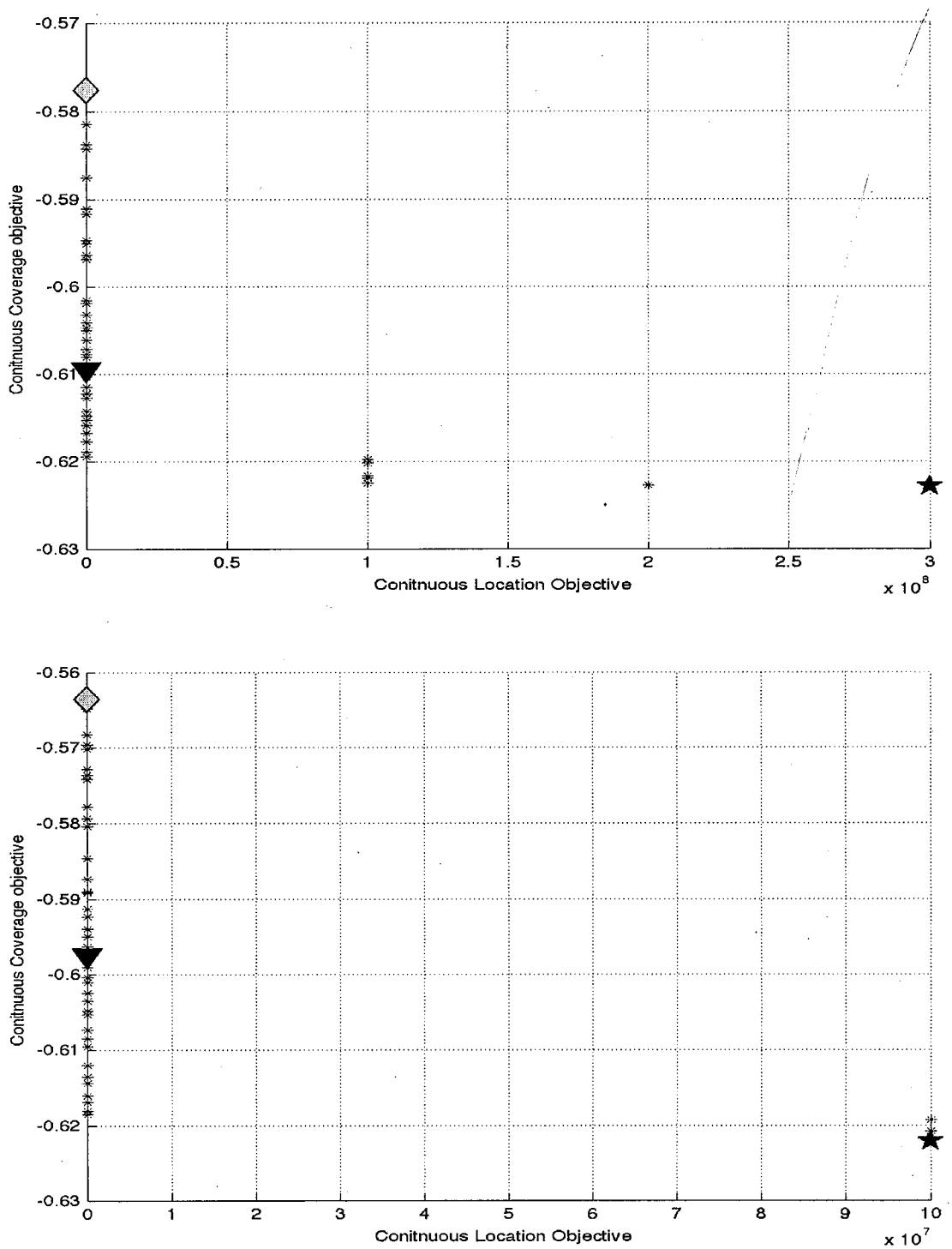


Figure 5.21: Pareto front with grid $G = 31 \times 31$, $C_{Demand=45}$, for relaxation values = 0.5 and 0.7 (from top to bottom), Continuous Location Objective (x-axis) vs Continuous Coverage Objective (y-axis).

Table 5.3 shows the numerical results for the first set of test instances where $C_{Demand} = 22$, every row in the Table stands for one of the twelve test instances and its respective Pareto front, the explanation of the column labels from this Table is the following:

**T best 1** The average arrival time in minutes to the covered demand points from the ambulance fleet, according to the best solution of the Continuous Location Objective.

**T knee point** The average arrival time in minutes to the covered demand points from the ambulance fleet, according to the knee point.

**T best 2** The average arrival time in minutes to the covered demand points from the ambulance fleet, according to the best solution of the Continuous Coverage Objective.

**Dc best 1** The fraction of demand covered, according to the best solution of the Continuous Location Objective.

**Dc knee point** The fraction of demand covered, according to the knee point.

**Dc best 1** The fraction of demand covered, according to the best solution of the Continuous Coverage Objective.

**Grid** The discretization used when the result was obtained.

**Rx.** The relaxation factor used when the result was obtained.

The explanation of column labels in Table 5.4 is the following:

**Best 1 x-coor** The x-coordinate of the best Continuous Location Objective solution (the Continuous Location Objective coordinate).

**Best 1 y-coor** The y-coordinate of the best Continuous Location Objective solution (the Continuous Coverage Objective coordinate).

**Best 1 x-coor** The x-coordinate of the best Continuous Coverage Objective solution (the Continuous Location Objective coordinate).

**Best 1 y-coor** The y-coordinate of the best Continuous Coverage Objective solution (the Continuous Coverage Objective coordinate).

**Grid** The discretization used when the result was obtained.

**Rx.** The relaxation factor used when the result was obtained.

Tables 5.5 and 5.6 stand for the second set of test instances where $C_{Demand} = 45$, the column labels are the same as the former Tables.

Table 5.3: Results for the continuous coverage vs continuous location multi-objective model, $C_{Demand=22}$, Part I

| T best 1 | T knee point | T best 2 | Dc Best 1 | Dc knee point | Dc best 2 | Grid | Rx. |
|---|---|---|---|---|---|---|---|
| 7.74957 | 6.55288 | 7.64830 | 0.813 | 0.820 | 0.820 | 10 | 0.1 |
| 6.48421 | 7.55637 | 7.43314 | 0.700 | 0.700 | 0.713 | 10 | 0.3 |
| 7.73932 | 7.56308 | 5.43615 | 0.500 | 0.553 | 0.513 | 10 | 0.5 |
| 4.82272 | 5.77581 | 5.89357 | 0.307 | 0.420 | 0.327 | 10 | 0.7 |
| 7.09808 | 7.15454 | 8.10851 | 0.807 | 0.813 | 0.900 | 20 | 0.1 |
| 7.24374 | 8.36837 | 8.20000 | 0.667 | 0.733 | 0.700 | 20 | 0.3 |
| 7.19642 | 7.31662 | 6.26907 | 0.500 | 0.473 | 0.507 | 20 | 0.5 |
| 5.10892 | 5.39207 | 4.98780 | 0.253 | 0.327 | 0.333 | 20 | 0.7 |
| 5.05369 | 5.01961 | 6.94518 | 0.713 | 0.847 | 0.867 | 30 | 0.1 |
| 6.88752 | 7.34987 | 7.64808 | 0.700 | 0.700 | 0.727 | 30 | 0.3 |
| 5.89388 | 6.41950 | 6.34403 | 0.500 | 0.620 | 0.600 | 30 | 0.5 |
| 4.65795 | 4.57725 | 4.59435 | 0.300 | 0.307 | 0.313 | 30 | 0.7 |

Table 5.4: Results for the continuous coverage vs continuous location multi-objective model, $C_{Demand=22}$, Part II

| Best 1 x-coor | Best 1 y-coor | Best 2 x-coor | Best 2 y-coor | Grid | Rx. |
|---|---|---|---|---|---|
| 0.04440 | -0.55616 | 0.04735 | -0.55997 | 10 | 0.1 |
| 0.03489 | -0.56010 | 0.04025 | -0.56150 | 10 | 46 |
| 0.02234 | -0.55833 | 20000.00000 | -0.58735 | 10 | 0.5 |
| 0.01422 | -0.54485 | 20000.00000 | -0.59682 | 10 | 0.7 |
| 0.04206 | -0.55689 | 0.05489 | -0.57018 | 20 | 0.1 |
| 0.03326 | -0.54999 | 0.04885 | -0.57695 | 20 | 0.3 |
| 0.02284 | -0.56072 | 20000.00000 | -0.58734 | 20 | 0.5 |
| 0.01289 | -0.54510 | 30000.00000 | -0.59635 | 20 | 0.7 |
| 0.03890 | -0.55897 | 0.05491 | -0.57492 | 30 | 0.1 |
| 0.03490 | -0.55591 | 0.05596 | -0.58228 | 30 | 0.3 |
| 0.02388 | -0.55860 | 10000.10000 | -0.58743 | 30 | 0.5 |
| 0.01232 | -0.55643 | 30000.00000 | -0.60543 | 30 | 0.7 |

Table 5.5: Results for the continuous coverage vs continuous location multi-objective model, $C_{Demand=45}$, Part I

| T best 1 | T knee point | T best 2 | Dc Best 1 | Dc knee point | Dc best 2 | Grid | Rx. |
|---|---|---|---|---|---|---|---|
| 6.47053 | 6.66515 | 6.52403 | 0.900 | 0.900 | 0.900 | 10 | 0.1 |
| 5.46176 | 7.20517 | 5.07713 | 0.700 | 0.720 | 0.740 | 10 | 0.3 |
| 6.66556 | 7.48263 | 4.42840 | 0.500 | 0.573 | 0.587 | 10 | 0.5 |
| 6.86187 | 7.31178 | 6.06169 | 0.300 | 0.493 | 0.473 | 10 | 0.7 |
| 5.43351 | 6.18304 | 6.46209 | 0.900 | 0.900 | 0.900 | 20 | 0.1 |
| 4.42864 | 3.23795 | 5.23280 | 0.633 | 0.733 | 0.700 | 20 | 0.3 |
| 4.09417 | 3.56822 | 4.92886 | 0.500 | 0.500 | 0.540 | 20 | 0.5 |
| 1.19412 | 3.95304 | 2.81575 | 0.300 | 0.427 | 0.400 | 20 | 0.7 |
| 6.45016 | 6.46511 | 5.77096 | 0.900 | 0.900 | 0.913 | 30 | 0.1 |
| 4.49069 | 4.59978 | 4.83377 | 0.700 | 0.727 | 0.700 | 30 | 0.3 |
| 2.79012 | 4.61165 | 3.60430 | 0.500 | 0.507 | 0.520 | 30 | 0.5 |
| 4.94466 | 3.61945 | 3.50771 | 0.300 | 0.407 | 0.480 | 30 | 0.7 |

Table 5.6: Results for the continuous coverage vs continuous location multi-objective model, $C_{Demand=45}$, Part II

| Best 1 x-coor | Best 1 y-coor | Best 2 x-coor | Best 2 y-coor | Grid | Rx. |
|---|---|---|---|---|---|
| 0.03818 | -0.56208 | 20000.00000 | -0.60445 | 10 | 0.1 |
| 0.02689 | -0.56264 | 20000.00000 | -0.61479 | 10 | 0.3 |
| 0.02047 | -0.55279 | 30000.00000 | -0.61806 | 10 | 0.5 |
| 0.01224 | -0.55788 | 10000.00000 | -0.60700 | 10 | 0.7 |
| 0.03599 | -0.55956 | 10000.10000 | -0.59796 | 20 | 0.1 |
| 0.02665 | -0.55429 | 10000.10000 | -0.61774 | 20 | 0.3 |
| 0.02003 | -0.56512 | 20000.10000 | -0.61896 | 20 | 0.5 |
| 0.01261 | -0.56880 | 50000.00000 | -0.62111 | 20 | 0.7 |
| 0.03667 | -0.56039 | 0.06561 | -0.60727 | 30 | 0.1 |
| 0.02682 | -0.56253 | 20000.10000 | -0.61610 | 30 | 0.3 |
| 0.01915 | -0.57756 | 30000.00000 | -0.62279 | 30 | 0.5 |
| 0.01219 | -0.56358 | 10000.00000 | -0.62193 | 30 | 0.7 |

### 5.2.2 Interpretation of the Results

In Table 5.3, if we pay attention to the first column and compare between the results obtained for different discretizations, we can observe that better results were found for the first grid $G = 31 \times 31$, for example, the average time it takes for the fleet associated to $G = 11 \times 11$ and relaxation factor $= 0.1$ is 7.74957 minutes, while the average time for the discretization $G = 31 \times 31$ with the same relaxation factor is 5.05369 minutes, the average arrival time for the discretization $G = 21 \times 21$ and same relaxation factor is 7.09808 minutes, again, less than the first mentioned. This trend is also observed on the other relaxation factors.

This difference does not occur if we consider the fraction of demand covered and compare between the different grids, in fact, the fraction value is almost always the same, and no more than the allowed by the setting of the problem.

We can also notice that, in most of the cases and for both sets of experiments, when the relaxation factor value grows the average arrival time decreases, what this decrement indicates is that when the problem is increasingly relaxed then the ambulances start to get closer to their targets, because the strings with which they are being pulled (the coverage constraints) tend to disappear.

If we compare the fraction covered between Tables, instead of the discretization grids, we notice that a improvement is achieved when the value of $C_{Demand}$ grows, for example when comparing the first rows of both Tables attending this metric, then for the Table associated to $C_{Demand} = 22$ the fraction covered is around the 80%, while the fraction covered by its counterpart is the 90%, in addition to that, the average arrival time for the experiments set with $C_{Demand} = 22$ is on average greater than for the experiments set with $C_{Demand} = 45$.

The effects of a greater value for $C_{Demand}$ are observable in:

- Pareto fronts: the number of points in the Pareto fronts associated to the largest value of $C_{Demand}$ is greater for most of the cases, also, this setting allows the NSGA-II algorithm to retrieve solutions in which some of the ambulances in the fleet doest no cover any demand point (compare Pareto set from Figure 5.10 against Pareto set on Figure 5.16).

- Tables 5.4 and 5.6: the best values of the Continuous Location Objective at the first column of these Tables are greater on average at the Table 5.4, while better coverage values are observed in Table 5.6 for the fourth column, this is, the best values of the Continuous Coverage Objective. Again, the number of penalized solutions is great at Table 5.6 (third column).

- Location Graphs: Greater values for $C_{Demand}$ favors solutions in which some ambulances share almost the same locations, this is, they tend to form clusters (compare Figure A.8 against Figure A.20 )

Greater values of $C_{Demand}$ allow an improvement in the fraction of coverage of both demand and geographical area, and also a decrement in the average arrival time of the fleet, but there are costs for these improvements: some of the ambulances are allowed to share locations and the same time that some of the do not cover any demand point.

From Tables 5.4 and 5.6, the observer can notice that when the relaxation factor increases then the factor of demand covered grows (third column), for example in Table 5.6, the ninth column has a value of -0.60625, while the twelfth column value is -0.62345.

In order to explain the meaning of an increment or decrement on the units for the objective 1, the Continuous Location Problem modeled as a weighted sum of distances, we used one of the previous results (the Pareto set obtained from the first experiment in Section 5.2), in which the solution to the problem was restricted allowing each ambulance to cover, at most, 22 demand points, and considering that 150 is total number of demand points expecting attendance by all the fleet. On this experiment a set of 10 Pareto points was obtained.

When calculated the sum of distances from each ambulance fleet (each solution from the Pareto set) to the most important points, ordered by their weight value, from least to greatest, we observed that: that sum of distances grows as we move along the Pareto front, starting from the objective 1 best solution towards the objective 2 best solution, i.e., when the objective 1 evaluation decreases, the time response to the most important points in the model decreases as well.

The sum of distances was calculated from every ambulance fleet to the first: 10 (Figure 5.22), 20 (Figure 5.23), 30 (Figure 5.24), 40 (Figure 5.25) and 50 (Figure 5.26) most important points. Green diamond stands for the best solution for objective 1, magenta triangle stands for the knee point and the blue star the best solution for objective 2 (coverage).

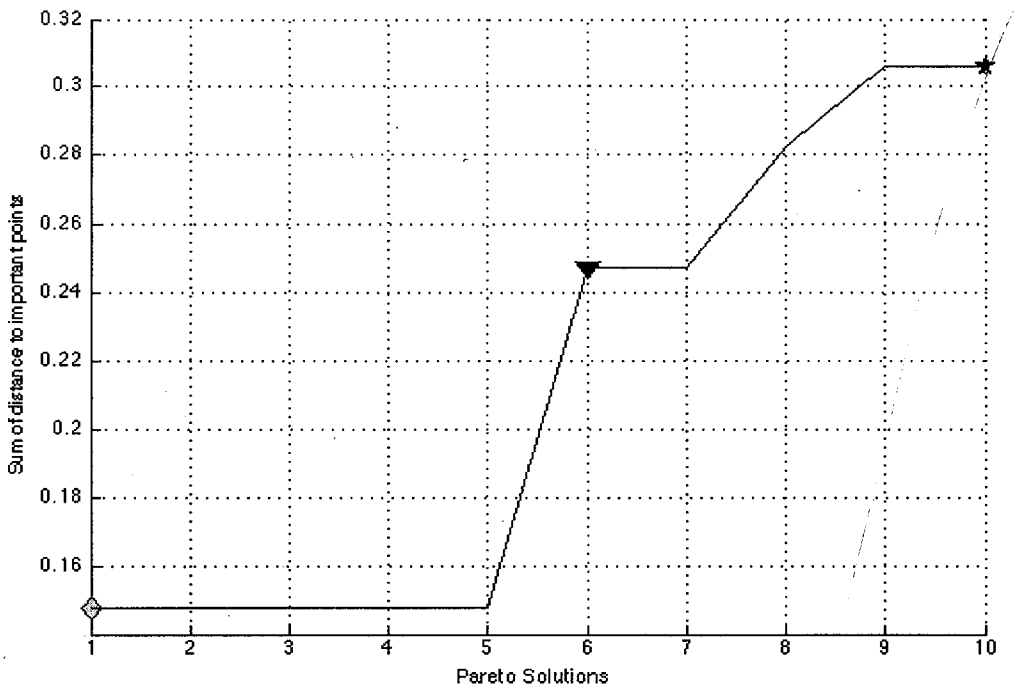


Figure 5.22: Sum of distance per solution to the 10 most important points.

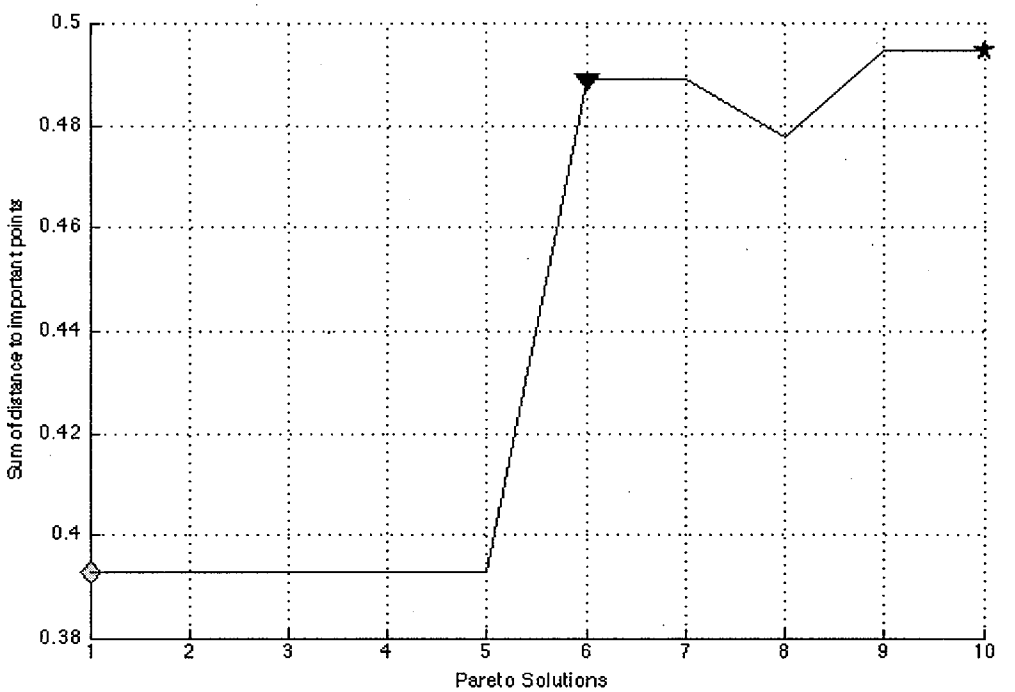


Figure 5.23: Sum of distance per solution to the 20 most important points.

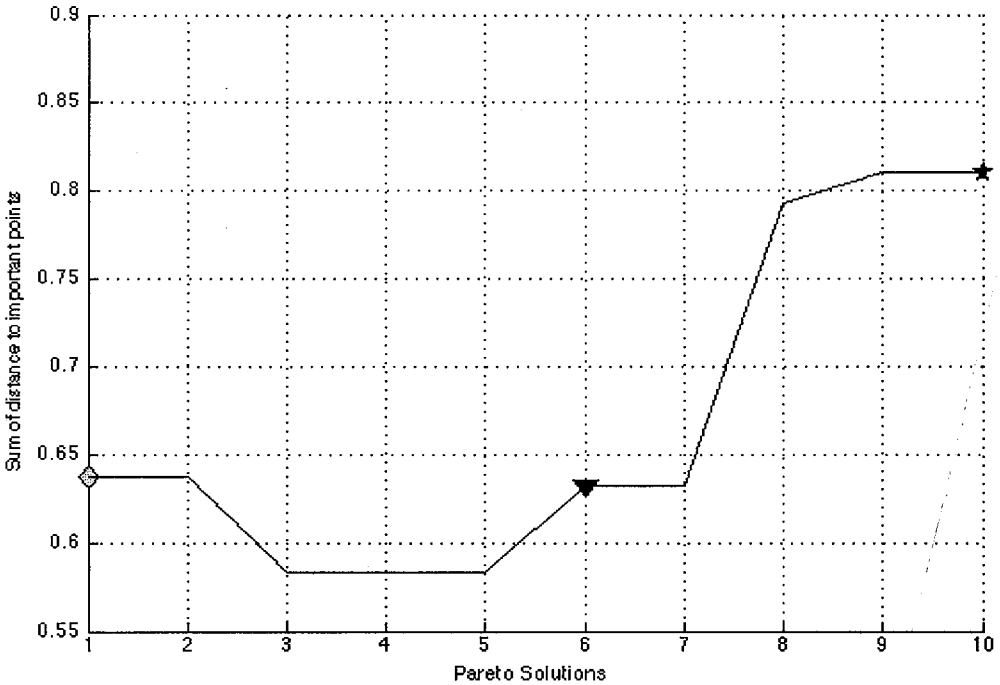


Figure 5.24: Sum of distance per solution to the 30 most important points.

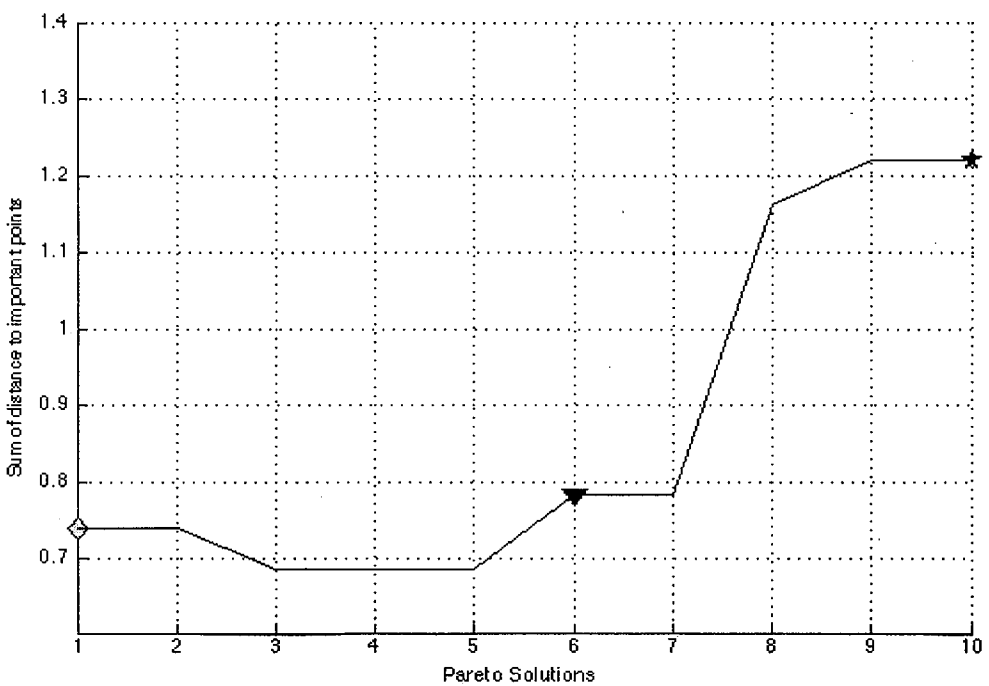


Figure 5.25: Sum of distance per solution to the 40 most important points.

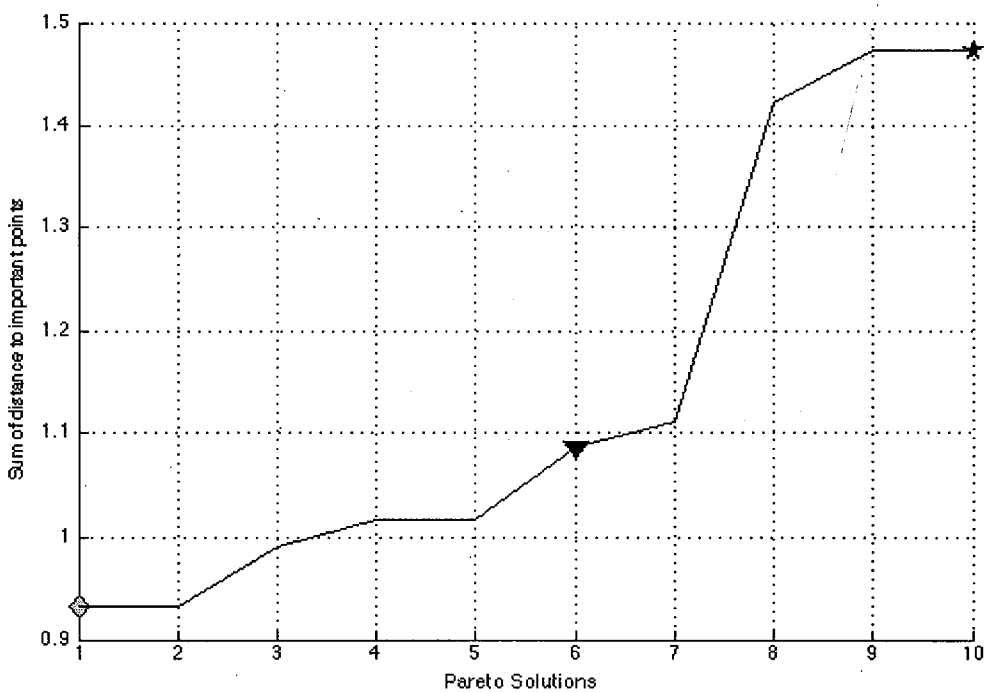


Figure 5.26: Sum of distance per solution to the 50 most important points.

## 5.3 Multi-Criteria Model

In this section, the experiments performed for the multi-criteria model described in Section 4.2 are presented. As in the former section, we have designed different test instances where every test instance has a different setting of the same problem, in order to understand which of these settings deliver the best results to locate the ambulances fleet. We have solved the problem using the two previously mentioned criteria into the model: the demand and the priority criteria.

### 5.3.1 Experiments

In the case of the multi-criteria model, we noticed that when we used a small discretization of the feasible area to solve the problem, then we obtained a Pareto set with only one element, instead, when using a larger discretization the genetic algorithm is able to find Pareto sets consisting of 3 or more elements, therefore, in this section we only include the results of the experiments performed using the largest discretization available, this is, the grid $G = 31 \times 31$.

The different settings we have considered for the test instances in this section are variations in the value of the constant $C_{Demand}$ and changes in the value of the relaxation factor, there are twelve test instances and their corresponding settings are the following:

1. $C_{Demand} = 18$, Relaxation factor $= 0.1$.
2. $C_{Demand} = 18$, Relaxation factor $= 0.3$.
3. $C_{Demand} = 18$, , Relaxation factor $= 0.5$.
4. $C_{Demand} = 37$, Relaxation factor $= 0.1$.
5. $C_{Demand} = 37$, Relaxation factor $= 0.3$.
6. $C_{Demand} = 37$, , Relaxation factor $= 0.5$.
7. $C_{Demand} = 56$, Relaxation factor $= 0.1$.
8. $C_{Demand} = 56$, Relaxation factor $= 0.3$.
9. $C_{Demand} = 56$, , Relaxation factor $= 0.5$.
10. $C_{Demand} = 75$, Relaxation factor $= 0.1$.
11. $C_{Demand} = 75$, Relaxation factor $= 0.3$.
12. $C_{Demand} = 75$, , Relaxation factor $= 0.5$.

However, not all of the experiments had retrieved a Pareto set with more than 3 elements, the Figures with the Pareto front for such experiments are no included, The experiments for which we have included its respective Pareto front are listed as follows:

$C_{Demand} = 18$, , **Relaxation factor = 0.5** Pareto front in Figure 5.27, Location Graphs included from Figure B.1 to Figure B.2.

$C_{Demand} = 37$, **Relaxation factor = 0.3.** Pareto front in Figure 5.28 (top), Location Graphs included from Figure B.3 to Figure B.2.

$C_{Demand} = 37$, , **Relaxation factor = 0.5.** Pareto front in Figure 5.28 (bottom).

$C_{Demand} = 56$, **Relaxation factor = 0.1.** Pareto front in Figure 5.29, Location Graphs included from Figure B.5 to Figure B.6.

$C_{Demand} = 75$, **Relaxation factor = 0.3.** Pareto front in Figure 5.30 (top).

$C_{Demand} = 75$, , **Relaxation factor = 0.5.** Pareto front in Figure 5.30 (bottom), Location Graphs included from Figure B.7 to Figure B.8.

For some of the experiments we have also included the location graphs of the solutions in Appendix B (page 109).

Tables 5.7 and 5.8 include the numerical results of all the test instances, even those for which we did not obtained a Pareto set with 3 or more elements. The only difference among these Tables and the Tables included for the multi-objective location model lies in the column labeled «C Demand», since on these experiments the discretization of the area was always same, varying instead the $C_{Demand}$ constant setting.

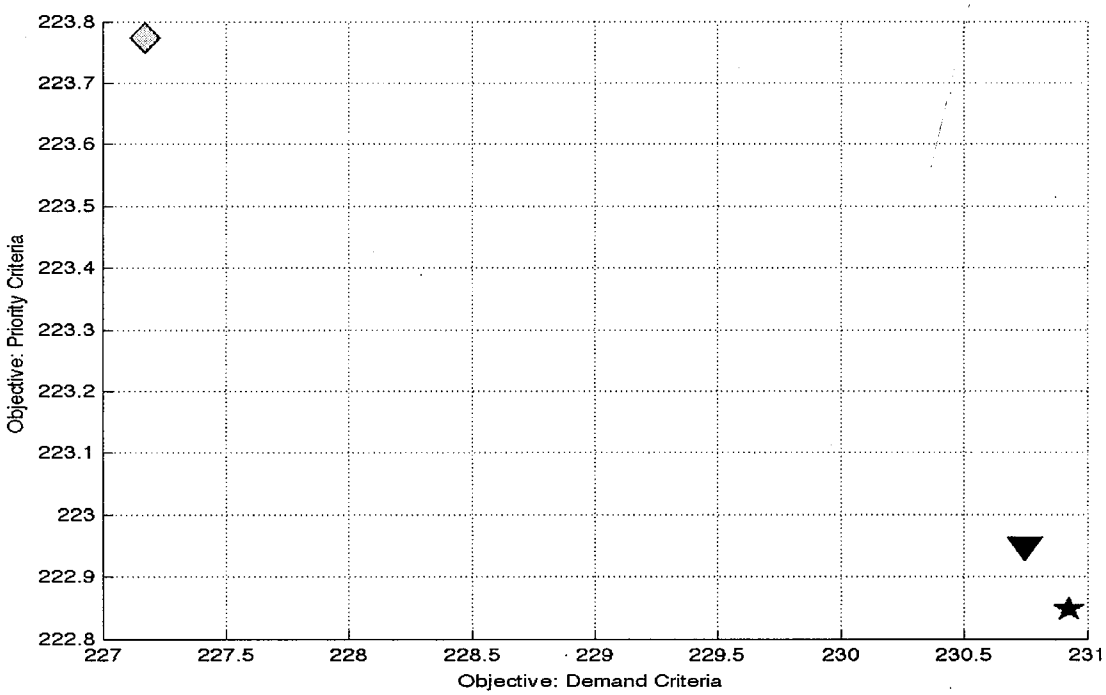


Figure 5.27: Pareto front with grid $G = 31 \times 31$, $C_{Demand=18}$, for relaxation values = 0.1, Multi-criteria model: demand vs priority.

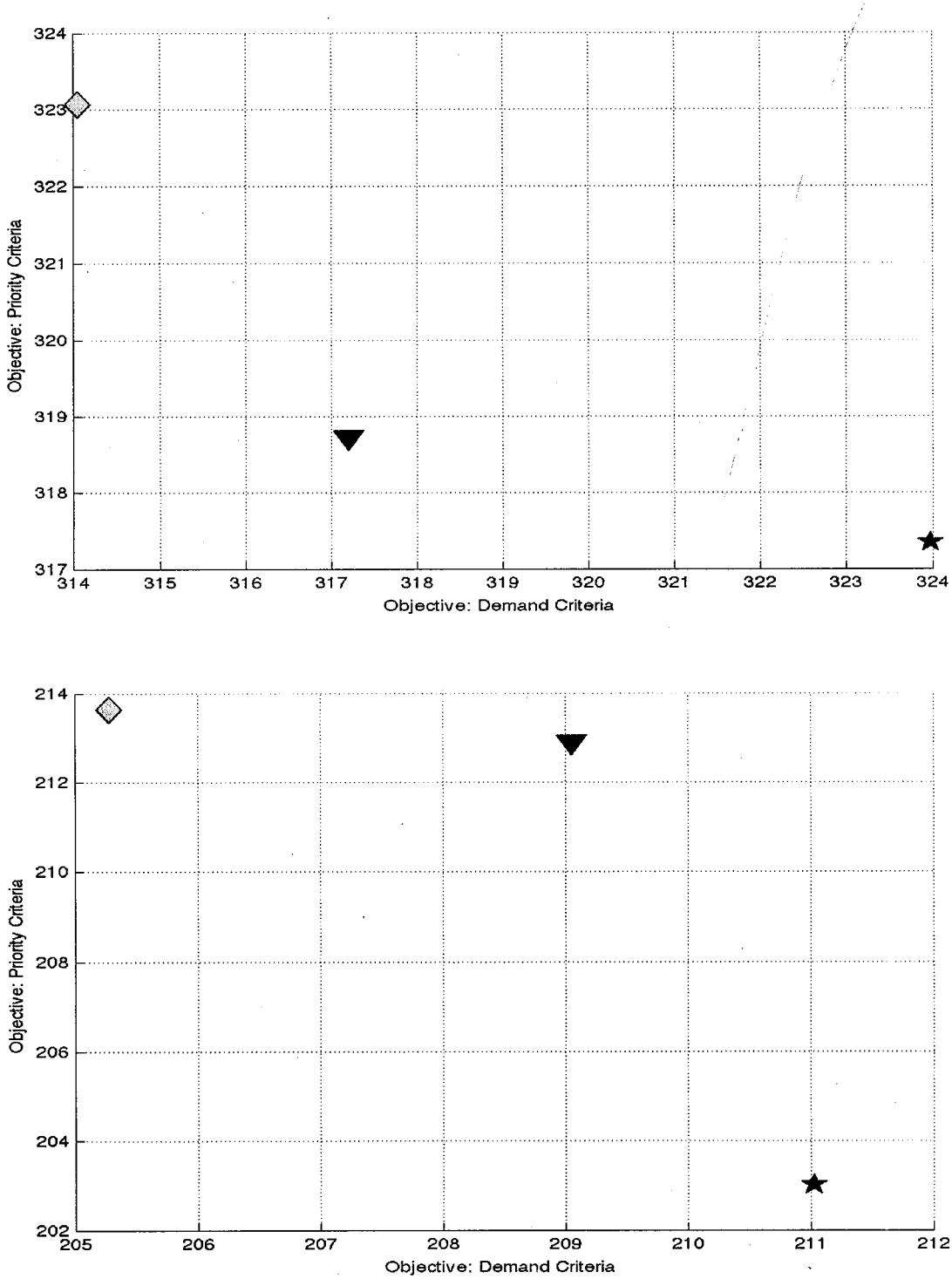


Figure 5.28: Pareto front with grid $G = 31 \times 31$, $C_{Demand=37}$, for relaxation values = 0.3 and 0.5, Multi-criteria model: demand vs priority.

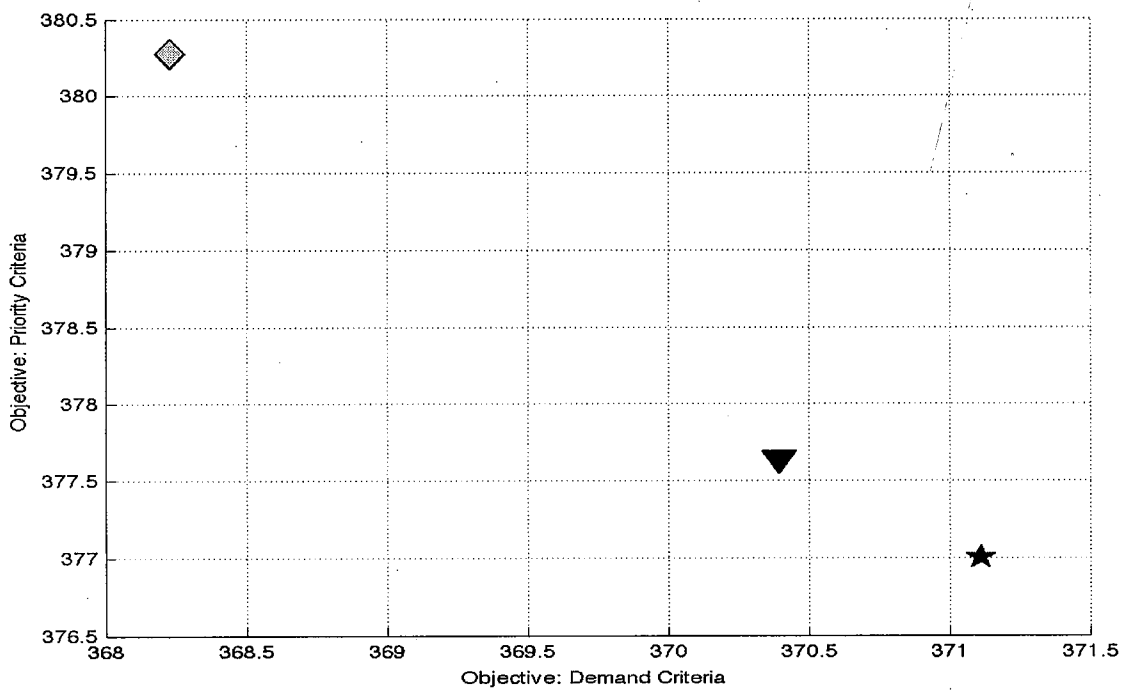


Figure 5.29: Pareto front with grid $G = 31 \times 31$, $C_{Demand=56}$, for relaxation values = 0.1, Multi-criteria model: demand vs priority.

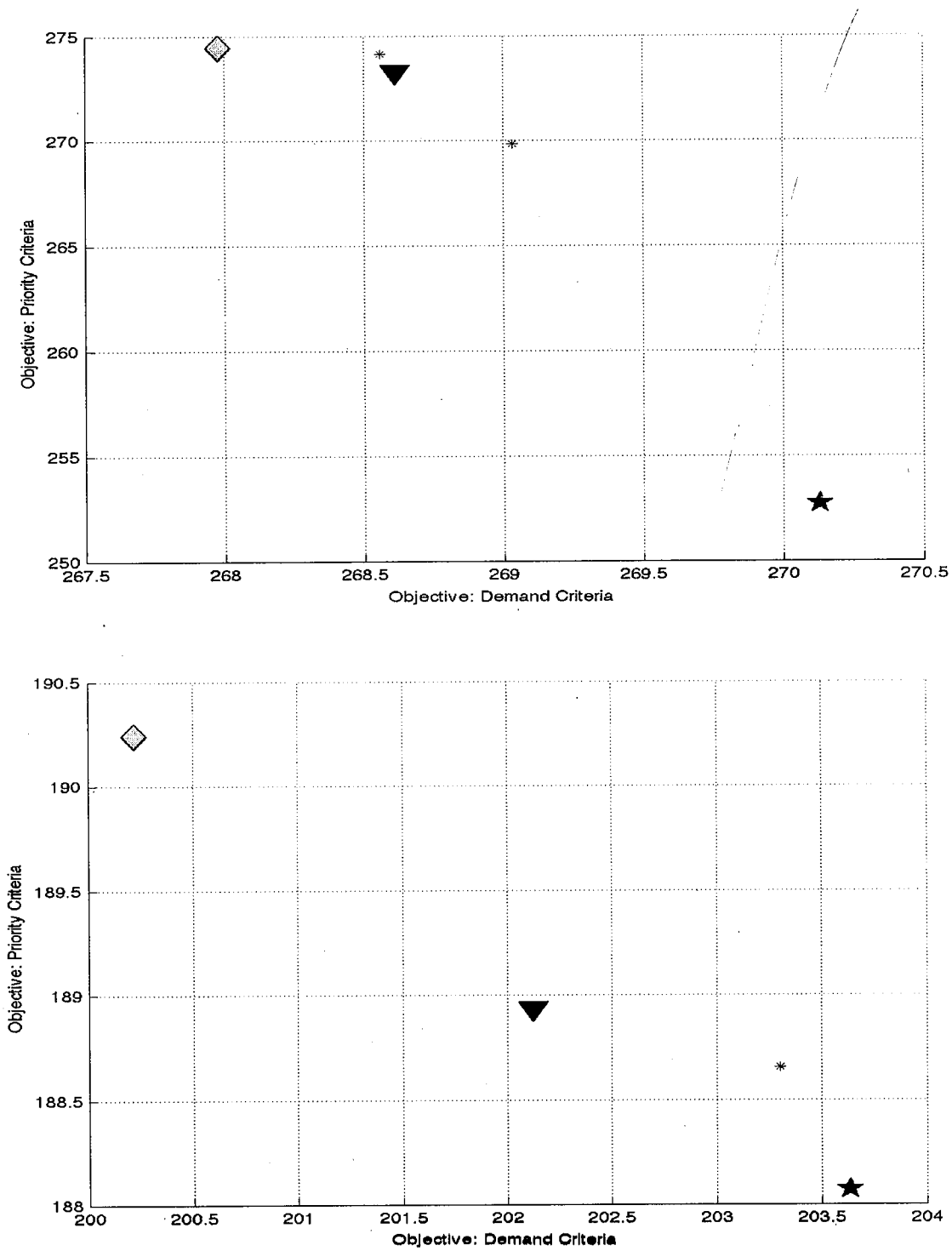


Figure 5.30: Pareto front with grid $G = 31 \times 31$, $C_{Demand=75}$, for relaxation values = 0.3 and 0.5 (from top to bottom), Multi-criteria model: demand vs priority.

Table 5.7: Results for the multi-criteria optimization model, Part I

| T best 1 | T knee point | T best 2 | Dc Best 1 | Dc knee point | Dc best 2 | C Demand | Rx. |
|---|---|---|---|---|---|---|---|
| 7.790 | 7.790 | 7.719 | 0.840 | 0.840 | 0.840 | 18 | 0.1 |
| 6.789 | 6.789 | 6.760 | 0.700 | 0.700 | 0.700 | 18 | 0.3 |
| 5.149 | 6.358 | 6.277 | 0.507 | 0.500 | 0.500 | 18 | 0.5 |
| 5.563 | 5.563 | 5.563 | 0.900 | 0.900 | 0.900 | 37 | 0.1 |
| 6.130 | 6.098 | 5.943 | 0.700 | 0.700 | 0.700 | 37 | 0.3 |
| 6.266 | 5.824 | 5.619 | 0.500 | 0.500 | 0.500 | 37 | 0.5 |
| 5.754 | 5.579 | 5.511 | 0.900 | 0.900 | 0.900 | 56 | 0.1 |
| 5.621 | 5.621 | 5.817 | 0.700 | 0.700 | 0.700 | 56 | 0.3 |
| 3.763 | 3.763 | 3.763 | 0.500 | 0.500 | 0.500 | 56 | 0.5 |
| 4.336 | 4.336 | 3.147 | 0.900 | 0.900 | 0.900 | 75 | 0.1 |
| 5.682 | 5.682 | 4.575 | 0.720 | 0.700 | 0.700 | 75 | 0.3 |
| 2.352 | 3.940 | 2.894 | 0.500 | 0.520 | 0.507 | 75 | 0.5 |

Table 5.8: Results for the multi-criteria optimization model, Part II

| Best 1 x-coor | Best 1 y-coor | Best 2 x-coor | Best 2 y-coor | C Demand | Rx. |
|---|---|---|---|---|---|
| 399.82600 | 411.13600 | 400.94200 | 408.82000 | 18 | 0.1 |
| 315.24800 | 315.66700 | 317.33500 | 314.91400 | 18 | 0.3 |
| 227.17500 | 223.77400 | 230.93100 | 222.84700 | 18 | 0.5 |
| 437.91600 | 437.63300 | 437.91600 | 437.63300 | 37 | 0.1 |
| 314.04500 | 323.07100 | 323.98100 | 317.34000 | 37 | 0.3 |
| 205.28100 | 213.62700 | 211.03200 | 202.99800 | 37 | 0.5 |
| 368.23300 | 380.27600 | 371.11500 | 376.99900 | 56 | 0.1 |
| 280.88100 | 289.53600 | 281.80900 | 287.88500 | 56 | 0.3 |
| 198.23400 | 200.97500 | 198.23400 | 200.97500 | 56 | 0.5 |
| 355.11200 | 348.10500 | 357.50200 | 348.01700 | 75 | 0.1 |
| 267.97700 | 274.44900 | 270.13200 | 252.72300 | 75 | 0.3 |
| 200.22100 | 190.23800 | 203.63500 | 188.07100 | 75 | 0.5 |

### 5.3.2 Interpretation of the Results

A confirmation of the effects that the variation on the value of the $C_{Demand}$ constant brings to the results arose with these experiments, here again, we observe better results when its value grows, this is, the average arrival time in Table 5.7 decreases with greater values of such setting; a clear example can be found by comparing the values at the first column («T best 1») for the first, the fourth, the seventh, and the tenth rows, the best average arrival time for the density criteria goes from 7.339 minutes to 6.078 minutes.

The same decrement occurs at the third column («T best 2») for the same rows, where the average arrival time goes from 7.301 minutes to 6.075 minutes. However, no penalized solutions were obtained for this model, because here penalized solutions do not deliver any advantage, as it did in the former model, where penalized solutions had the best performance in terms of geographical area coverage, instead, the notion of coverage is the same for both objectives, and a penalized solution would only lead to a waste of resources.

Moreover, the increment on the value of the relaxation factor, in most of the cases, leads to decrements on the value of the average arrival time when maintaining the constant $C_{Demand}$ fixed. In general, many of the observations made for the results of the former model can be applied for this one.

Nonetheless, such observations have different implications; for example: in the case of the relaxation factor for the multi-objective location model, an increment on it allows the ambulances to be located at distant regions improving the metrics of the second objective, but for the multi-criteria model such relaxation means an improvement in quality of the EMS services provided to the most important points according to the sets of weights and a deterioration of the quality for those points considered less relevant. But we have seen that there exist different ways to attend most of the demand points with the ambulance fleet, therefore, such relaxation might not be recomended.

# Chapter 6

# Conclusions and Future Work

## Conclusions

### Continuous Location Model

With this work we offer a method to look for the best locations to deploy an ambulance fleet, to solve this problem the method requieres the following:

- A set of demand points distributed over the feasible area (Tijuana city) in which the demand is concentrated.
- Every demand point has a weight value associated, such value is proportional to the relevance of the point in terms of EMS services, economic affairs, geo-political fairness, et cetera.
- Every demand point has associated a time threshold within the ambulance must be located in order to deliver the EMS service.
- The estimated travel time to go from and to any point in the feasible area.

With the former requirements fulfilled, this method is able to deliver:

The locations of the ambulance fleet in which all or most of the demand points are covered within their defined time thresholds and considering their associated weight values, this is, the ambulances will be located closer to some points than others according to the priority defined in the set of weight values.

In Section 5.1, the results obtained for the solution of the ambulance location problem using our proposed optimization model are presented, however, this work lies under some assumptions that is worthy to mention in order to explain its relevance:

- The calculations on how the demand is distributed over the set of demand points was performed based on the information provided by the Tijuana Red Cross Unit over a specific period of time, assuming such period effectively reflects the demand of EMS services.

- The problem is solved considering that the demand remains quiet over the time.
- The number of demand points is fixed.

Nevertheless, such assumptions do not impact the value of this work, because they are not part of the definition of the optimization model (neither its extensions), they are implied in the setting of the problem, however, such assumptions affect the precision of the solution, since the problem only consider a static distribution of the demand in the time.

## Multi-Objective Location Model

A very satisfying result from the solution of the multi-objective location problem was to find the possibility to locate the ambulance fleet attending the main restrictions of the ambulance location problem (demand coverage and time thresholds) at the same time that the restrictions of the geographical coverage were addressed.

This possibility means that there are ways to satisfy the EMS demand from the urban areas, where the population is most concentrated, and to offer EMS services to distant or isolated areas of the city which accomplish the time restrictions. This multi-objective optimization problem is solved by following a logic of political fairness, where the people living in distant regions do not remain uncovered (vulnerable).

In Section 5.2, the results obtained for 24 test instances were presented, where every test instance stands for a different setting of the multi-objective location model, from these experiments the settings which lead to better result were noticed, our conclusions are listed as follows:

- Discretization Grid: better results in terms of average arrival time and geographical coverage were observed for greater discretizations, and no improvements in terms of demand coverage, moreover, the number of points in the Pareto front tend to increase as the discretization grows, which might be a good feature to offer to the decision maker.
- $C_{Demand}$ value: greater values of the constant $C_{Demad}$ leads to better results in terms demand and geographical area coverage, it also reduces the average arrival time from the ambulance fleet to the demand points. However, greater values also estimate configurations of the ambulance fleet in which some of the ambulances relatively too close to each other and configurations in which some ambulances do not cover any demand point, this configurations have the best performance in terms os geographical coverage, as expected. Finally, the number of points in the Pareto points tend to be larger for greater values of $C_{Demand}$.

- Relaxation factor: the relaxation of the coverage constraints leads to slights improvements in the average arrival time of the ambulance fleet and in the geographical area coverage, nonetheless, the amount required for observable improvements of the demand coverage sacrifice is too high.

- Differences between the solutions: when the value of the $C_{Demand}$ constant grows, the differences between opposite the corners of the Pareto front grows, this, is by allowing the ambulances to gather around the solver is able to find solutions in which more significant changes arise between the elements in the Pareto set, however, all of them accomplish the time restrictions, the difference in time for some solutions in of almost one minute in the average arrival time (ninth row of the table 5.4 in page 61).

## Multi-criteria Model

With the incursion of this model and its corresponding solution we deliver a model to which finds compromised solutions for different criteria without forgetting the time and coverage restrictions of the ambulance location problem. We think that this model can be really helpful for a decision maker, since it helps to show wether there are ways to deploy the ambulance fleet by pondering the problem over many factors. In the future, this model can be extended with many more objectives, every objective standing for a conflictive feature of the original problem. With the solution of the multi-criteria ambulance location problem we found that there are many ways to deploy the fleet, and that those different locations have different implications for the quality of the EMS services delivered.

In Section 5.3, the results obtained for 12 test instances were presented, where every test instance stands for a different setting of the multi-criteria location model, from these experiments the settings which lead to better result were noticed, our conclusions are listed as follows:

- Discretization Grid: we could only obtain Pareto set with 3 or more elements with the largest discretization available, however, as a future work the problem should be solve with larger discretization and other solver methods which might be able to find more feasible configurations of the ambulance fleet.

- $C_{Demand}$ value: greater values of the constant $C_{Demad}$ leads to better results in terms of demand coverage and average arrival time.

- Relaxation factor: the relaxation of the coverage reduces the average arrival time, nevertheless such relaxation is not recommended, since it leads to a deterioration in the quality of the EMS services without any advantage, like the advantage it represented for the multi-location model, where the fraction of area covered grows when the demand restrictions are relaxed.

# Future Work

In order to find solutions nearer to the real features of the problem some future work needs to be done:

- Estimate the demand distribution of EMS for different periods of time: considering the hour, the day of the week, and the season of the year in which the problem is requested to be solved. This might be done by implementing more sophisticated tool such as with a statistical and probabilistic analysis of the emergence of the demand in this city.
- Updated and performe the inclusion and/or the exclusion of elements from the set of demand points: when we compared against the current deployment of the ambulance fleet, we observed a large improvement, because our solution attends to the actual deployment of the demand based on recent historical data, the current ambulance fleet was deployed attending to a distribution of the demand which is not longer the same. The deployment of the ambulances must evolve at the same rate that the city evolves, a clear counterexample of this is the base station located at the beach of Tijuana city, which was placed to attend a demand that no longer is there.
- Build larger discretizations of the feasible area: we have observed that better results can be achieved in terms of average arrival time when the discretization of the domain $Q$ grows.

With the chosen genetic algorithm we have proved that this problem can be solved, and this was our main objective, this is to solve the problem and find good solutions. However, a solver method which solves the problem in less time still needs to be found.

# Appendices

# Appendix A

# Multi-Objective Location Model Location Graphs

## A.1 C demand = 22

Here we present the location graphs of the ambulance fleet according to the solution of six different test instances of the Multi-Objective Location Model, these test instances were obtained by setting $C_{Demand} = 22$.

For every test instance we have included:

- A graph with the locations of the ambulance fleet according to the best solution of the Continuous Location Objective.
- A graph with the locations of the ambulance fleet according to the best solution of the Continuous Coverage Objective.
- A graph with the locations of the ambulance fleet according to the knee point.
- A graph with the locations of all the previous solutions.

The test instances for which the locations graphs have been included are:
(1) $G = 11 \times 11$, Relaxation factor = 0.1: Figure A.1 and Figure A.2.
(4) $G = 11 \times 11$, Relaxation factor = 0.7: Figure A.3 and Figure A.4.
(5) $G = 21 \times 21$, Relaxation factor = 0.1: Figure A.5 and Figure A.6.
(8) $G = 21 \times 21$, Relaxation factor = 0.7: Figure A.7 and Figure A.8.
(9) $G = 31 \times 31$, Relaxation factor = 0.1: Figure A.9 and Figure A.10.
(12) $G = 31 \times 31$, Relaxation factor = 0.7: Figure A.11 and Figure A.12.

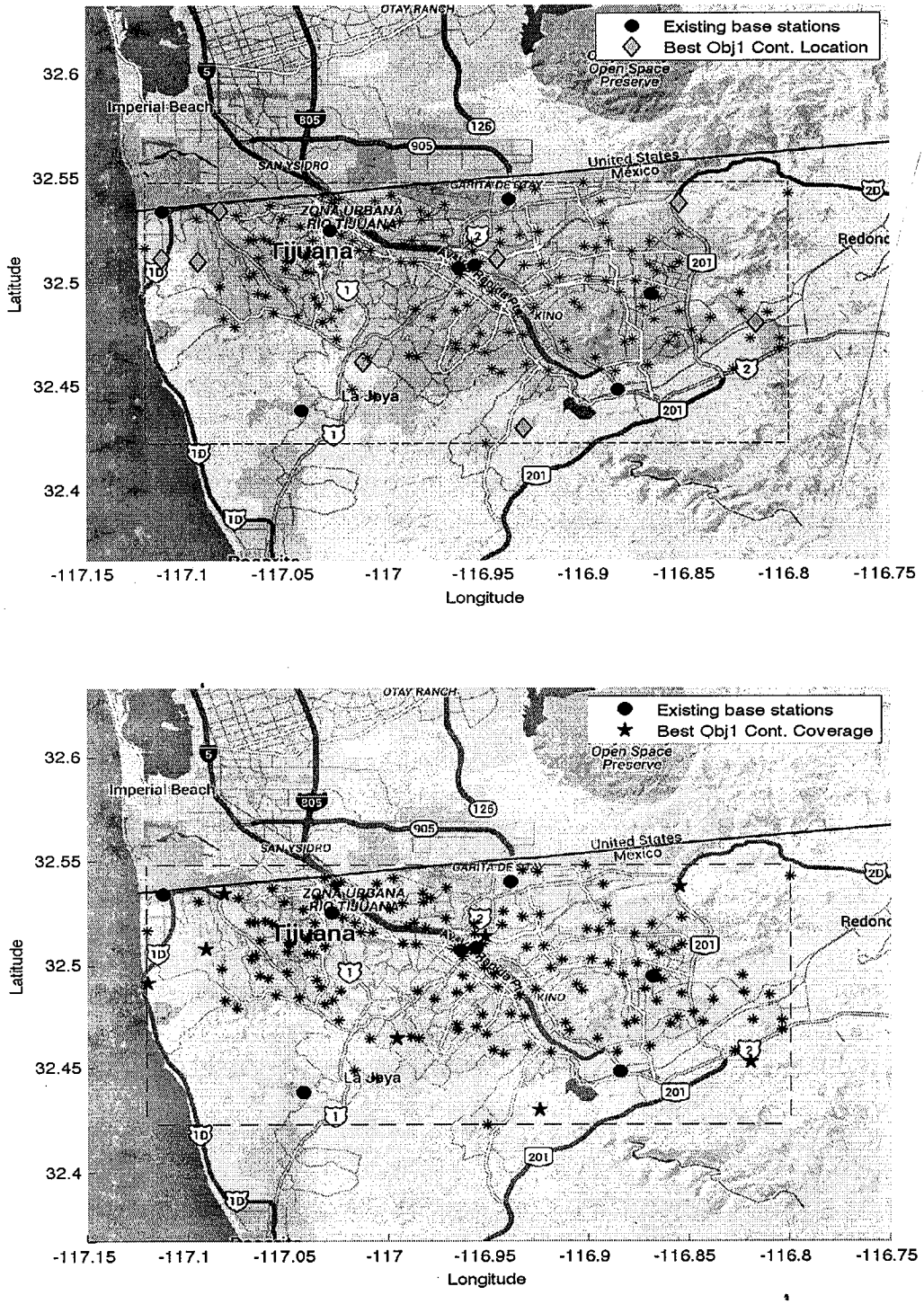


Figure A.1: Locations of the best solution for objetive 1 and for objective 2, $C_{Demand=22}$, Discretization $11 \times 11$ (from top to bottom), Relaxation factor $= 0.1$

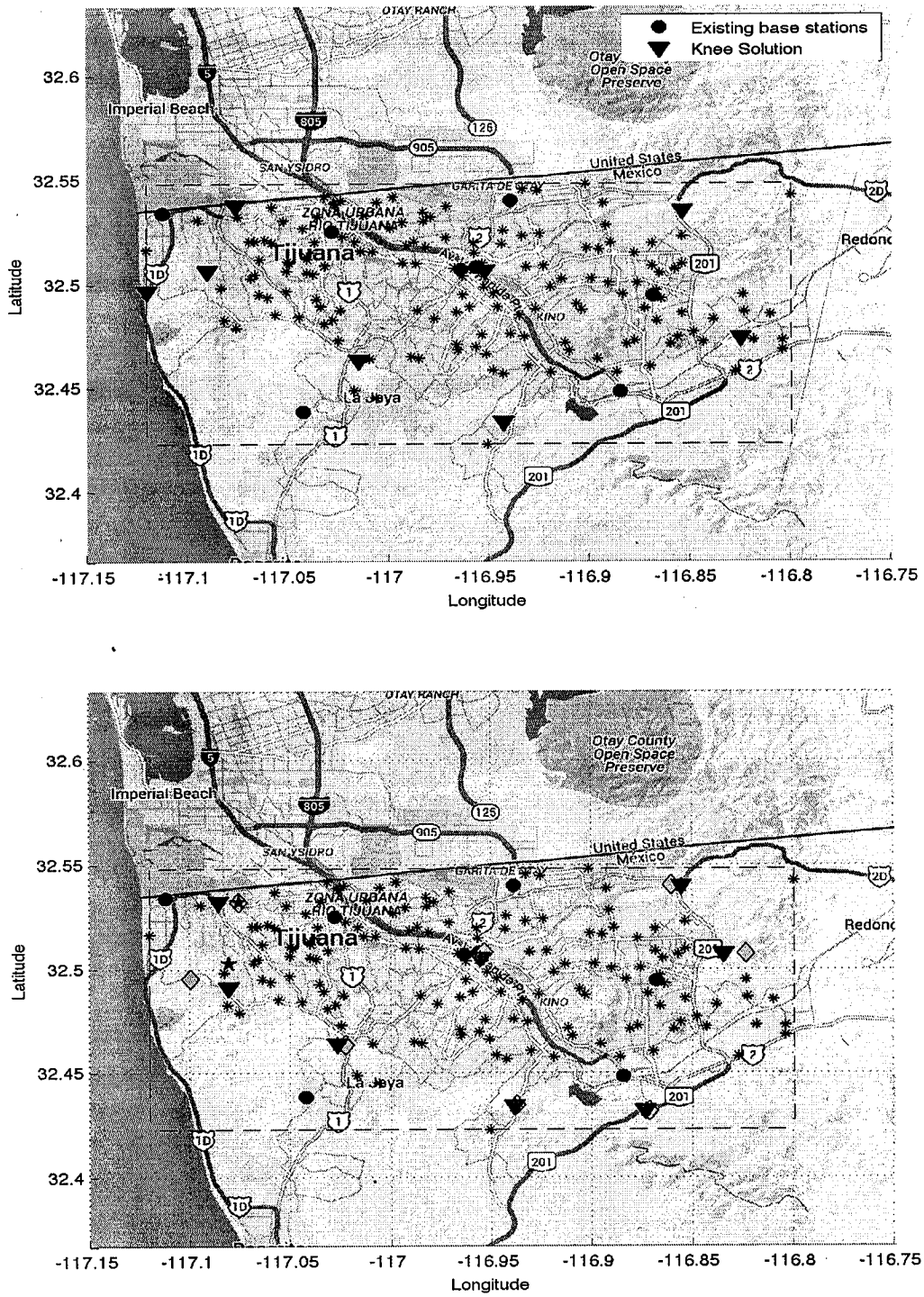


Figure A.2: Locations according to the knee point, The merge for all previous solution locations, $C_{Demand=22}$, Discretization $11 \times 11$ (from top to bottom), Relaxation factor $= 0.1$

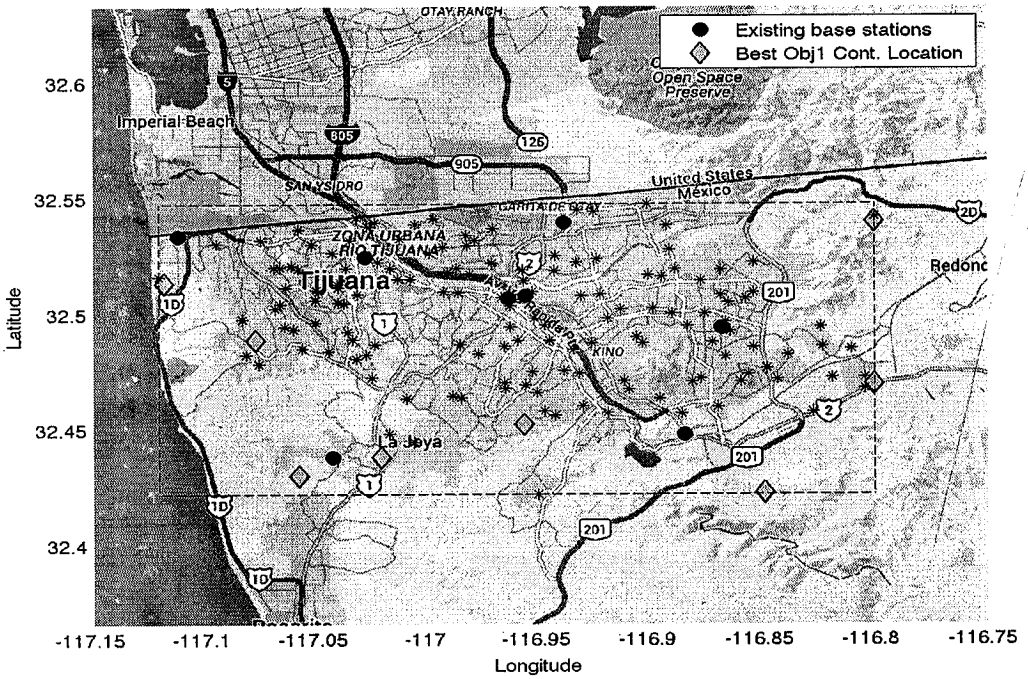


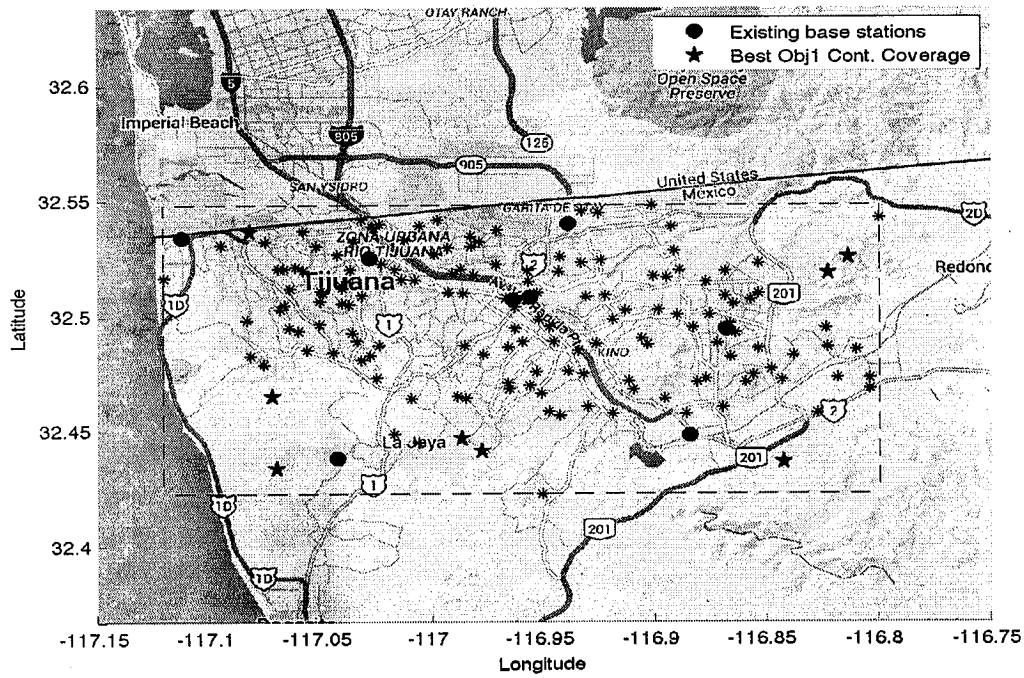


Figure A.3: Locations of the best solution for objetive 1 and for objective 2, $C_{Demand=22}$, Discretization $11 \times 11$ (from top to bottom), Relaxation factor $= 0.7$

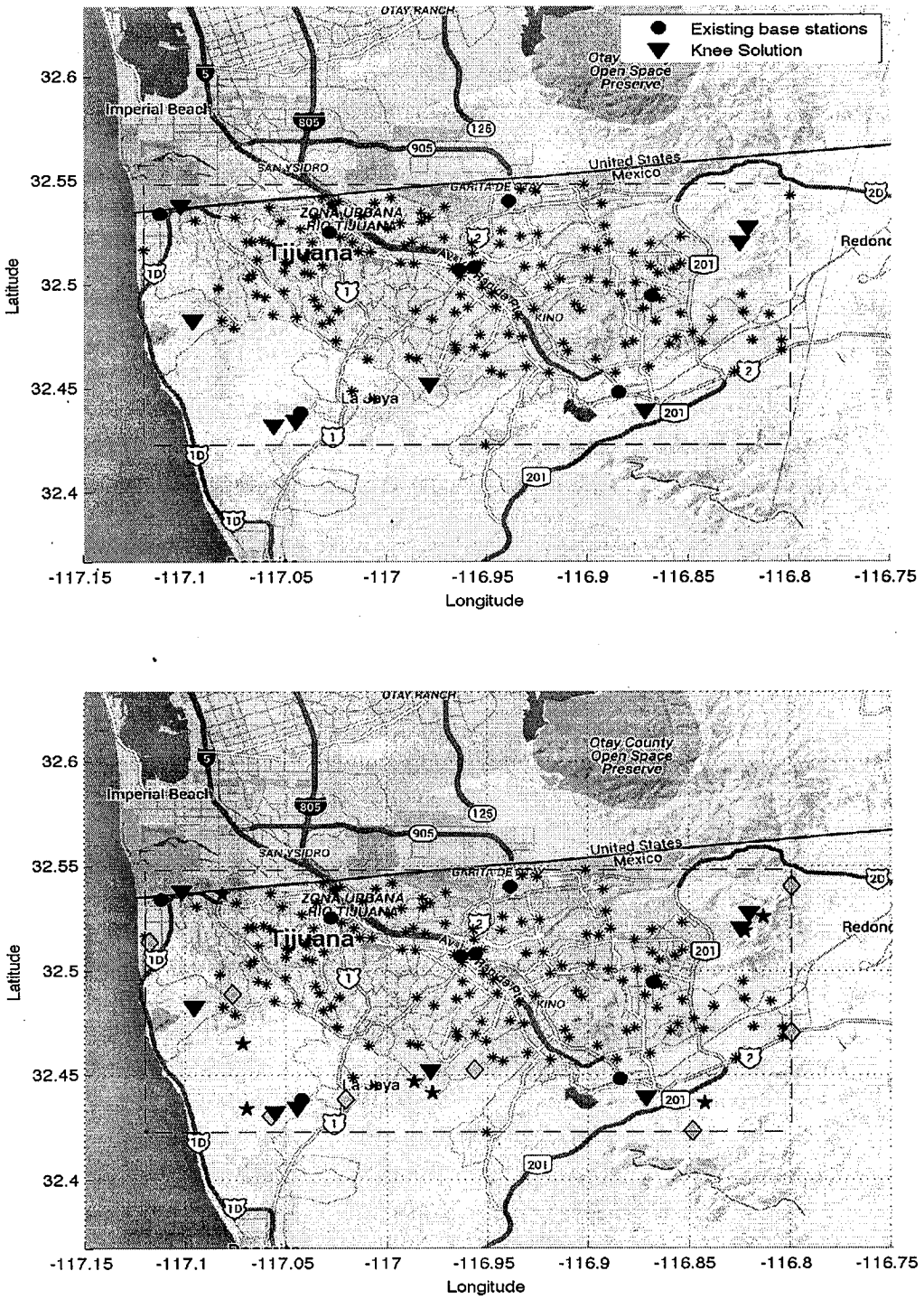


Figure A.4: Locations according to the knee point, The merge for all previous solution locations, $C_{Demand=22}$, Discretization $11 \times 11$ (from top to bottom), Relaxation factor $= 0.7$

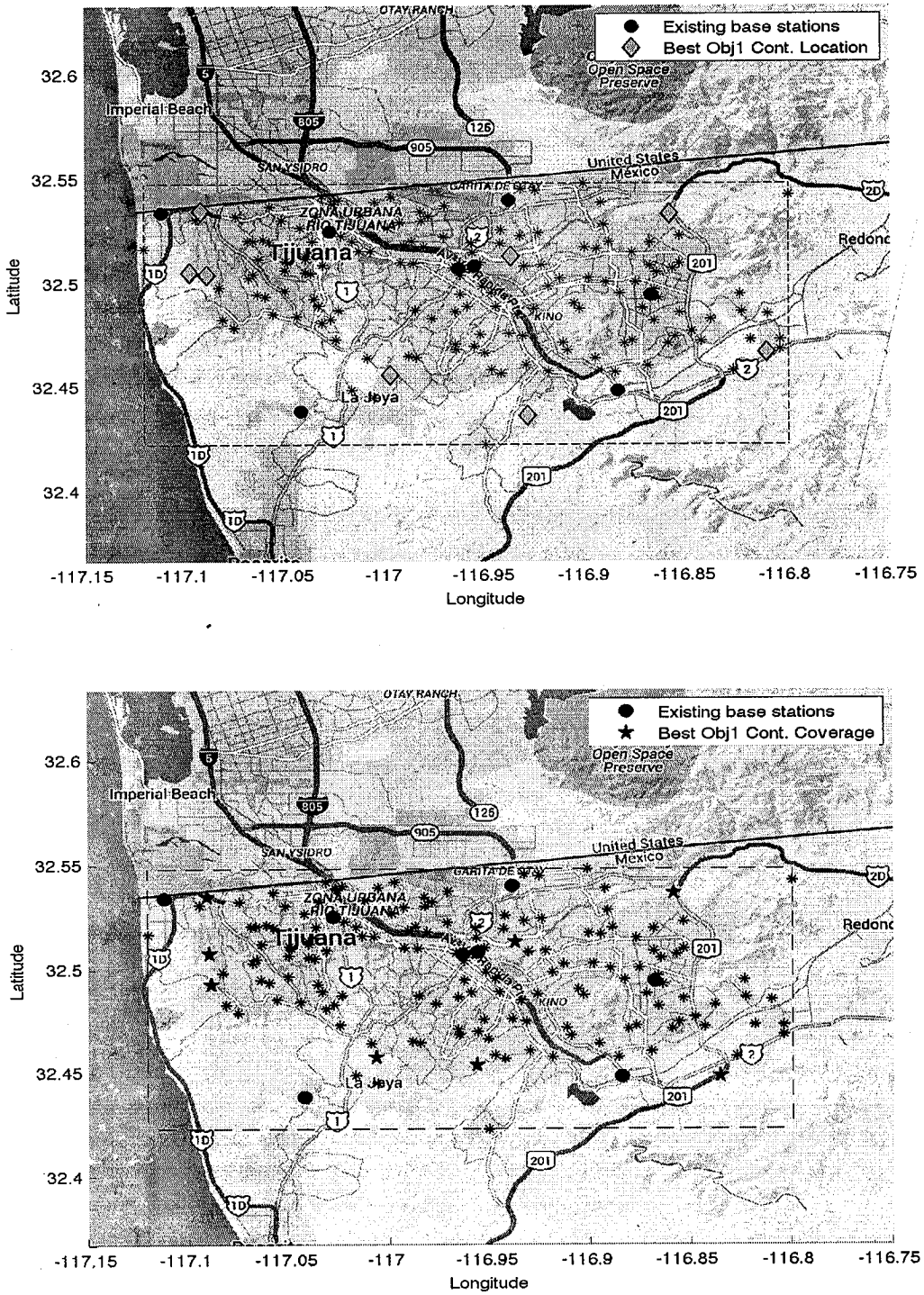


Figure A.5: Locations of the best solution for objetive 1 and for objective 2, $C_{Demand=22}$, Discretization $21 \times 21$, (from top to bottom), Relaxation factor $= 0.1$

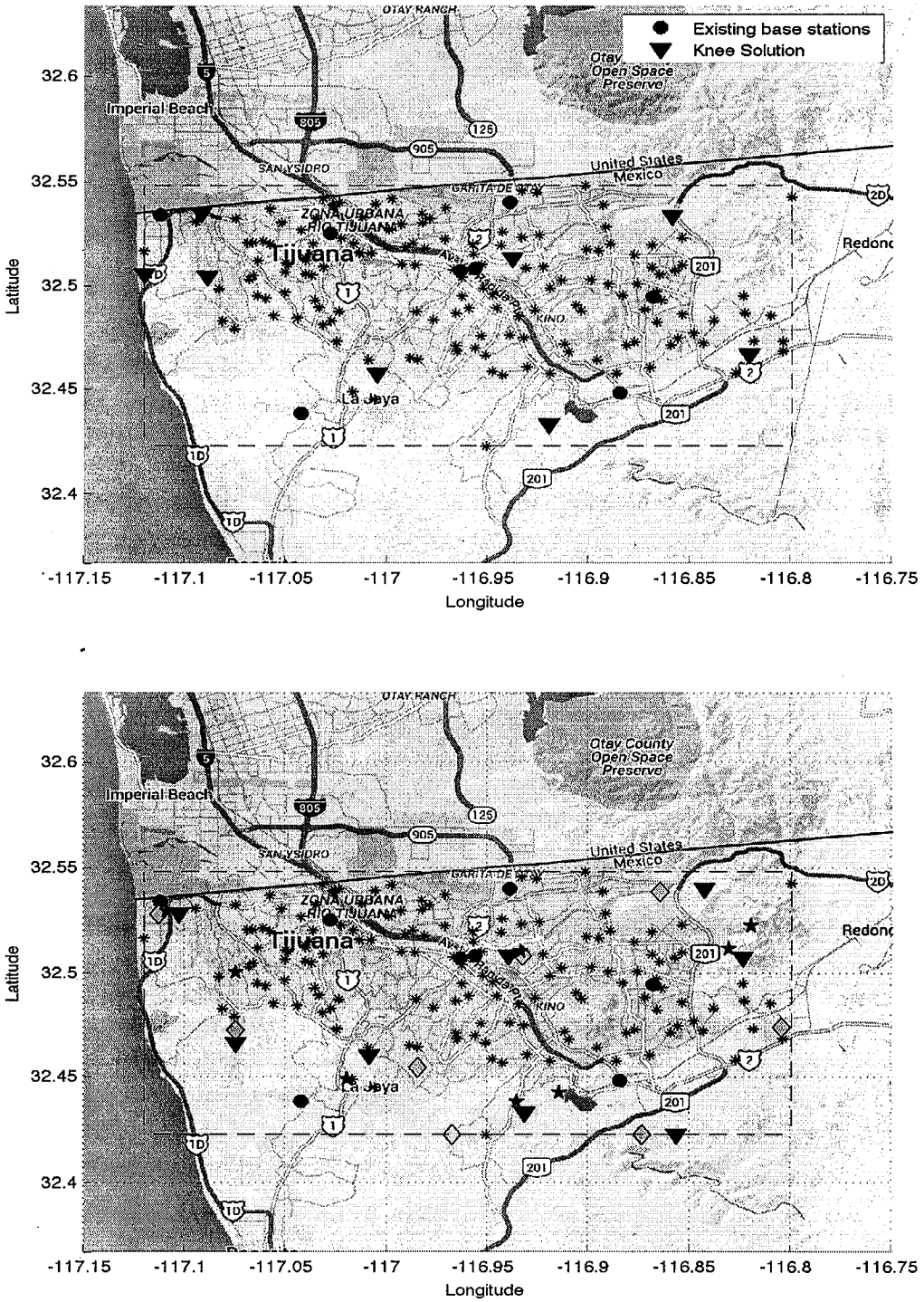


Figure A.6: Locations according to the knee point, The merge for all previous solution locations, $C_{Demand=22}$, Discretization $21 \times 21$, (from top to bottom), Relaxation factor $= 0.1$

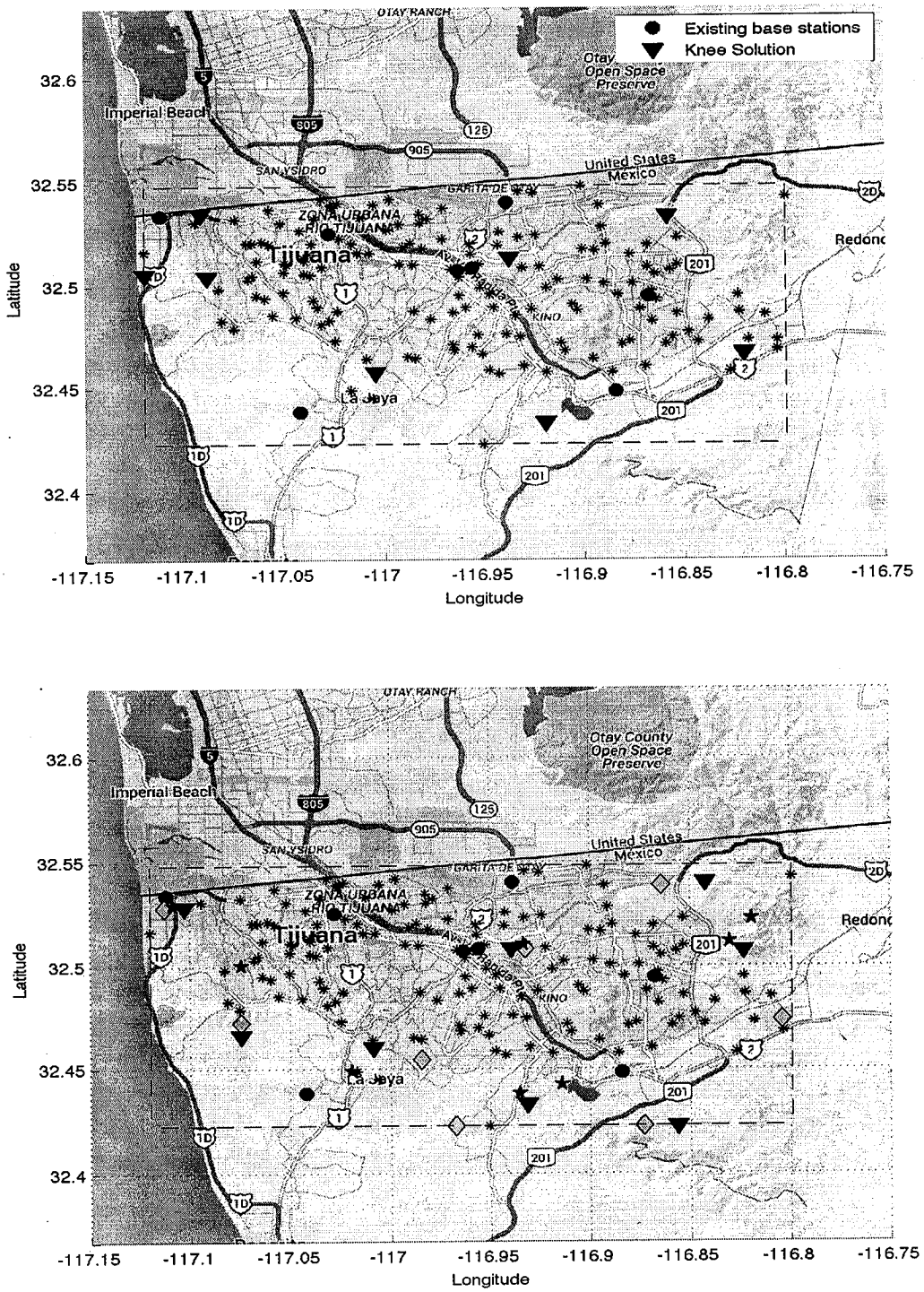


Figure A.6: Locations according to the knee point, The merge for all previous solution locations, $C_{Demand=22}$, Discretization $21 \times 21$, (from top to bottom), Relaxation factor $= 0.1$

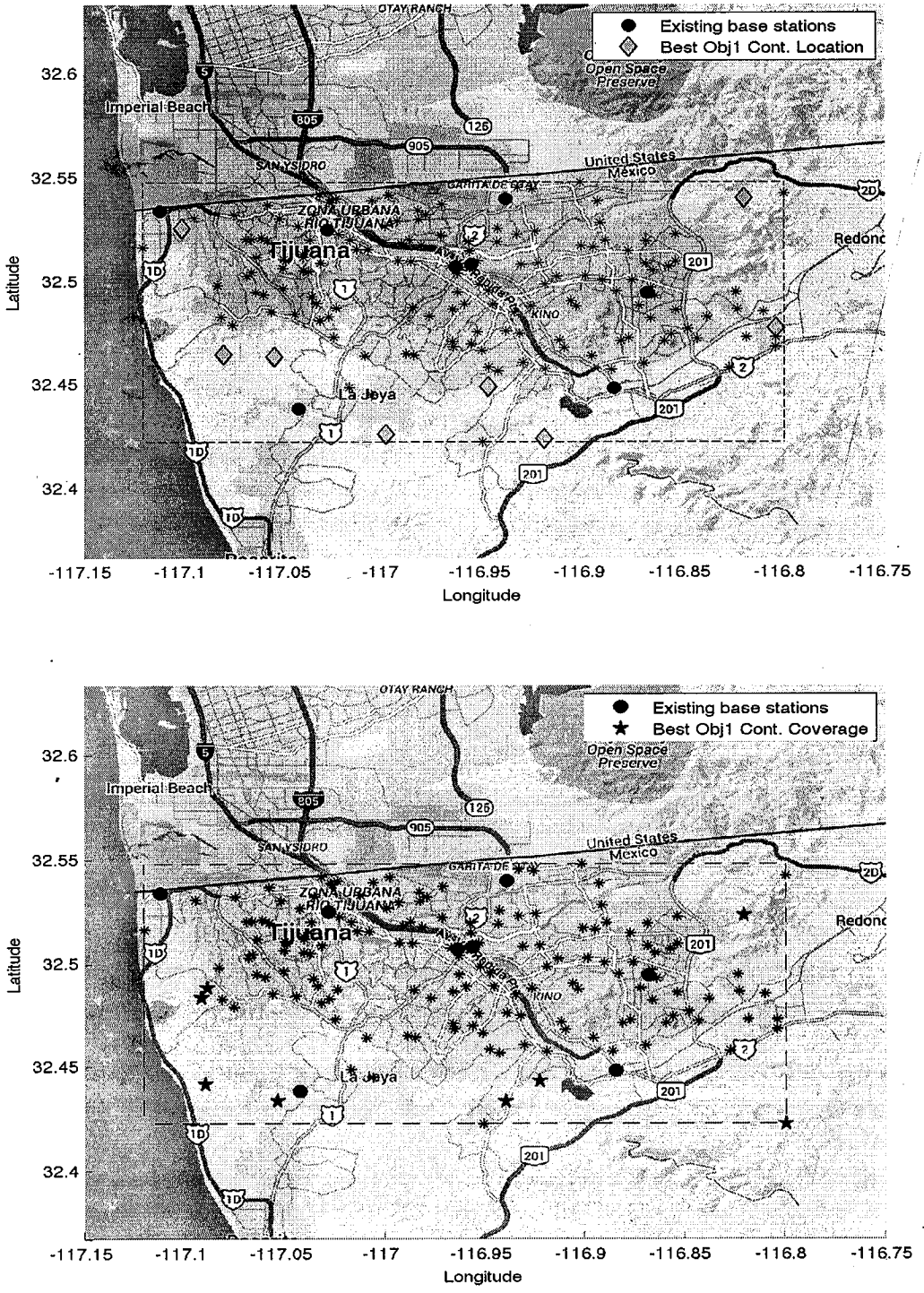


Figure A.7: Locations of the best solution for objetive 1 and for objective 2, $C_{Demand=22}$, Discretization $21 \times 21$, (from top to bottom), Relaxation factor = 0.7

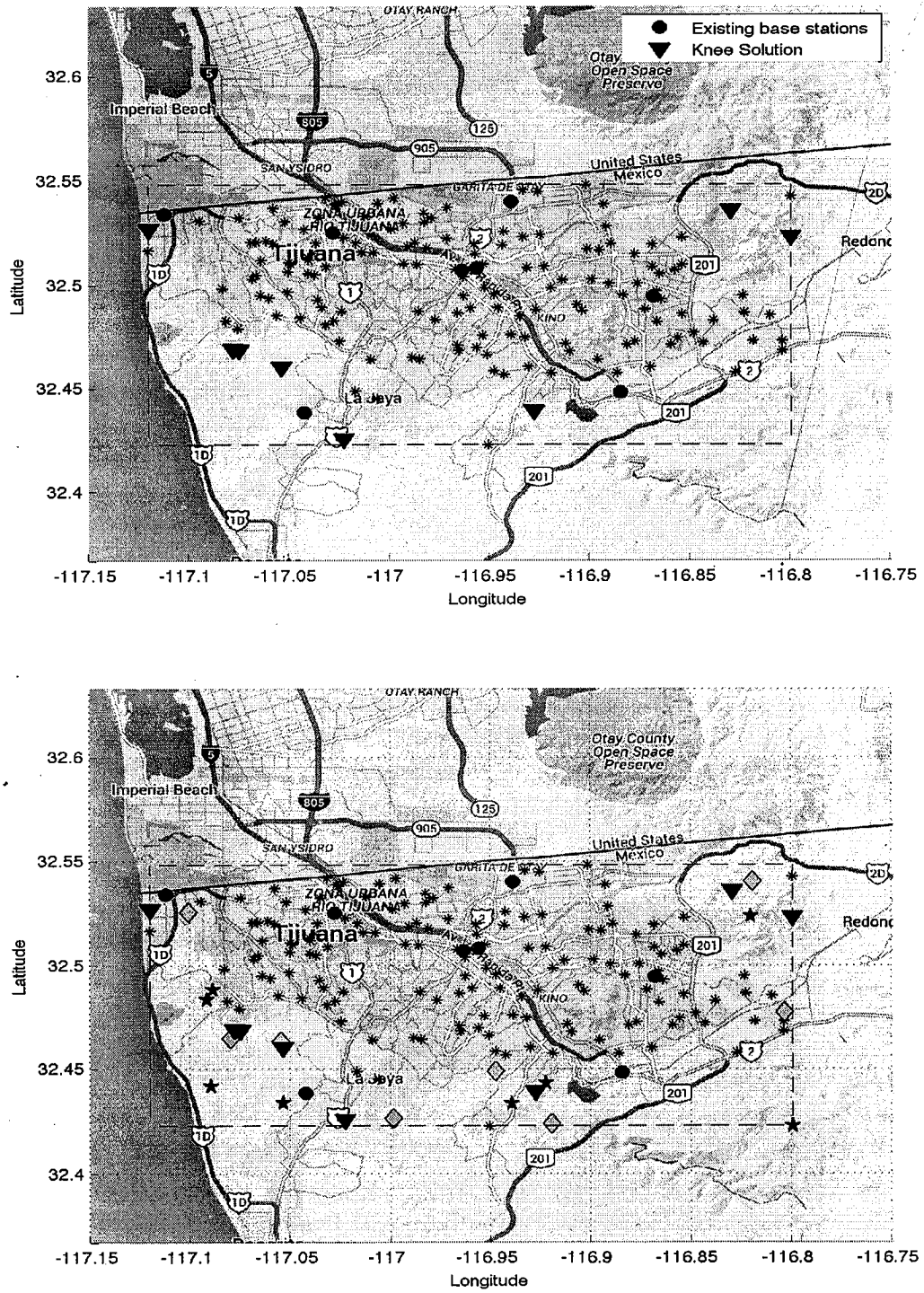


Figure A.8: Locations according to the knee point, The merge for all previous solution locations, $C_{Demand=22}$, Discretization $21 \times 21$, (from top to bottom), Relaxation factor $= 0.7$

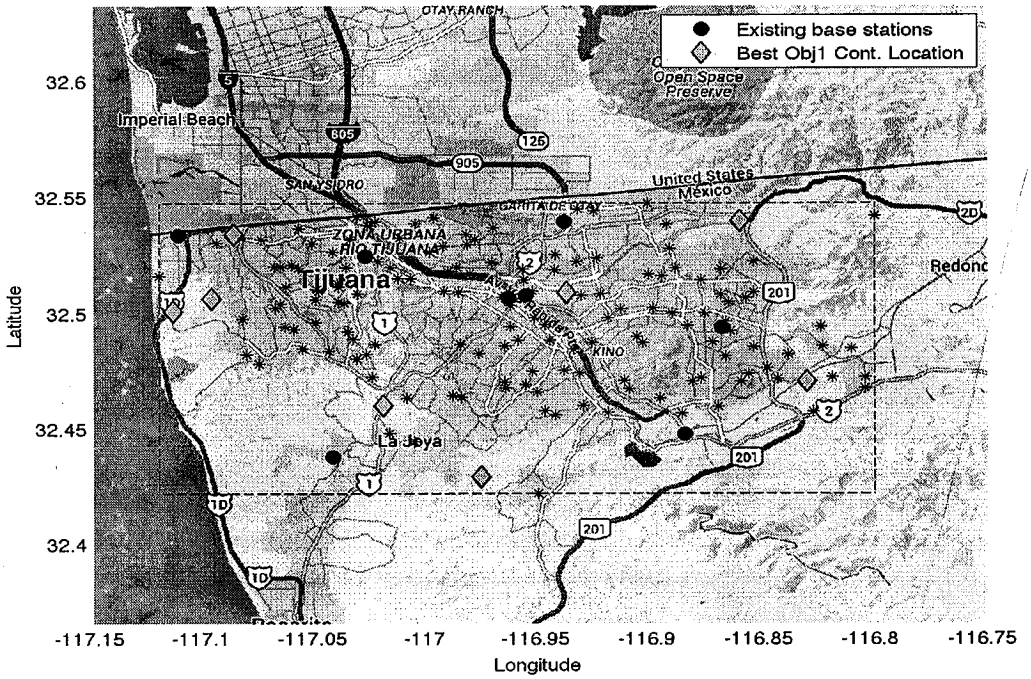


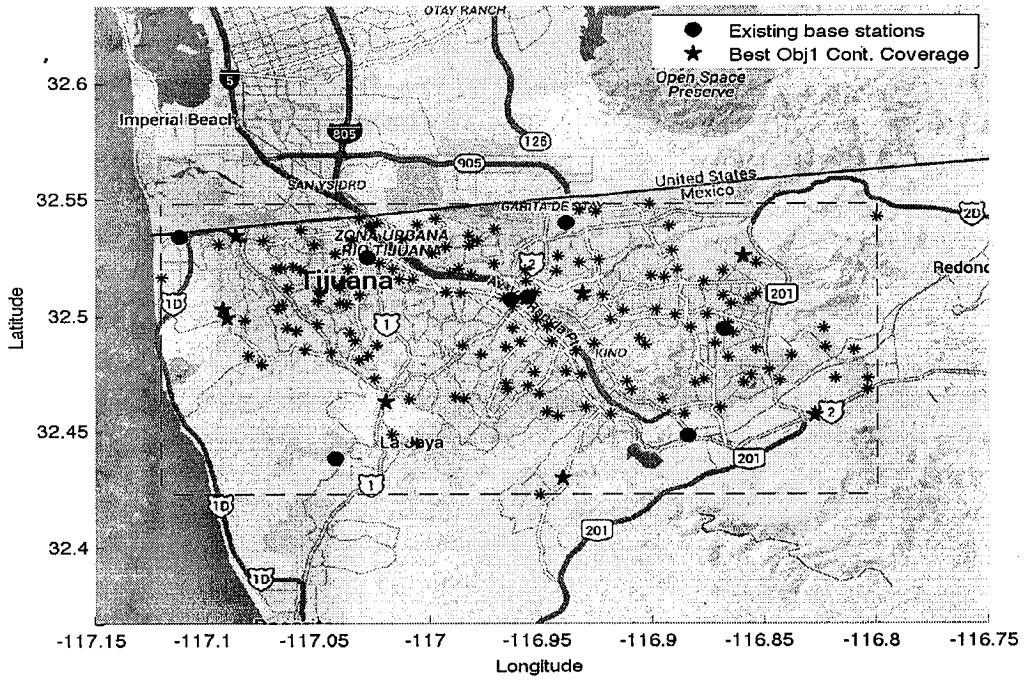


Figure A.9: Locations of the best solution for objetive 1 and for objective 2, $C_{Demand=22}$, Discretization $31 \times 31$, (from top to bottom), Relaxation factor $= 0.1$

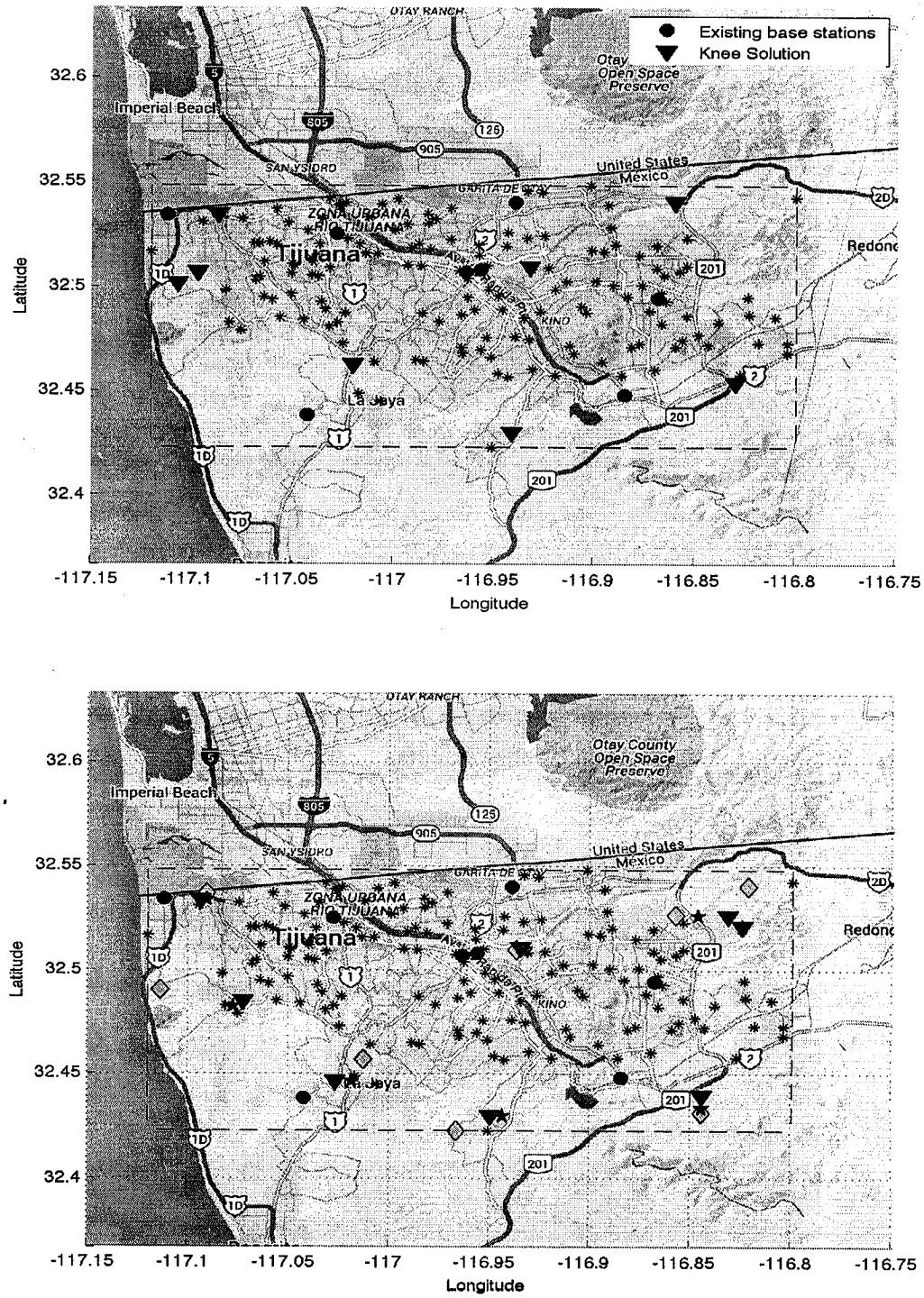


Figure A.10: Locations according to the knee point, The merge for all previous solution locations, $C_{Demand=22}$, Discretization $31 \times 31$, (from top to bottom), Relaxation factor $= 0.1$

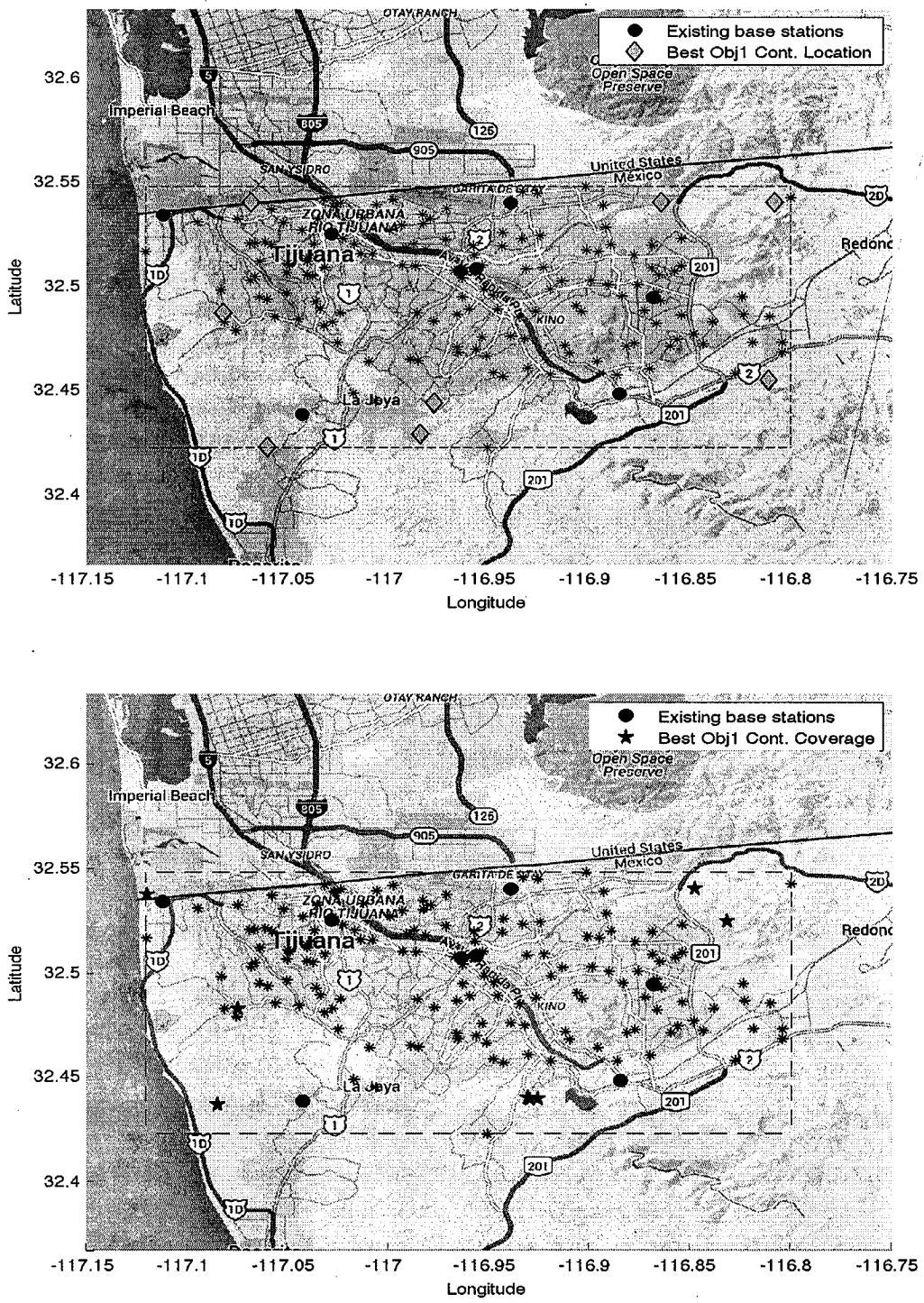


Figure A.11: Locations of the best solution for objetive 1 and for objective 2, $C_{Demand=22}$, Discretization $31 \times 31$, (from top to bottom), Relaxation factor $= 0.7$

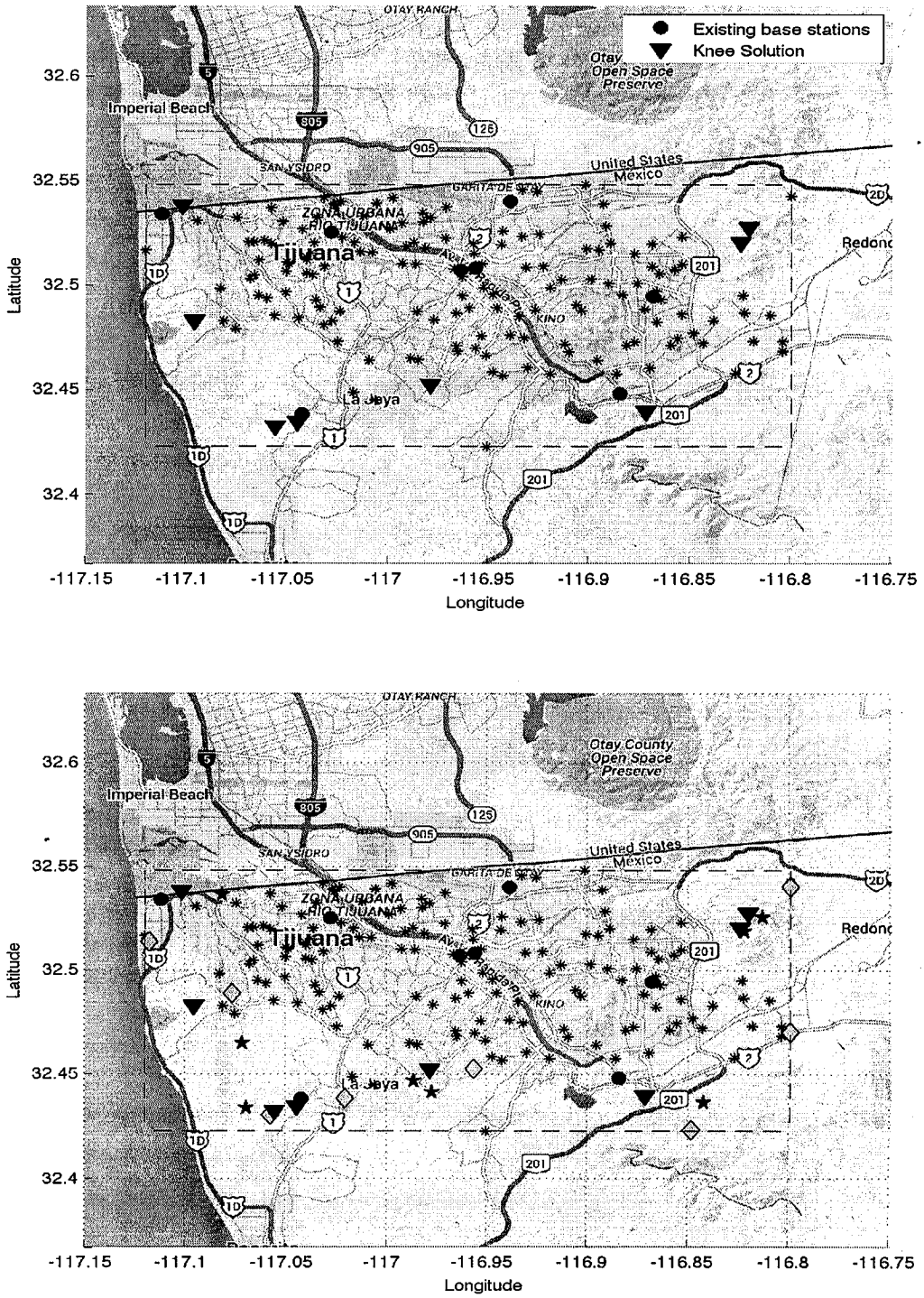


Figure A.12: Locations according to the knee point, The merge for all previous solution locations, $C_{Demand=22}$, Discretization $31 \times 31$, (from top to bottom), Relaxation factor $= 0.7$

## A.2 C demand = 45

As in previous section, here we present the location graphs of the ambulance fleet according to the solution of six different test instances of the Multi-Objective Location Model, these test instances were obtained by setting $C_{Demand} = 45$.

The test instances for which the locations graphs have been included are:
(1) $G = 11 \times 11$, Relaxation factor = 0.1: Figure A.13 and Figure A.14.
(4) $G = 11 \times 11$, Relaxation factor = 0.7: Figure A.15 and Figure A.16.
(5) $G = 21 \times 21$, Relaxation factor = 0.1: Figure A.17 and Figure A.18.
(8) $G = 21 \times 21$, Relaxation factor = 0.7: Figure A.19 and Figure A.20.
(9) $G = 31 \times 31$, Relaxation factor = 0.1: Figure A.21 and Figure A.22.
(12) $G = 31 \times 31$, Relaxation factor = 0.7: Figure A.23 and Figure A.24.

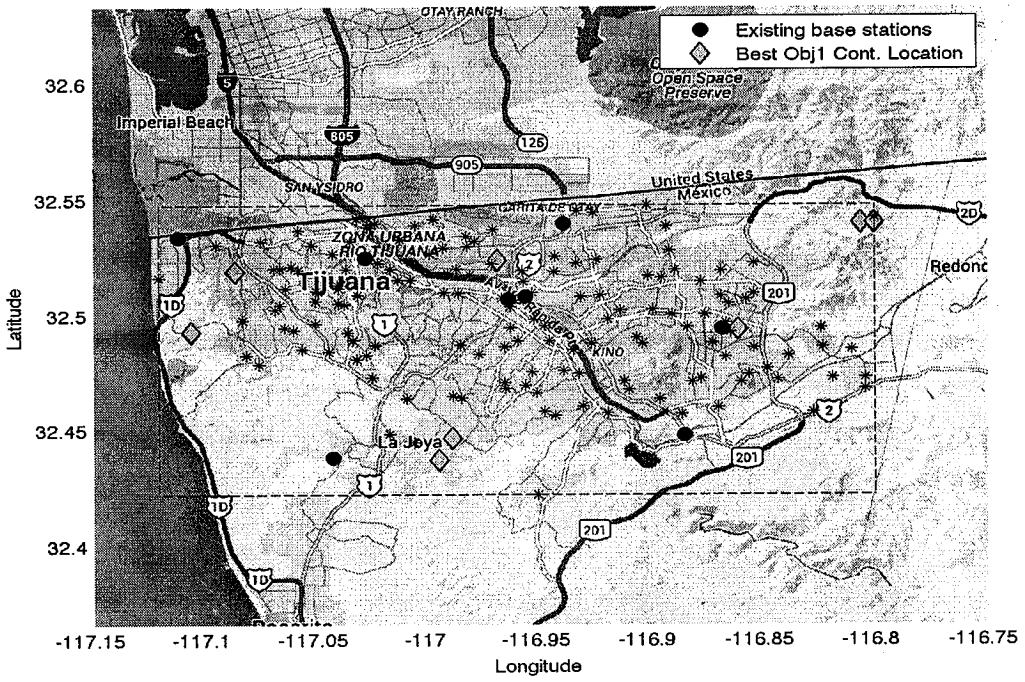


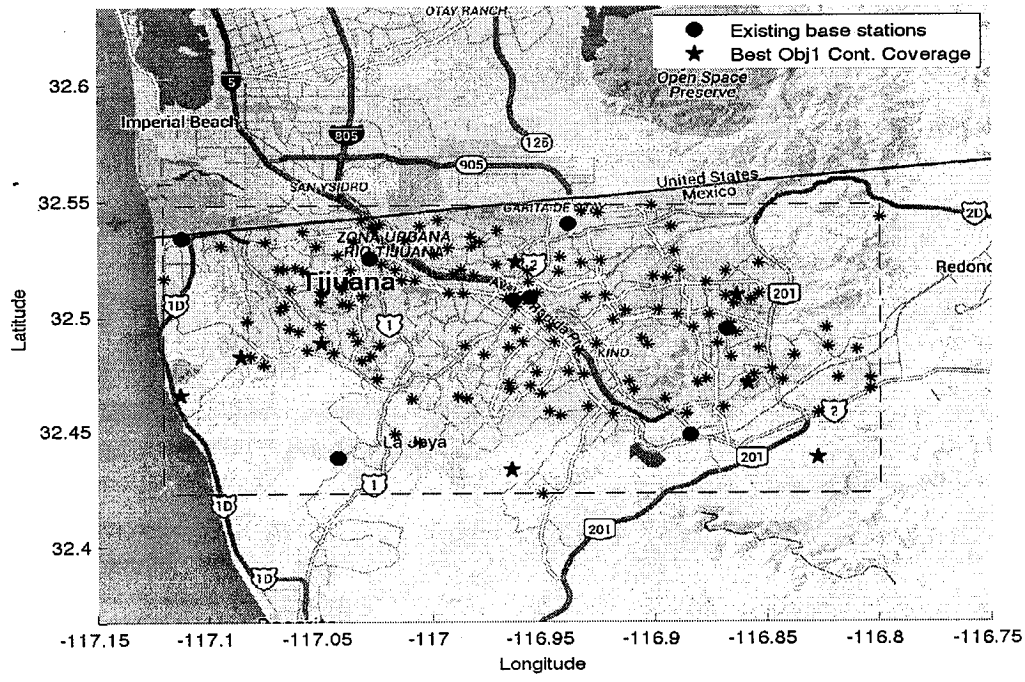


Figure A.13: Locations of the best solution for objetive 1 and for objective 2, $C_{Demand=45}$, Discretization $11 \times 11$ (from top to bottom), Relaxation factor = 0.1

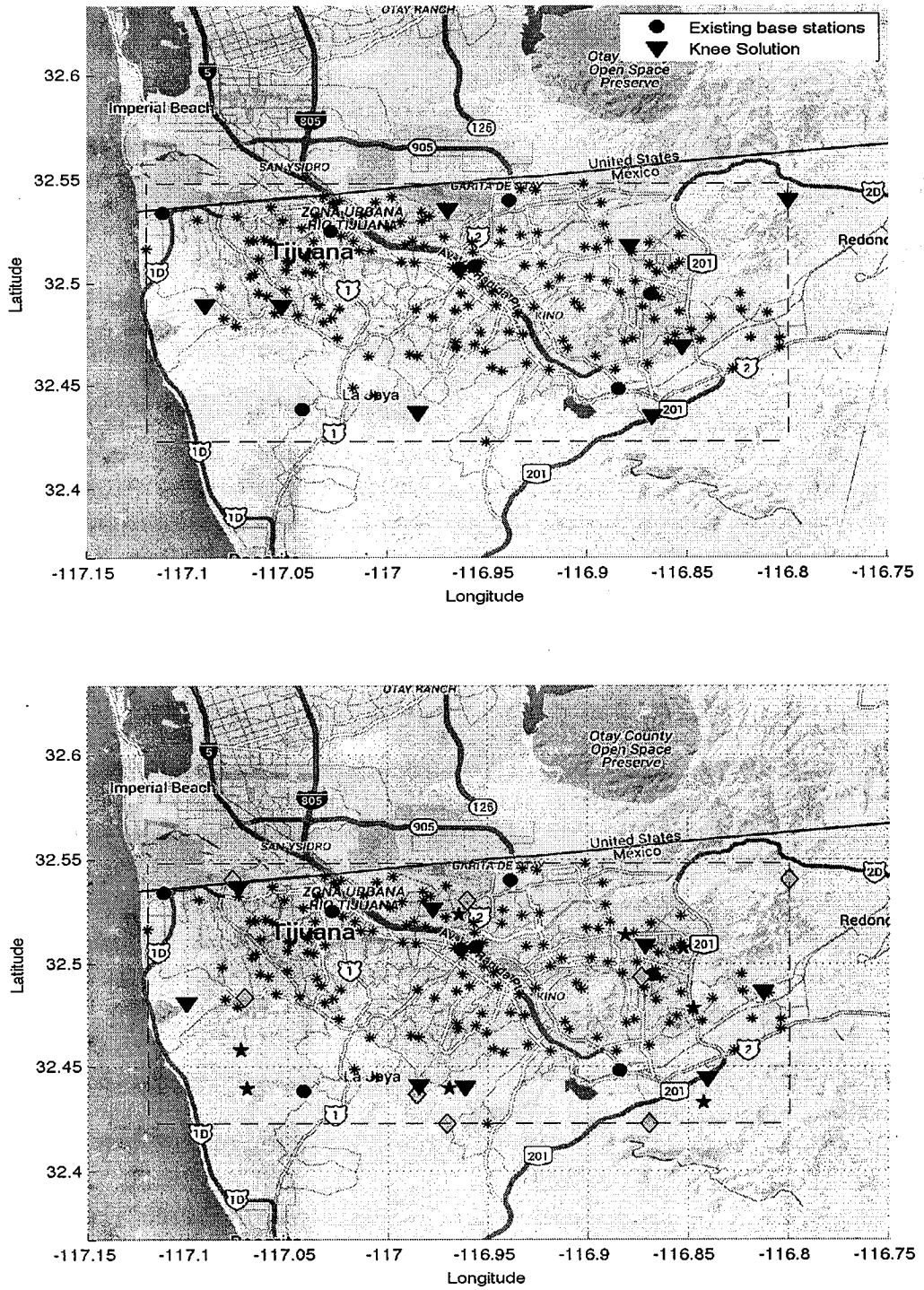


Figure A.14: Locations according to the knee point, The merge for all previous solution locations, $C_{Demand=45}$, Discretization $11 \times 11$ (from top to bottom), Relaxation factor = 0.1

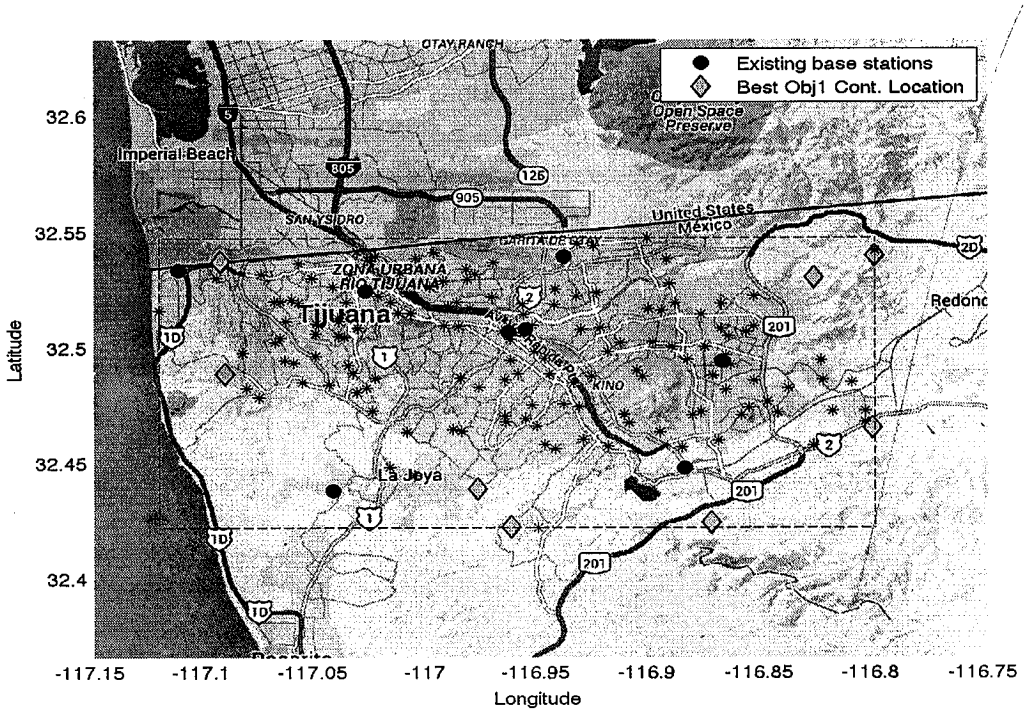


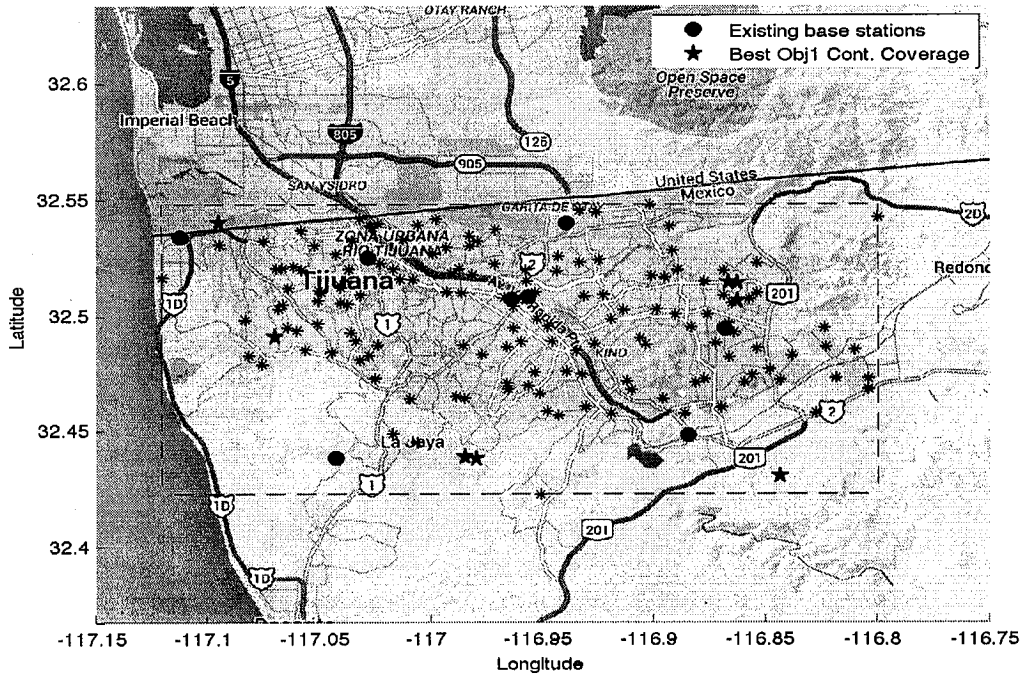


Figure A.15: Locations of the best solution for objetive 1 and for objective 2, $C_{Demand=45}$, Discretization $11 \times 11$ (from top to bottom), Relaxation factor = 0.7

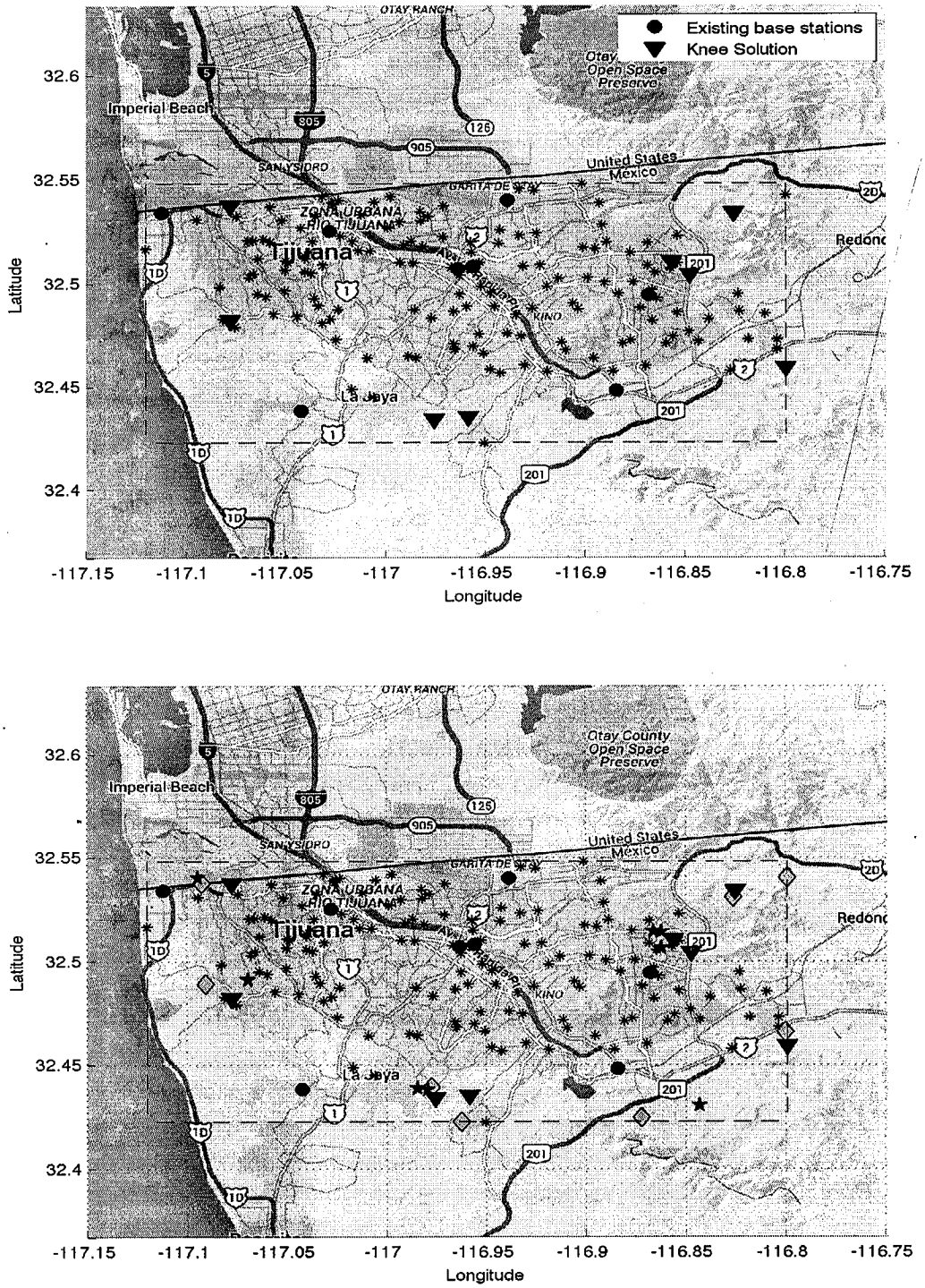


Figure A.16: Locations according to the knee point, The merge for all previous solution locations, $C_{Demand=45}$, Discretization $11 \times 11$ (from top to bottom), Relaxation factor $= 0.7$

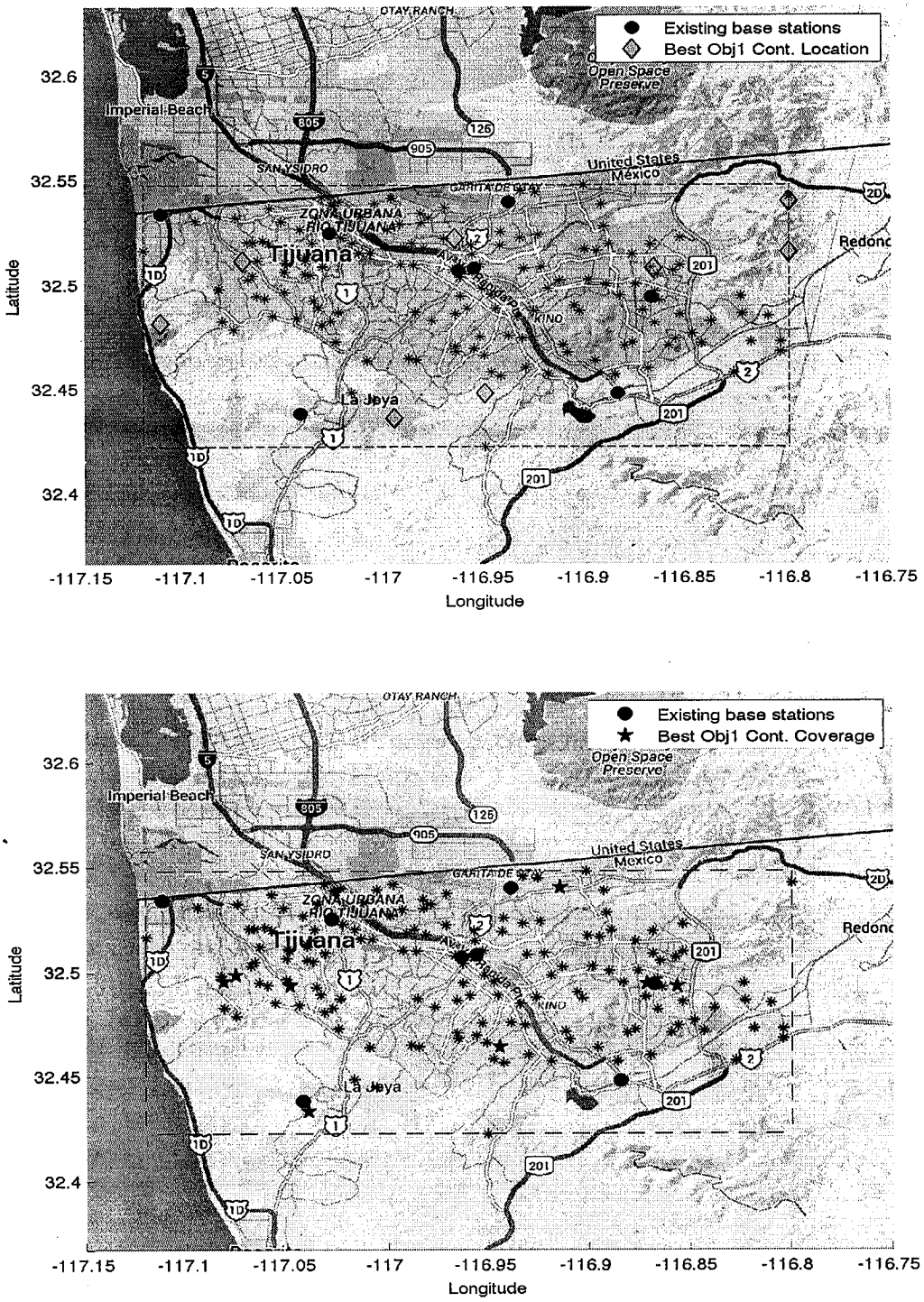


Figure A.17: Locations of the best solution for objetive 1 and for objective 2, $C_{Demand=45}$, Discretization $21 \times 21$, (from top to bottom), Relaxation factor $= 0.1$

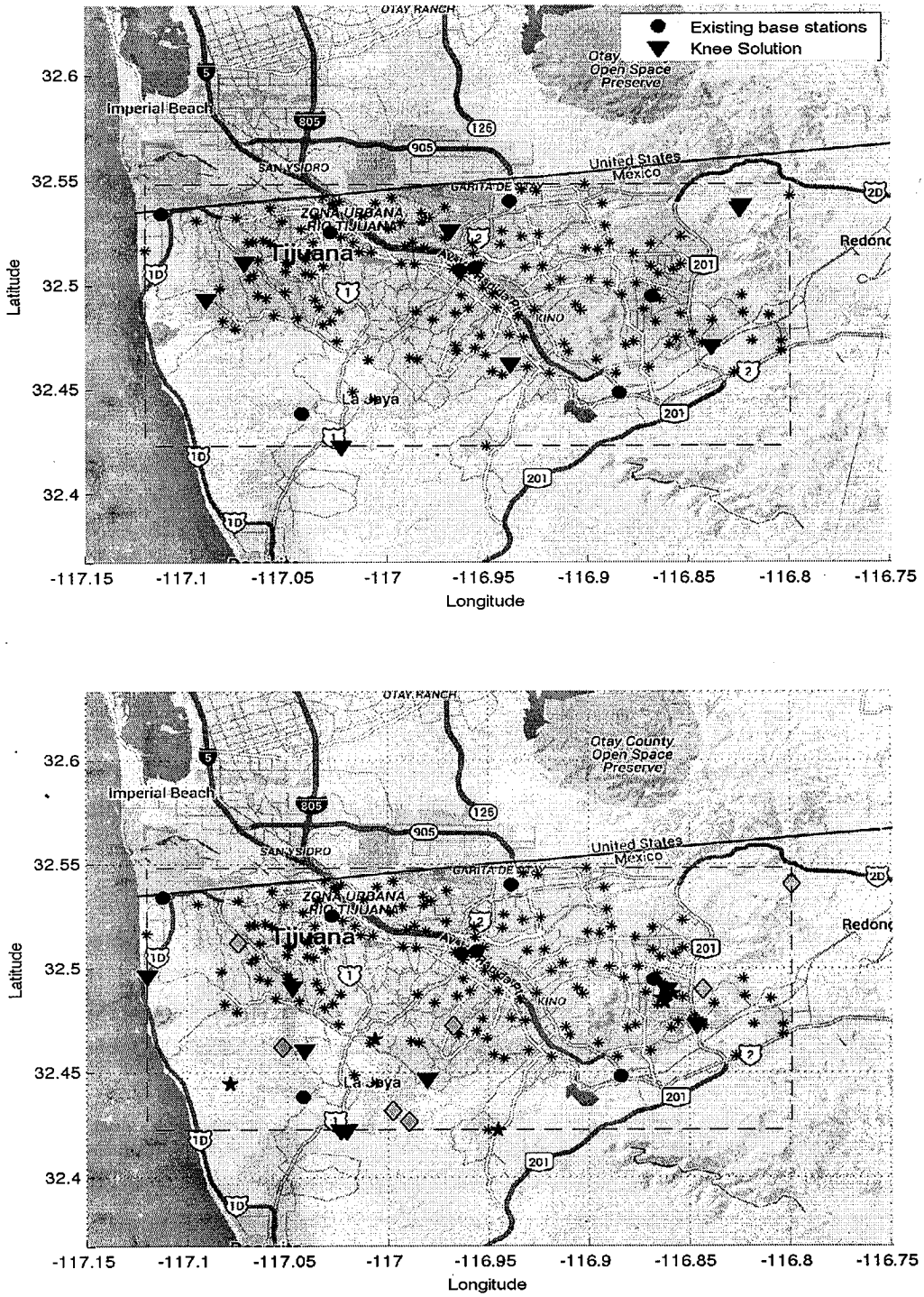


Figure A.18: Locations according to the knee point, The merge for all previous solution locations, $C_{Demand=22}$, Discretization $21 \times 21$, (from top to bottom), Relaxation factor $= 0.1$

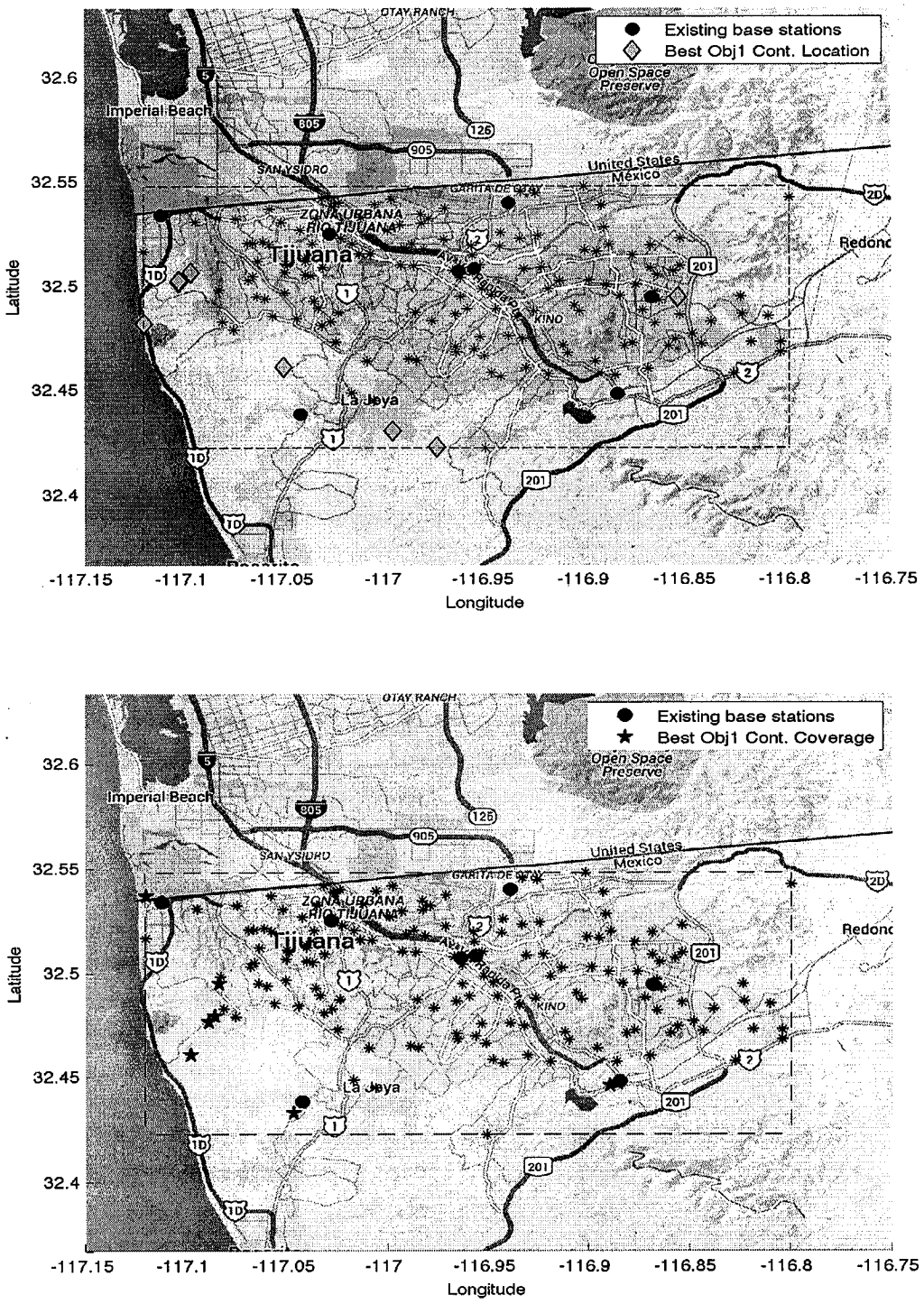


Figure A.19: Locations of the best solution for objetive 1 and for objective 2, $C_{Demand=45}$, Discretization $21 \times 21$, (from top to bottom), Relaxation factor $= 0.7$

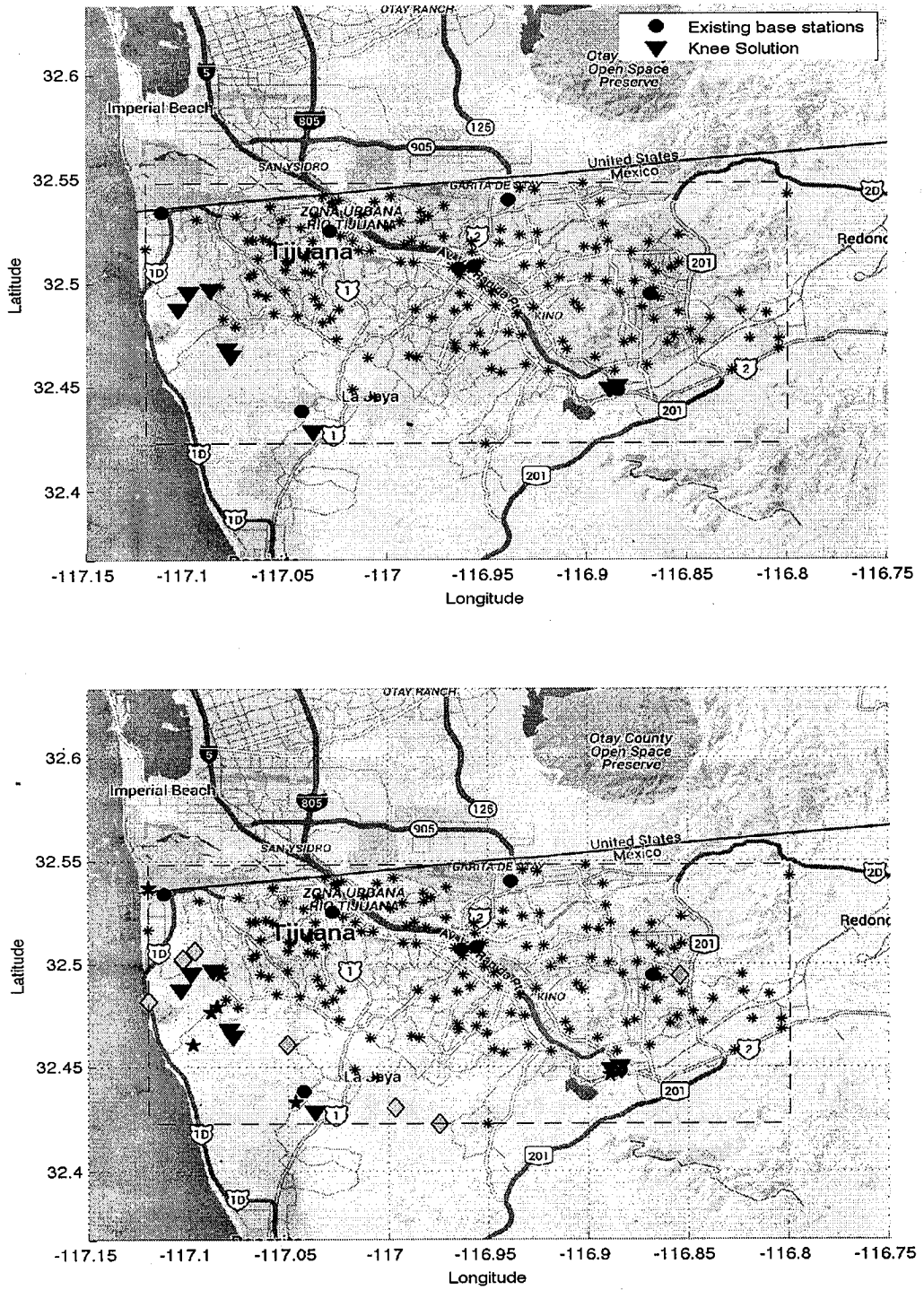


Figure A.20: Locations according to the knee point, The merge for all previous solution locations, $C_{Demand=45}$, Discretization $21 \times 21$, (from top to bottom), Relaxation factor $= 0.7$

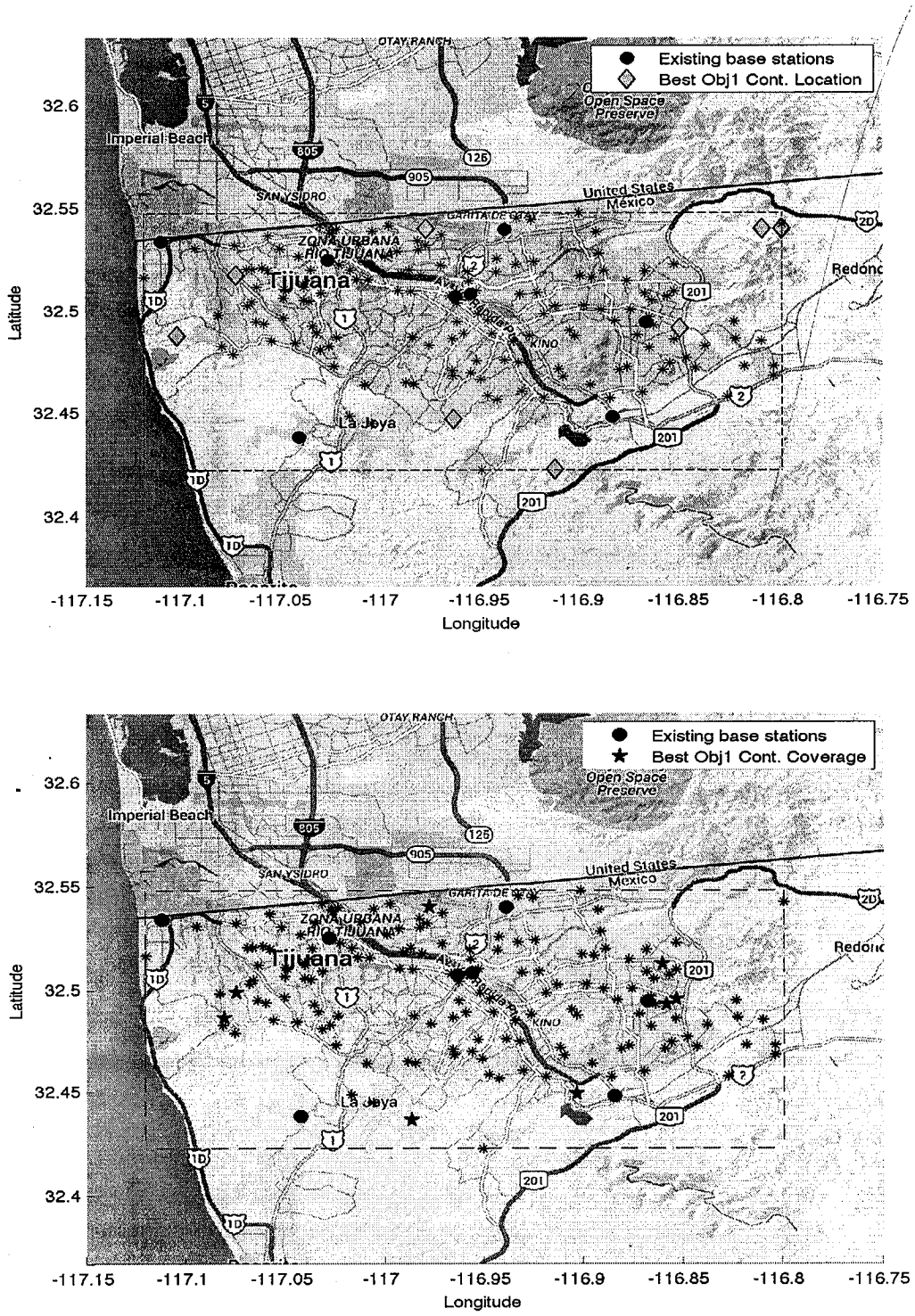


Figure A.21: Locations of the best solution for objetive 1 and for objective 2, $C_{Demand=45}$, Discretization $31 \times 31$, (from top to bottom), Relaxation factor $= 0.1$

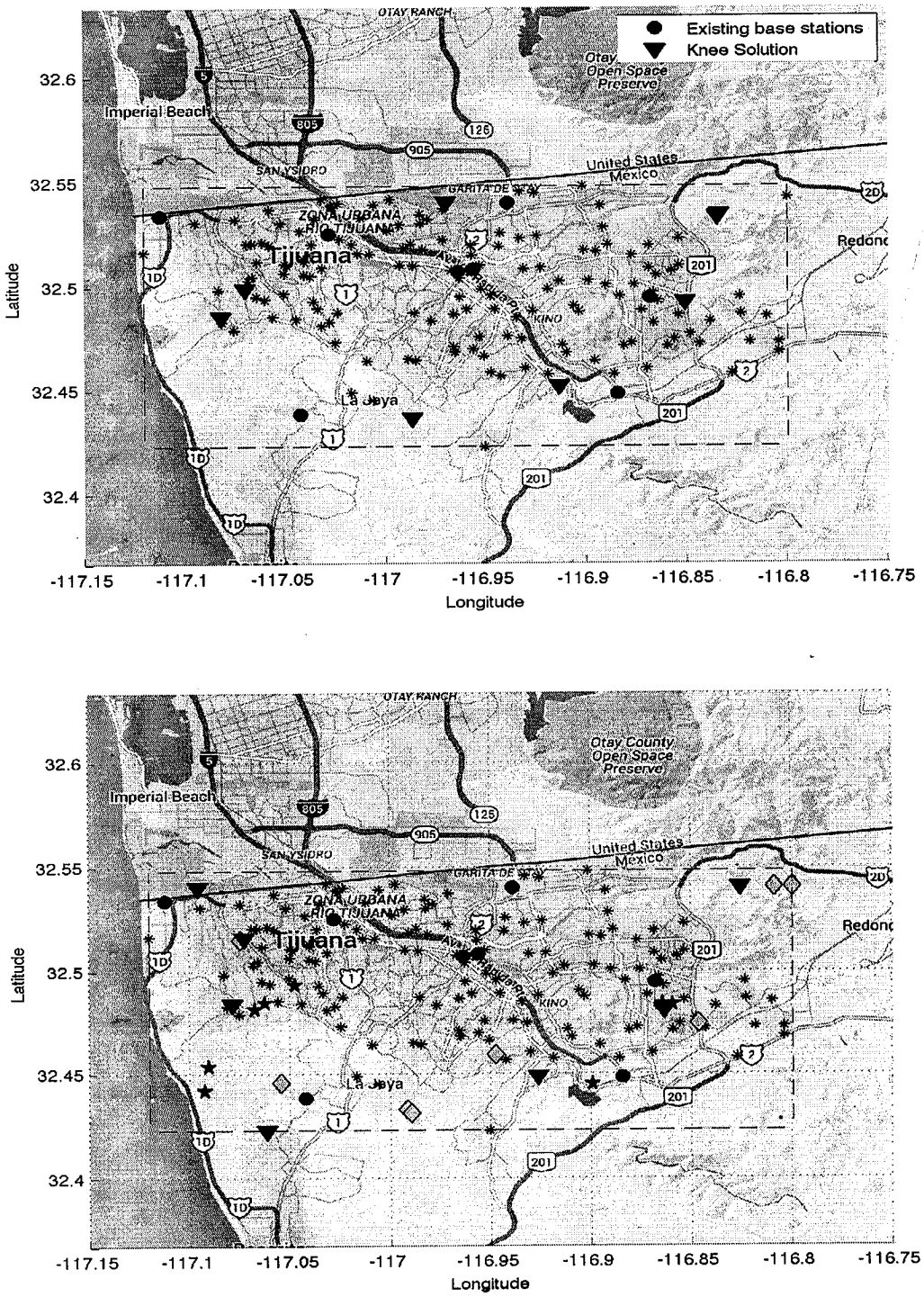


Figure A.22: Locations according to the knee point, The merge for all previous solution locations, $C_{Demand=45}$, Discretization $31 \times 31$, (from top to bottom), Relaxation factor $= 0.1$

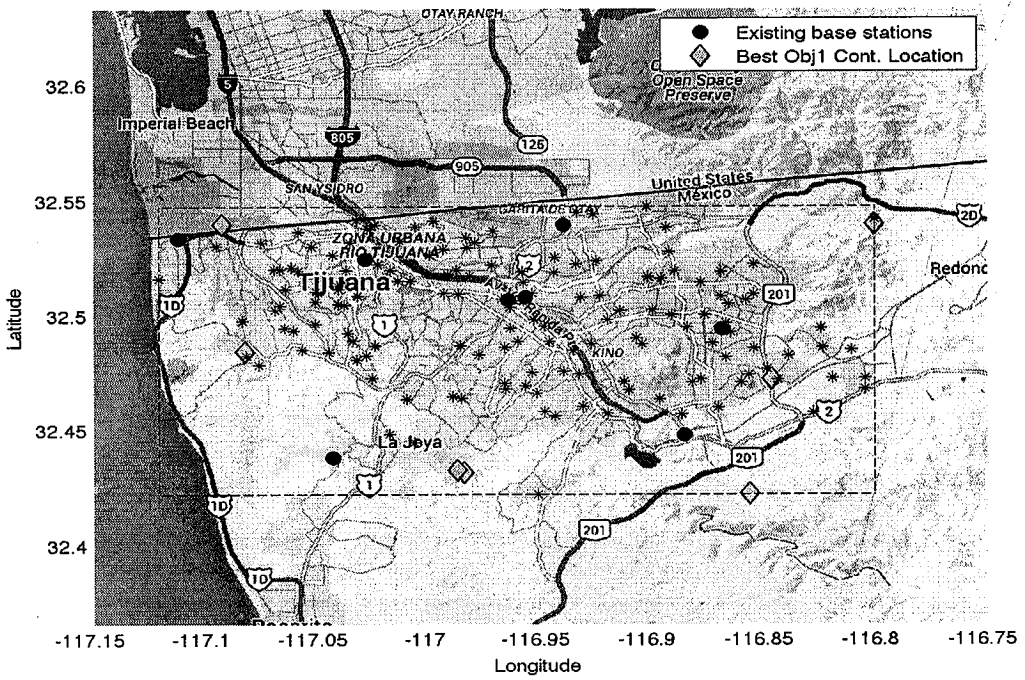


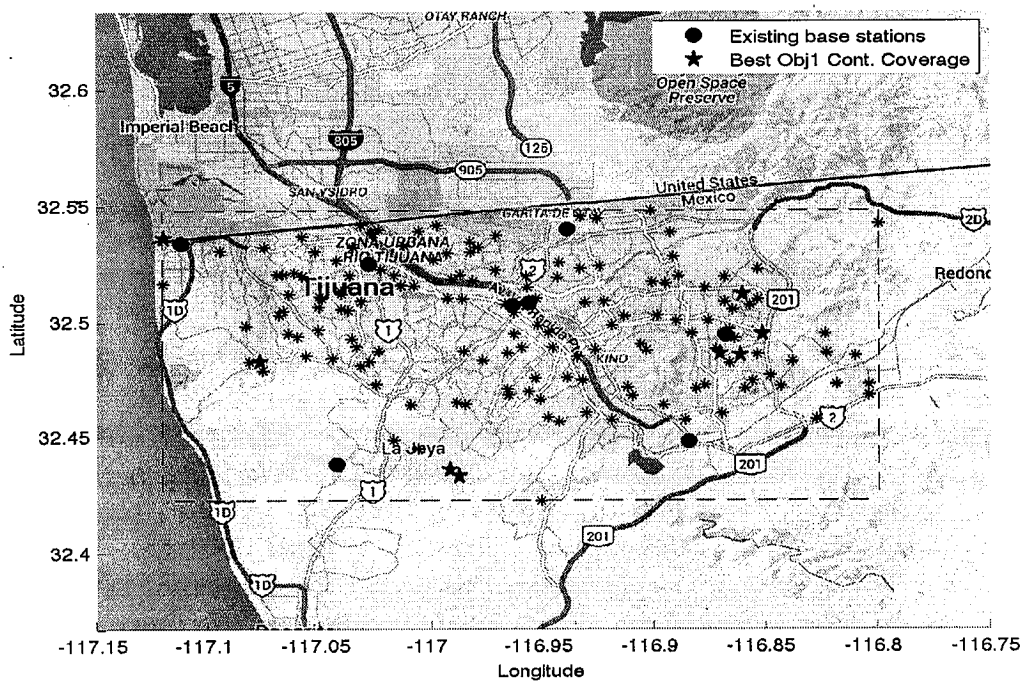


Figure A.23: Locations of the best solution for objetive 1 and for objective 2, $C_{Demand=45}$, Discretization $31 \times 31$, (from top to bottom), Relaxation factor $= 0.7$

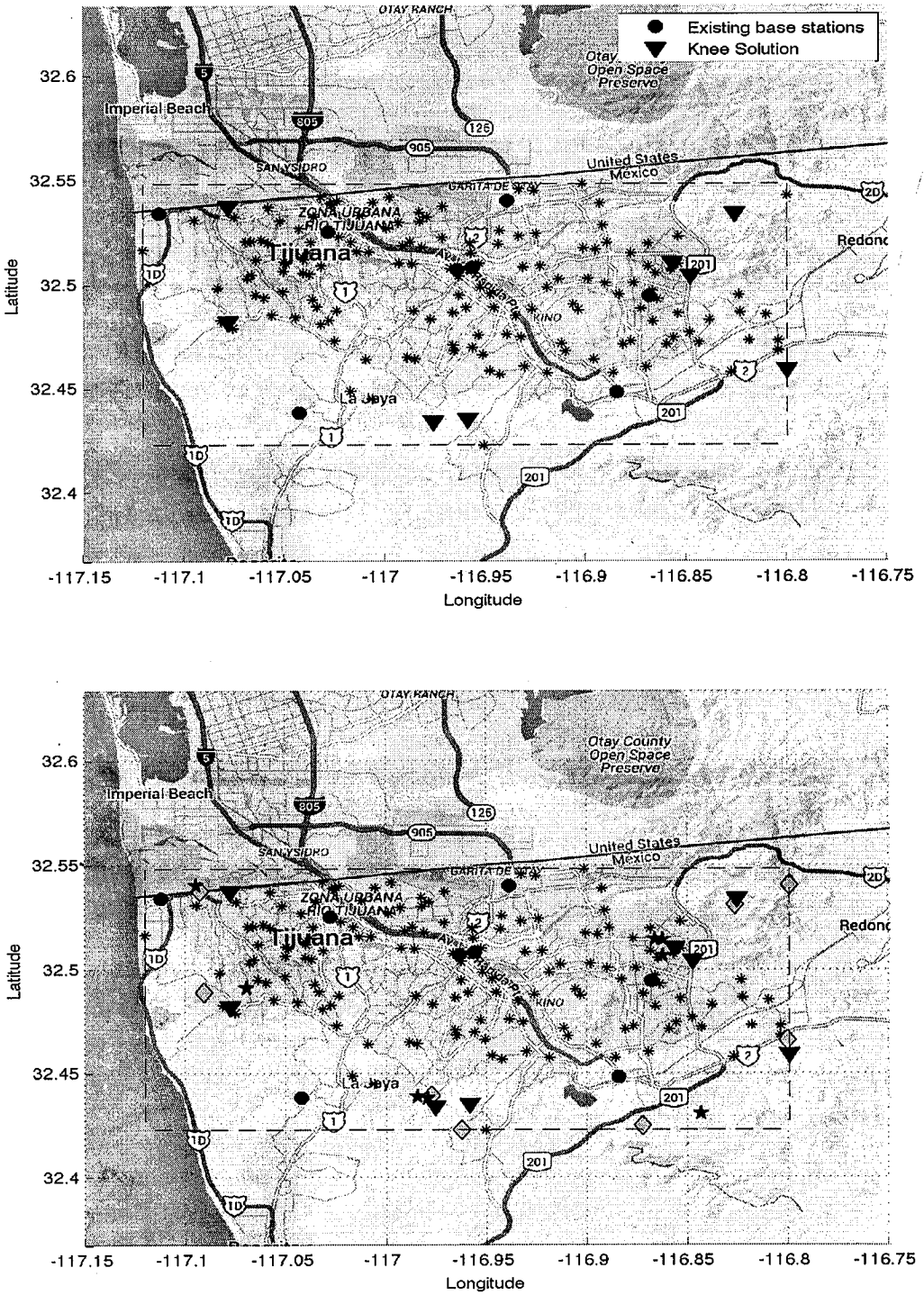


Figure A.24: Locations according to the knee point, The merge for all previous solution locations, $C_{Demand=45}$, Discretization $31 \times 31$, (from top to bottom), Relaxation factor = 0.7

# Appendix B

# Multi-Criteria Model Location Graphs

In this section the location graphs of the ambulance fleet according to the solution of six different test instances of the Multi-Criteria Model Location Graphs are included.

The test instances for which the locations graphs have been included are:

$C_{Demand} = 18$, **Relaxation factor = 0.5** , Location Graphs from Figure B.1 to Figure B.2.

$C_{Demand} = 37$, **Relaxation factor = 0.3** , Location Graphs from Figure B.3 to Figure B.2.

$C_{Demand} = 56$, **Relaxation factor = 0.1** , Location Graphs from Figure B.5 to Figure B.6.

$C_{Demand} = 75$, , **Relaxation factor = 0.5** , Location Graphs from Figure B.7 to Figure B.8.

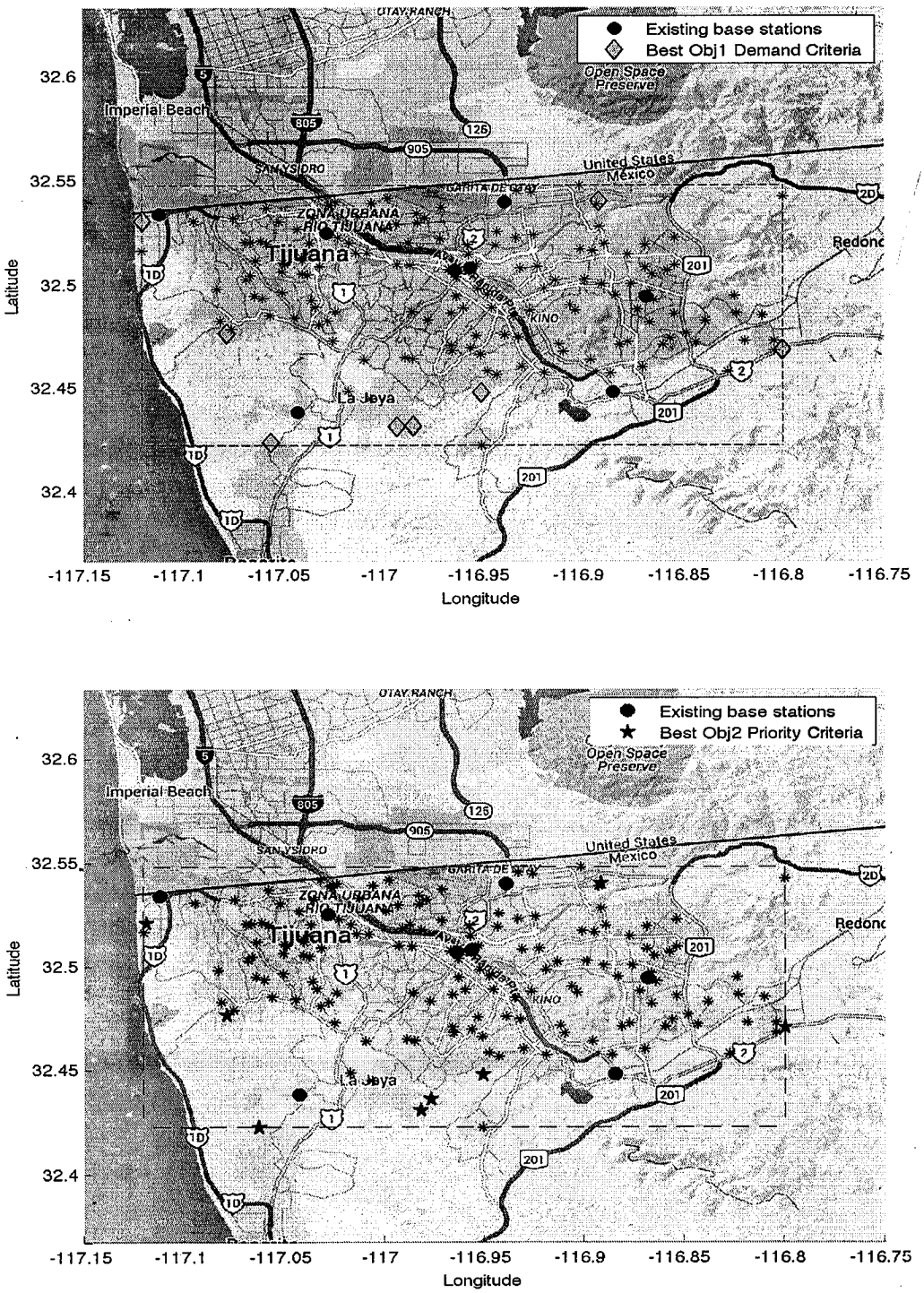


Figure B.1: Locations of the best solution for objetive 1 (Demand Criteria) and for objective 2 (Priority Criteria), $C_{Demand=18}$, Discretization $31 \times 31$, (from top to bottom), Relaxation factor = 0.5

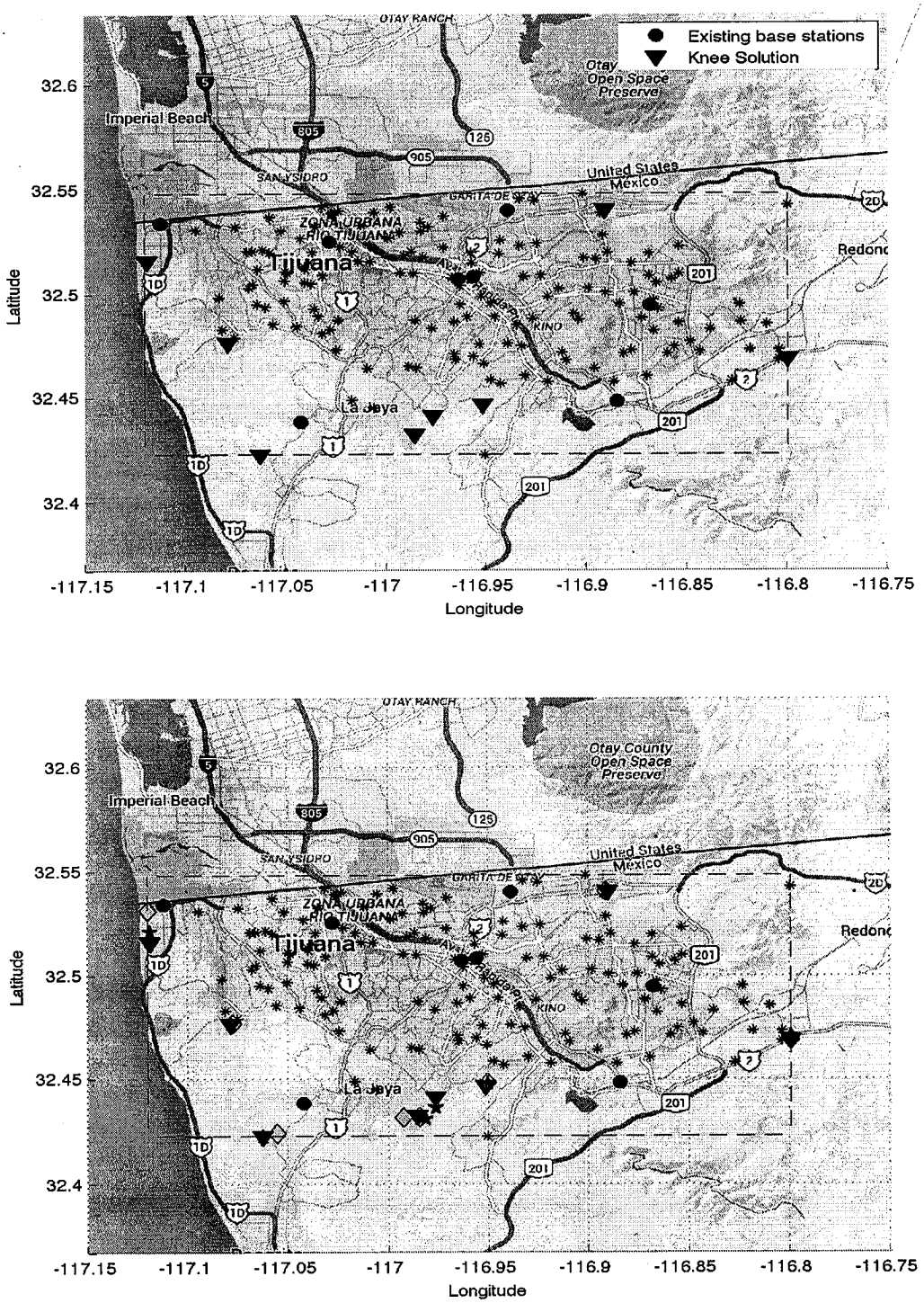


Figure B.2: Locations according to the knee point, The merge for all previous solution locations, $C_{Demand=18}$, Discretization $31 \times 31$, (from top to bottom), Relaxation factor $= 0.5$

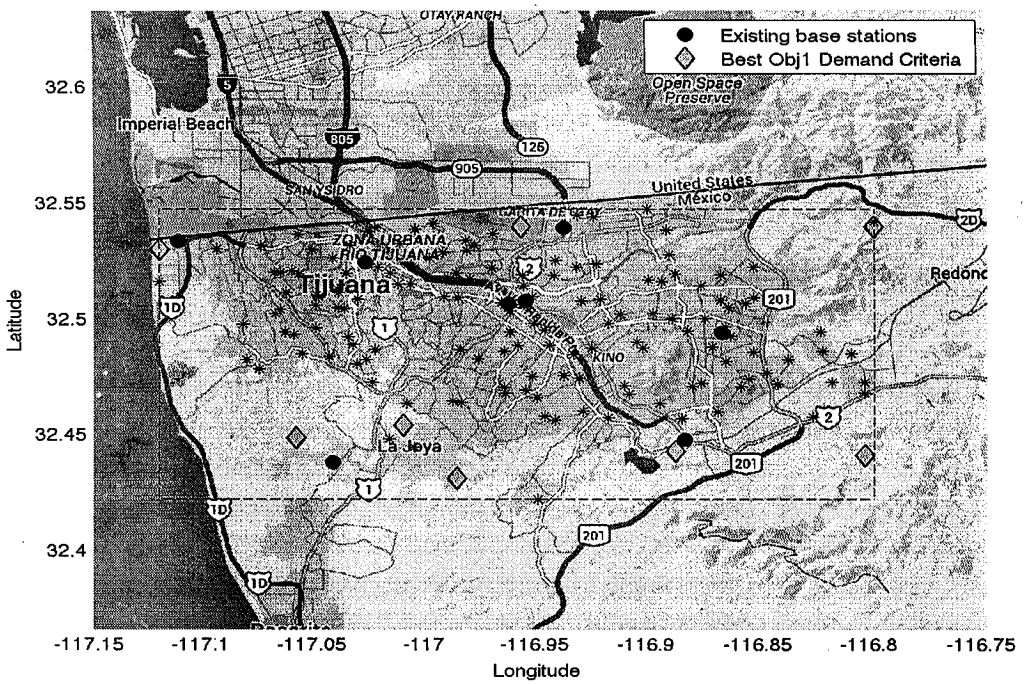


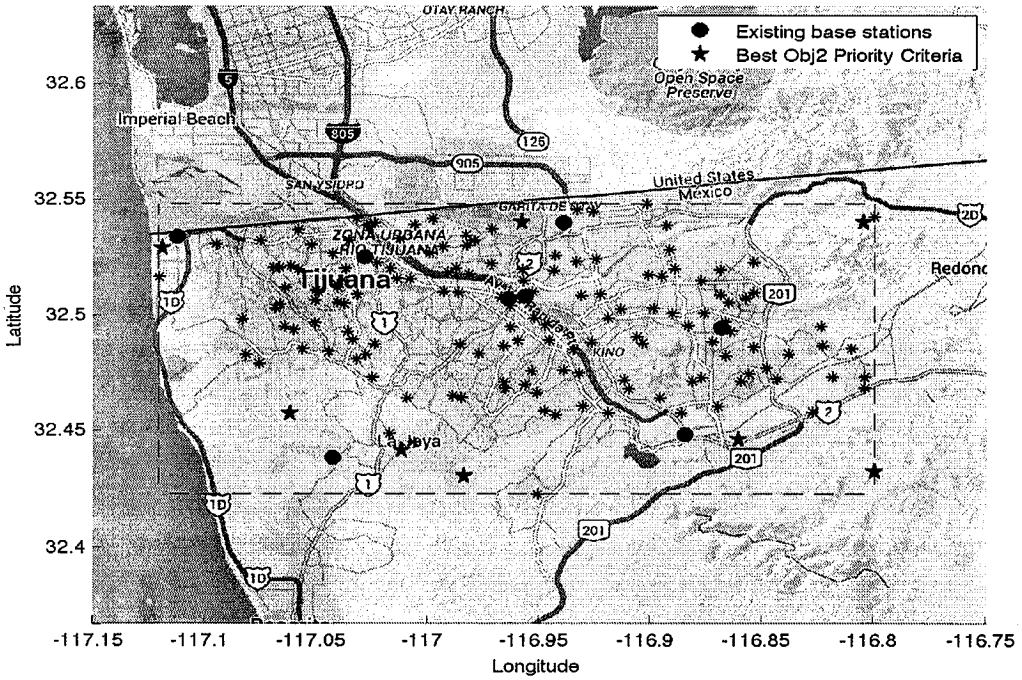


Figure B.3: Locations of the best solution for objetive 1 (Demand Criteria) and for objective 2 (Priority Criteria), $C_{Demand=37}$, Discretization $31 \times 31$, (from top to bottom), Relaxation factor $= 0.3$

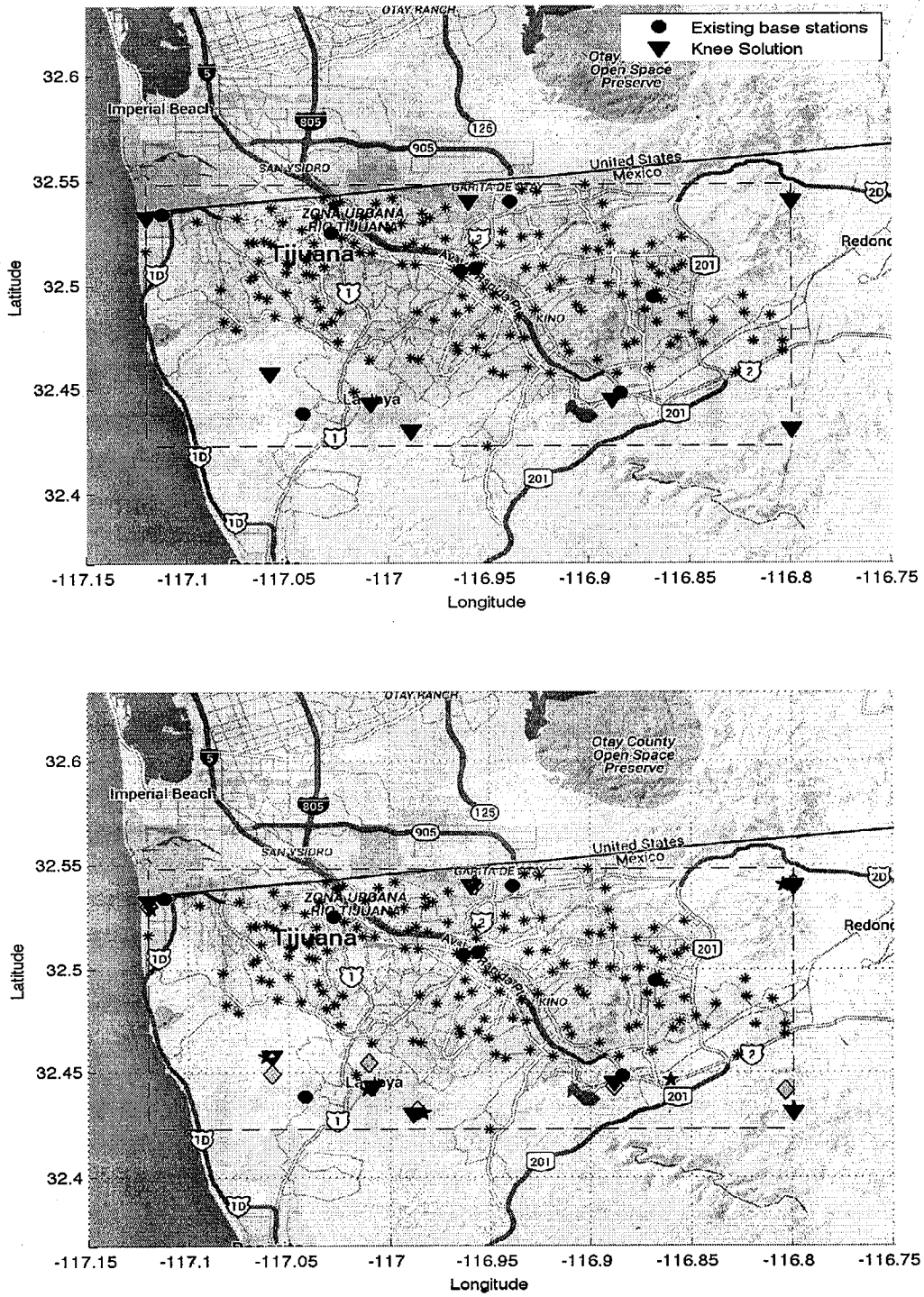


Figure B.4: Locations according to the knee point, The merge for all previous solution locations, $C_{Demand=37}$, Discretization $31 \times 31$, (from top to bottom), Relaxation factor $= 0.3$

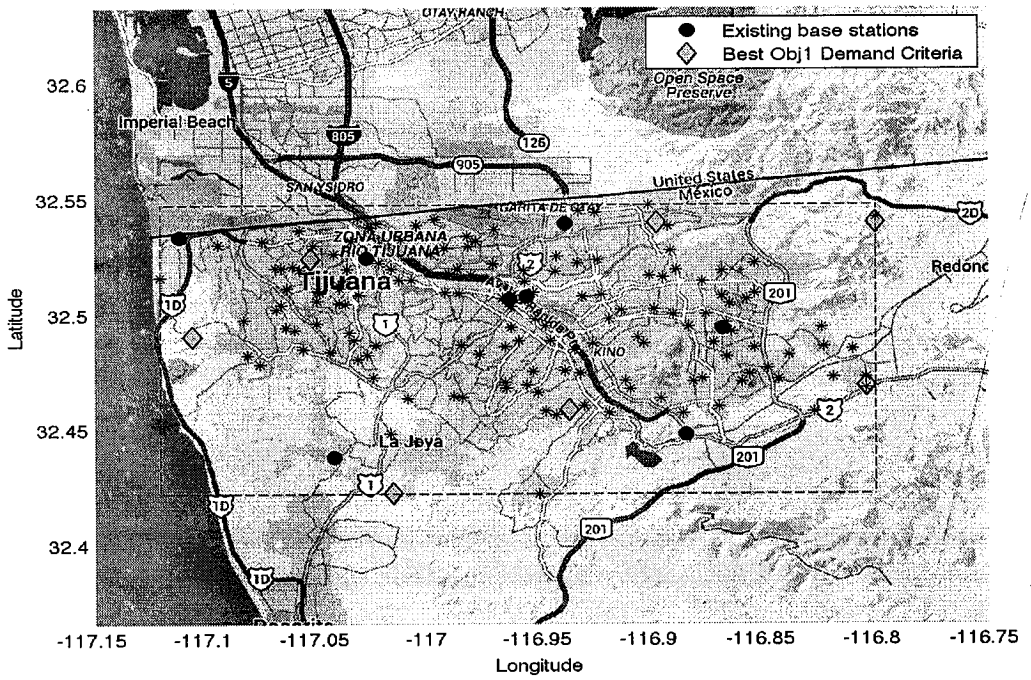


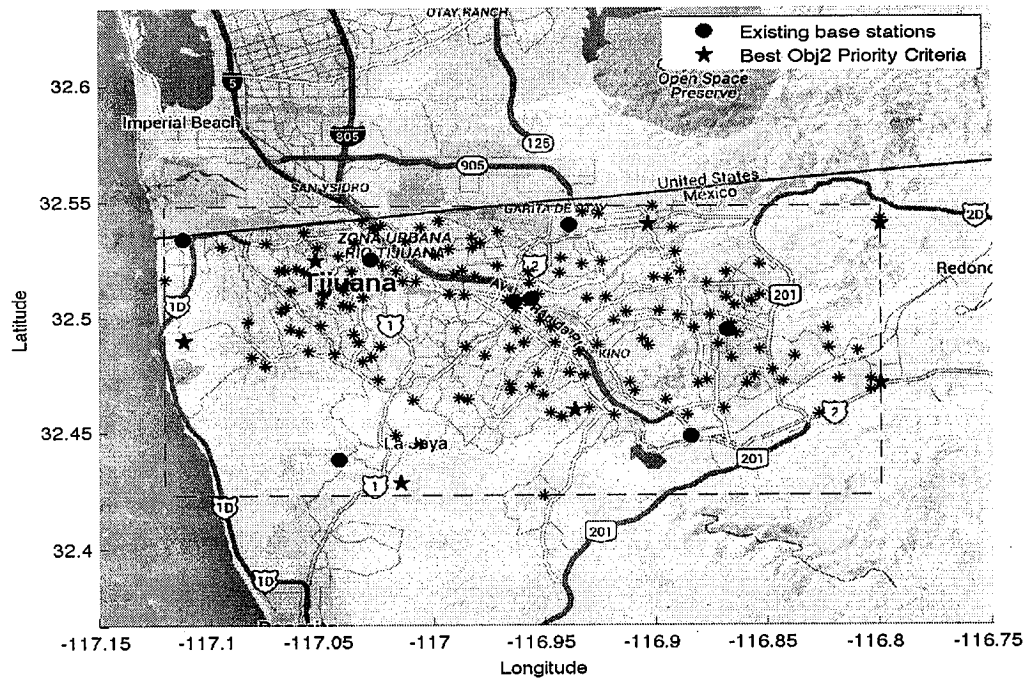


Figure B.5: Locations of the best solution for objetive 1 (Demand Criteria) and for objective 2 (Priority Criteria), $C_{Demand=56}$, Discretization $31 \times 31$, (from top to bottom), Relaxation factor = 0.1

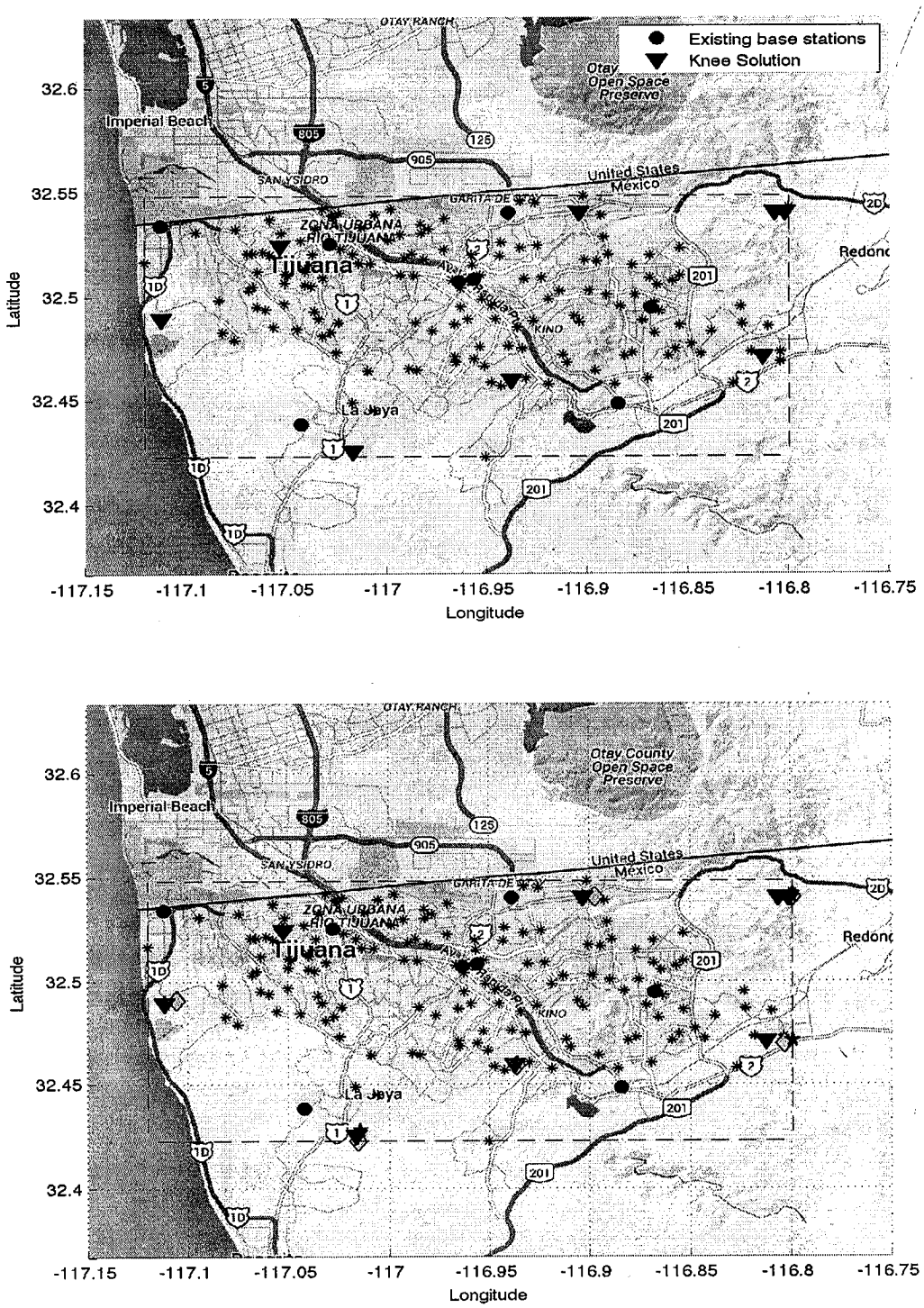


Figure B.6: Locations according to the knee point, The merge for all previous solution locations, $C_{Demand=56}$, Discretization $31 \times 31$, (from top to bottom), Relaxation factor $= 0.1$

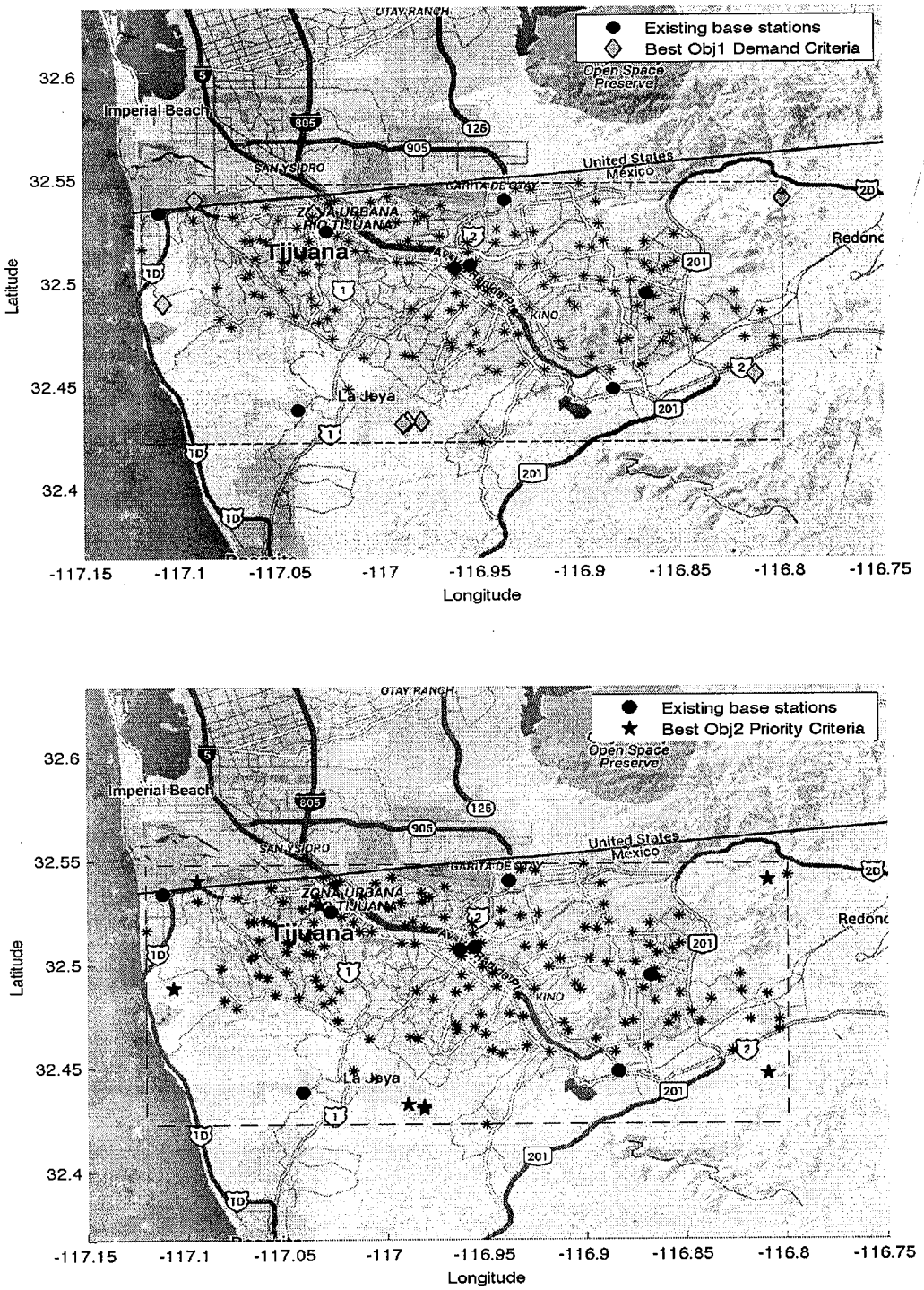


Figure B.7: Locations of the best solution for objetive 1 (Demand Criteria) and for objective 2 (Priority Criteria),$C_{Demand=75}$, Discretization 31 × 31, (from top to bottom), Relaxation factor = 0.5

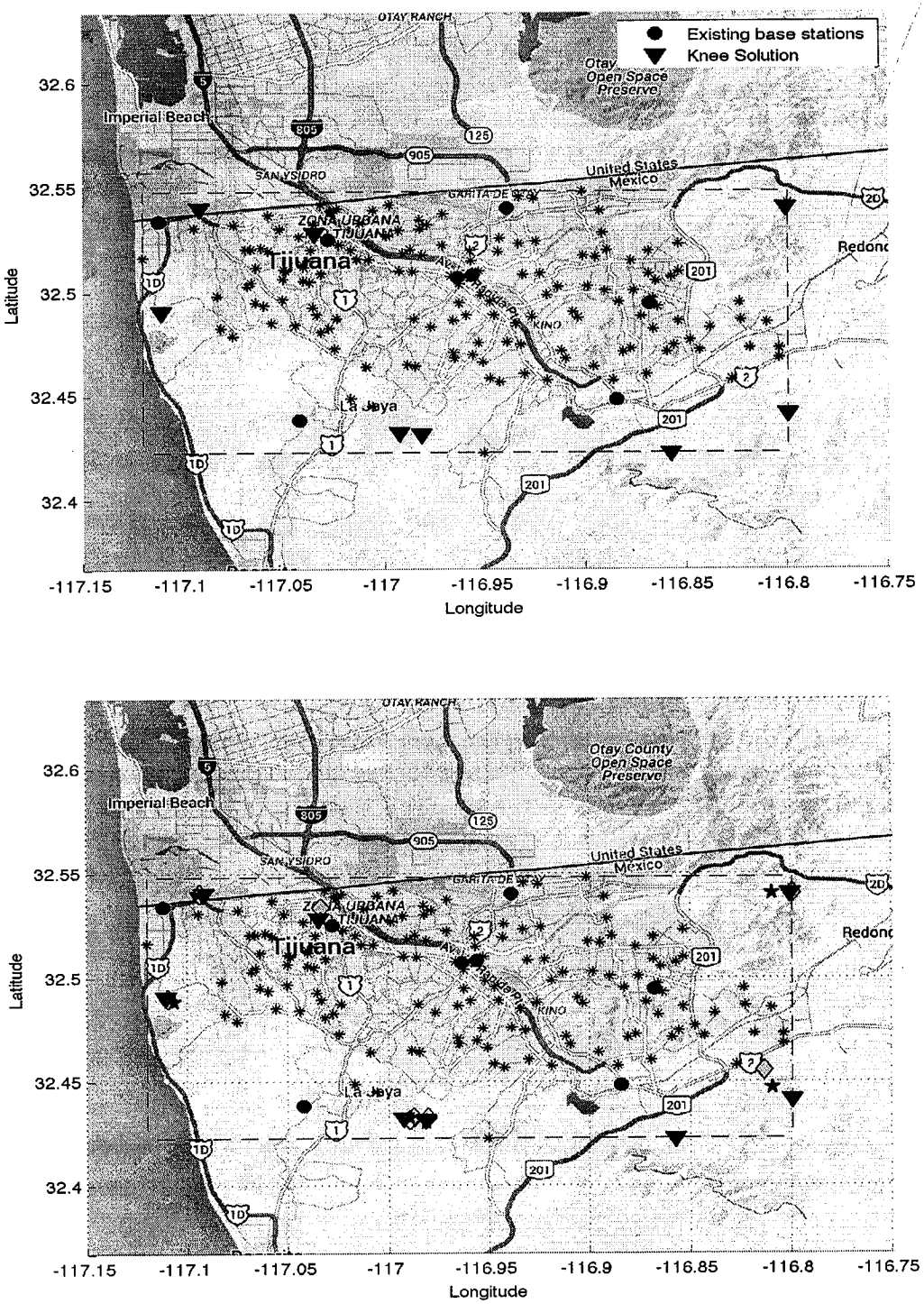


Figure B.8: Locations according to the knee point, The merge for all previous solution locations, $C_{Demand=75}$, Discretization $31 \times 31$, (from top to bottom), Relaxation factor $= 0.5$

# Bibliography


[1] Julius Atlason, Marina A. Epelman, and Shane G. Henderson. Optimizing call center staffing using simulation and analytic center cutting-plane methods. *Management Science*, 54(2):295–309, 2008.

[2] J. Brimberg, R. Chen, and D. Chen. Accelerating convergence in the Fermat-Weber location problem. *Operations Research Letters*, 22(4):152–157, 1998.

[3] Jack Brimberg, Pierre Hansen, Nenad Mladenovic, and Éric D. Taillard. Improvement and comparison of heuristics for solving the uncapacitated multisource weber problem. *Operations Research*, 48(3):444–460, 2000.

[4] Luce Brotcorne, Gilbert Laporte, and Frédéric Semet. Ambulance location and relocation models. *European Journal of Operational Research*, 147:451–463, 2003.

[5] John Cavazos, J Eliot B Moss, and Michael FP O?Boyle. Hybrid optimizations: Which optimization algorithm to use? In *Compiler Construction*, pages 124–138. Springer, 2006.

[6] K. Deb, A. Pratap, S. Agarwal, and T. Meyarivan. A fast and elitist multiobjective genetic algorithm: NSGA-II. *Evolutionary Computation, IEEE Transactions on*, 6(2):182–197, Apr 2002.

[7] Michael Dellnitz, Sina Ober-BlÃ¶baum, Marcus Post, Oliver SchÃ¼tze, and Bianca Thiere. A multi-objective approach to the design of low thrust space trajectories using optimal control. *Celestial Mechanics and Dynamical Astronomy*, 105(1-3):33–59, 2009.

[8] Marco Dorigo and Mauro Birattari. Ant colony optimization. In *Encyclopedia of machine learning*, pages 36–39. Springer, 2010.

[9] Z. Drezner, A. Mehrez, and G. O. Wesolowsky. The facility location problem with limited distances. *Transportation Science*, 25(3):183–187, 1991.

[10] Zvi Drezner, Jack Brimberg, Nenad Mladenovia, and Said Salhi. New local searches for solving the multi-source weber problem. *Annals of Operations Research*, pages 1–23, 2015.

[11] Zvi Drezner, Avram Mehrez, and George O Wesolowsky. The facility location problem with limited distances. *Transportation Science*, 25(3):183–187, 1991.

[12] I. Fernandes, D. Aloise, D. Aloise, and P. Hansen. On the Weber facility location problem with limited distances and side constraints. *Optimization Letters, Springer*, 8(2):407–424, 2014.

[13] V. Filipović. Fine-grained tournament selection operator in genetic algorithms. *Computing and Informatics*, 22:143–161, 2003.

[14] Christodoulos A Floudas and Panos M Pardalos. *Recent advances in global optimization.* princeton University press, 2014.

[15] Lawrence J. Fogel. *Intelligence Through Simulated Evolution: Forty Years of Evolutionary Programming.* John Wiley & Sons, Inc., New York, NY, USA, 1999.

[16] M Gendrau, G. Laporte, and F. Semet. Solving an ambulance location model by tabu search. *Location Sciences*, 5:75–88, 1997.

[17] M. Gendrau, G. Laporte, and F. Semet. Solving an ambulance location model by tabu search. *Location Sciences*, 5(2):75–88, 2012.

[18] John H. Holland. *Adaptation in Natural and Artificial Systems: An Introductory Analysis with Applications to Biology, Control and Artificial Intelligence.* MIT Press, Cambridge, MA, USA, 1992.

[19] J. H. Jaramillo, J. Bhadury, and R. Batta. On the use of genetic algorithms to solve location problems. *Computers and Operations Research*, 29(6):761–779, 2002.

[20] A. Klose and A. Drexl. Facility location models for distribution system design. *European Journal of Operational Research*, 15(2):4–29, 2005.

[21] John R. Koza. *Genetic Programming: On the Programming of Computers by Means of Natural Selection.* MIT Press, Cambridge, MA, USA, 1992.

[22] Jozef Kratica. Improvement of simple genetic algorithm for solving the uncapacitated warehouse location problem. In Rajkumar Roy, Takeshi Furuhashi, and PravirK. Chawdhry, editors, *Advances in Soft Computing*, pages 390–402. Springer London, 1999.

[23] Jozef Kratica, Duän Tošic, Vladimir Filipović, and Ivana Ljubić. Solving the simple plant location problem by genetic algorithm. *RAIRO - Operations Research*, 35:127–142, 1 2001.

[24] Gilbert Laporte, François V. Louveaux, Frédéric Semet, and Arnaud Thirion. Application of the double standard model for ambulance location. Bertazzi, Luca (ed.) et al., Innovations in distribution logistics. Selected papers based on the presentations at the workshop IWDL 2006, Brescia, Italy, October 2006. Berlin: Springer. Lecture Notes in Economics and Mathematical Systems 619, 235-249 (2009)., 2009.

[25] A. Lara, G. Sanchez, Carlos A. Coello Coello, and O. Schutze. Hcs: A new local search strategy for memetic multiobjective evolutionary algorithms. *Evolutionary Computation, IEEE Transactions on*, 14(1):112–132, Feb 2010.

[26] Xueping Li, Zhaoxia Zhao, Xiaoyan Zhu, and Tami Wyatt. Covering models and optimization techniques for emergency response facility location and planning: A review. *Math. Meth. of OR*, 74(3):281–310, 2011.

[27] K. F. Man, K. S. Tang, and S. Kwong. *Genetic Algorithms: Concepts and Designs with Disk.* Springer-Verlag New York, Inc., Secaucus, NJ, USA, 2nd edition, 1999.

[28] M. Marić. An efficient genetic algorithm for solving the multi-level uncapacited facility location problem. *Computing and Informatics*, 29(2):183?201, 2010.

[29] Nimrod Megiddo and Kenneth J. Supowit. On the complexity of some common geometric location problems. *SIAM J. Comput.*, 13(1):182–196, 1984.

[30] Zbigniew Michalewicz. *Genetic Algorithms + Data Structures = Evolution Programs (2Nd, Extended Ed.).* Springer-Verlag New York, Inc., New York, NY, USA, 1994.

[31] S. Morales Pacheco, O. Schutze, C. Vera, L. Trujillo, and Y. Maldonado. Solving the ambulance location problem in tijuana-mexico using a continuous location model. In *Evolutionary Computation (CEC), 2015 IEEE Congress on*, pages 2631–2638, May 2015.

[32] Maik Ringkamp, Sina Ober-BlÃ¶baum, Michael Dellnitz, and Oliver SchÃ¼tze. Handling high-dimensional problems with multi-objective continuation methods via successive approximation of the tangent space. *Engineering Optimization*, 44(9):1117–1146, 2012.

[33] Oliver SchÃ¼tze, Carlos A. Coello Coello, Sanaz Mostaghim, El-Ghazali Talbi, and Michael Dellnitz. Hybridizing evolutionary strategies with continuation methods for solving multi-objective problems. *Engineering Optimization*, 40(5):383–402, 2008.

[34] Oliver Schütze, Adanay Martín, Adriana Lara, Sergio Alvarado, Eduardo Salinas, and Carlos A Coello Coello. The directed search method for multi-objective memetic algorithms. *Computational Optimization and Applications*, 8 2015.

[35] Jan A. Snyman. *Practical mathematical optimization : an introduction to basic optimization theory and classical and new gradient-based algorithms.* Applied optimization. Springer, New York, 2005.

[36] R. Sridharan. The capacitated plant location problem. *European Journal of Operational Research*, 87(2):203 – 213, 1995.

[37] C. Toregas, R. Swaim, C.S. ReVelle, and L. Bergman. The location of emergency service facilities. *Operations Research*, 19(6):1363–1373, 1971.

[38] Prahalad Venkateshan and Kamlesh Mathur. A heuristic for the multisource weber problem with service level constraints. *Transportation Science*, 49(3):472–483, 2015.

[39] Fu-Rui Xiong, Zhi-Chang Qin, Yang Xue, Oliver SchÃ$\frac{1}{4}$tze, Qian Ding, and Jian-Qiao Sun. Multi-objective optimal design of feedback controls for dynamical systems with hybrid simple cell mapping algorithm. *Communications in Nonlinear Science and Numerical Simulation*, 19(5):1465 – 1473, 2014.

[40] Xin-She Yang. Genetic algorithms. *Engineering Optimization*, pages 171–180, 2014.

[41] Xin-She Yang, Zhihua Cui, Renbin Xiao, Amir Hossein Gandomi, and Mehmet Karamanoglu. *Swarm intelligence and bio-inspired computation: theory and applications.* Newnes, 2013.